Diffusion, Viscosity, and Thermodynamics in Liquid Systems

vom Fachbereich Maschinenbau und Verfahrenstechnik
der Technischen Universität Kaiserslautern
zur Verleihung des akademischen Grades
Doktor-Ingenieur (Dr.-Ing.)
genehmigte Dissertation

von
Dipl.-Ing. Dennis Bosse
aus Remscheid

Eingereicht am:	14. Oktober 2004
Tag der mündlichen Prüfung:	28. Januar 2005
Dekan:	Prof. Dr.-Ing. P. Steinmann
Vorsitzender:	Prof. Dr.-Ing. habil. G. Maurer
Referenten:	Prof. Dipl.-Ing. Dr. techn. H.-J. Bart
	Prof. dr. ir. A. B. de Haan

Acknowledgement

Looking back over the last couple of years I know feel relieved that I really finished my research work at the Technical University of Kaiserslautern, Germany. Back in 1999, Prof. Dipl.-Ing. Dr. techn. Hans-Jörg Bart welcomed me on board of his Process Engineering research group. What started initially as a “simple” task, doing some diffusion coefficient measurements and extending the range of applicability of an already developed theory, turned into a real adventure. At that time I never thought of going as deep into the theoretical aspects of diffusion as the present thesis witnesses. During this journey I met of a lot of interesting and smart people who directly or indirectly contributed to the success of this work.

First of all, I am very grateful to Prof. Bart for promoting this work. Working in his group was a pleasure for me. I highly appreciate his guidance and I enjoyed the freedom and patience he gave me to accomplish my work.

Secondly, I would like to express my appreciation to Prof. dr. ir. André de Haan for being a member of the committee. Thank you for your professional advice but also for the joyful times I had during the DAE courses.

Prof. Dr.-Ing. habil. Gerd Maurer I thank for being the chairman of the PhD committee and for his thoughts on thermodynamic modelling.

I would also like to express my deepest appreciation to Harry Kooijman, Ross Taylor, and Andreas Klamt for all the fruitful discussions on various theoretical topics. Thank you all.

Finally, I want to thank my parents and my wife for their faith in me but also for their endless patience, especially during the last two years while writing up and revising this thesis.

Summary

Diffusion is the basis for all kinds of chemical engineering processes, like distillation or liquid-liquid extraction. With the increasing usage of nonequilibrium stage modelling, a deeper insight into mass transfer has become more important to allow accurate and reliable predictions of e.g. concentration profiles in many kinds of equipment. Therefore, fundamental knowledge of various physical and thermodynamic properties such as diffusion coefficients, viscosities, and vapour-liquid equilibria (VLE) is required. Diffusion coefficients of these three properties are the most difficult to predict. Many of the empirical and semi-empirical models developed for this transport property rely on accurate information of the viscosity and thermodynamic models. In almost all diffusion coefficient models a thermodynamic correction factor accounts for deviations from an ideal system. This factor is computed from the second derivative of an excess Gibbs energy model. Small deviations in the prediction of thermodynamics may result in prediction errors for the diffusion coefficients. The largest inaccuracies in the calculated diffusion coefficients are, therefore, to be expected for highly nonideal systems.

To improve the current state of diffusion coefficient prediction, it does not suffice to solely focus on the diffusivity models. Instead, the thermodynamics and viscosity approaches must be assessed separately and revised as required. Only in this way the influence of prediction errors for these properties used to compute the diffusion coefficients can be minimized.

This thesis aims at an overall improvement of the diffusion coefficient predictions. For this reason the theoretical determination of diffusion, viscosity, and thermodynamics in liquid systems is discussed. Furthermore, the experimental determination of diffusion coefficients is also part of this work. All investigations presented are carried out for organic binary liquid mixtures.

The experimental set-up employed in the determination of diffusion coefficients is a Taylor dispersion unit. Such an apparatus consists of standard HPLC-equipment and is well-known for its rapidity and accuracy. A three parameter form of the theoretically derived distribution function is fitted to the detector output, a concentration-time-curve. Diffusion coefficient measurements of 9 highly nonideal binary mixtures have been carried out over the whole concentration range at various temperatures, (25, 30, and 35) °C. All mixtures investigated consist of an alcohol (ethanol, 1-propanol, or 1-butanol) dissolved in hexane, cyclohexane, carbon tetrachloride, or toluene. The uncertainty of the reported data is estimated to be within $3 \cdot 10^{-11}$ $m^2 \cdot s^{-1}$.

Only recently a new model, called COSMOSPACE, was proposed for the description of the excess Gibbs energy. In contrast to other excess Gibbs energy models, like the Wilson equation or UNIQUAC, this model is thermodynamically consistent and its parameters have a physical meaning. Furthermore, the Wilson equation and UNIQUAC may be derived as special cases of the more general COSMOSPACE approach, which is based on the analytical solution to the statistical thermodynamics of the pairwise interacting surface model COSMO-RS. The required molecular parameters like segment types, areas, volumes, and interaction parameters are derived by means of a new technique. So called sigma profiles form the basis of this approach which describe the screening charge densities appearing on a molecule’s surface. In contrast to COSMO-RS, these profiles are not continuously evaluated but divided into as many fragments as peaks appear in the profile. Each of these peaks refers to a separate segment type. From the corresponding peak area and a weighted distribution function applied to this peak, the area and the screening charge of the segment may be derived. However, the interaction parameters determined in this way yield only rough estimates. To improve the model performance, a constrained two-parameter fitting strategy is developed. Within this method, the most negative segment screening charge of each molecule is used as a fitting parameter. To obey the electroneutrality constraint of a molecular surface, this constraint is used to recalculate the value of the most positive segment screening charge of each molecule. In total, 91 thermodynamically consistent experimental data sets covering the various thermodynamic situations appearing in reality are used to assess the quality of this approach and compare the results with the findings of the Wilson model and UNIQUAC. For moderate nonideal systems all models perform equally well while the UNIQUAC calculations fail in the case of systems containing an alcohol component due to erroneous computations of miscibility gaps. A comparison of Wilson and COSMOSPACE reveals that, on average, Wilson performs slightly better. On the other hand, Wilson is incapable of describing phase splitting while the range of applicability of COSMOSPACE is only limited by the number of available molecular parameters. Since these can be easily obtained from quantum chemical COSMO calculations, COSMOSPACE is a valuable tool for the calculation of thermodynamic properties.

On the basis of Eyring’s absolute reaction rate theory a new mixture viscosity model is developed. The nonidealities of the mixture are accounted for with the COSMOSPACE approach that has been successfully applied in the prediction of vapour-liquid equilibria. The required model and component parameters are adopted from the VLE calculations with COSMOSPACE. To improve the prediction quality of this approach, the newly introduced constraint optimisation procedure is employed. In this way the two unknown segment parameters can be obtained from a least-squares fit to experimental data while the parameters retain their physical meaning. Experimental data of 49 binary mixtures are used to compare the results of this approach with those of the Eyring–UNIQUAC model. These results show that with an average relative deviation of 1.21 % the new Eyring–COSMOSPACE approach is slightly superior to the frequently employed Eyring–UNIQUAC method with 1.41 % deviation. Though the performance improvement may seem small, the advantage of the new model is its theoretically consistent basis. Likewise to the VLE-modelling results, the COSMOSPACE approach is superior to the UNIQUAC method especially for highly nonideal systems. In this way, the calculated relative mean deviations can be reduced by a factor of 2 for some mixture classes.

A new model for the Maxwell-Stefan diffusivity is also developed on the basis of Eyring’s absolute reaction rate theory. This model, an extension of the Vignes equation, describes the concentration dependence of the diffusion coefficient in terms of the diffusivities at infinite dilution and an additional excess Gibbs energy contribution. This energy part allows the explicit consideration of thermodynamic nonidealities within the modelling of this transport property. Applying, for this part and for the thermodynamic correction factor, the same set of interaction parameters solely fitted to VLE data, a theoretically sound modelling of the VLE and diffusion can be achieved. The new diffusivity model is also presented in a modified form to account for viscosity effects. With these two models at hand, the influence of viscosity and thermodynamics on the prediction quality of diffusion coefficients is thoroughly investigated. In total, 85 binary mixtures consisting of alkanes, cycloalkanes, X-alkanes, aromatics, ketones, and alcohols are used to compare the prediction results of the new diffusivity approaches with those of the Vignes equation and the Leffler–Cullinan approach. The Wilson model and COSMOSPACE are used to compute the excess Gibbs energy contribution while the mixture viscosity is described by a polynomial of degree 3. All model parameters are derived from thermodynamically consistent Pxy-data and viscosity data that match the temperature of the diffusivity experiments. Since reliable VLE data have only been found for half of the diffusivity experiments, UNIFAC is chosen for a first performance assessment to compute the thermodynamic correction factor. The results indicate that the new model without viscosity correction is superior to the other models investigated. This outcome is also confirmed in subsequent investigations where the influence of the more accurate thermodynamic models is examined. These results demonstrate a clear dependence of the quality of the diffusion coefficient calculations on the accuracy of the thermodynamic model. The new diffusivity approach combined with UNIFAC leads to a relative mean deviation of 8.92 %. In contrast, the deviation of the combinations with COSMOSPACE or Wilson is 7.9 % which is in agreement with other methods recently developed.

In summary, it can be said that the new approach facilitates the prediction of diffusion coefficients. The final equation is mathematically simple, universally applicable, and the prediction quality is as good as other models recently developed without having to worry about additional parameters, like pure component physical property data, self diffusion coefficients, or mixture viscosities.

However, with the introduction of the additional excess Gibbs energy contribution, the influence of thermodynamics increases on the prediction of diffusion coefficients while the uncertainties introduced are undefined. Therefore, it is crucial to model the phase equilibrium behaviour properly to further improve the prediction quality of diffusion coefficients from now 7.9 % to below 2 %, a value typical for e.g. mixture viscosities. Here, the focus should be directed toward the diluted concentration regions where the thermodynamic models show the largest inaccuracies.

In contrast to many other models, the influence of the mixture viscosity can be omitted. Though a viscosity model is not required in the prediction of diffusion coefficients with the new equation, the models presented in this work allow a consistent modelling approach of diffusion, viscosity, and thermodynamics in liquid systems.

Zusammenfassung

Diffusion ist die Basis bei allen verfahrenstechnischen Prozessen, wie z.B. Rektifikation oder Flüssig-flüssig-Extraktion. Mit der verbreiteten Anwendung des Nichtgleichgewichtsmodells wird ein tieferes Verständnis des Stofftransports immer notwendiger, um genaue und zuverlässige Vorhersagen von z.B. Konzentrationsprofilen in jeder Art von Apparat zu ermöglichen. Hierzu sind grundlegende Kenntnisse der unterschiedlichsten physikalischen und thermodynamischen Stoffeigenschaften Voraussetzung, wie z.B. Diffusionskoeffizienten, Viskositäten oder Gas-Flüssig-Gleichgewichte. Von den vorgenannten Stoffeigenschaften sind die Diffusionskoeffizienten am schwierigsten vorherzusagen, da viele empirische und semi-empirische Modelle für die Beschreibung der Diffusion von den beiden anderen Eigenschaften abhängen. In nahezu allen Diffusionskoeffizientenmodellen berücksichtigt ein thermodynamischer Korrekturfaktor die Abweichungen von einem idealen System. Dieser Faktor wird über die zweite Ableitung eines Exzess-Gibbs-Energiemodells berechnet. Kleine Abweichungen in der Vorausberechnung der Thermodynamik können größere Vorhersagefehler bei der Diffusionsberechnung verursachen. Die größten Ungenauigkeiten sind daher in thermodynamisch stark nichtidealen Systemen zu erwarten.

Um die gegenwärtige Vorhersagegenauigkeit von Diffusionskoeffizientenmodellen zu verbessern, ist es nicht ausreichend, nur die Diffusionskoeffizientenmodelle zu verbessern. Die Thermodynamikansätze sowie die Viskositätsmodelle müssen separat evaluiert und, wenn nötig, verbessert werden. Nur so kann der Einfluss der Modellungenauigkeiten für diese Stoffeigenschaften auf die Diffusionsberechnung minimiert werden.

Das Ziel der vorliegenden Arbeit ist die Gesamtverbesserung von Diffusionskoeffizientenberechnungen. Um dieses Ziel zu erreichen, wird die theoretische Bestimmung von Diffusion, Viskosität und Thermodynamik in Flüssigsystemen gleichermaßen diskutiert. Experimentelle Untersuchungen von Diffusionskoeffizienten sind ebenfalls Gegenstand dieser Arbeit. Alle in dieser Arbeit durchgeführten Untersuchungen beschränken sich auf binäre, organische Flüssigsysteme.

Für die experimentelle Bestimmung von Diffusionskoeffizienten wird eine Taylor-Dispersions-Einheit verwendet. Eine solche Apparatur besteht aus Standard-HPLC-Equipment, die für ihre Schnelligkeit und Genauigkeit bekannt ist. Im Rahmen der Datenauswertung wird eine 3-Parameter-Form der theoretisch abgeleiteten Verteilungsfunktion an das Detektorausgangssignal, einem Konzentrations-Zeit-Verlauf, angepasst. Insgesamt werden Diffusionskoeffizienten-messungen von neun stark nichtidealen Mischungen über den gesamten Konzentrationsbereich bei verschiedenen Temperaturen (25, 30 und 35) °C durchgeführt. Alle untersuchten Mischungen bestehen aus einer Alkoholkomponente (Ethanol, 1-Propanol, 1-Butanol), die in Hexan, Cyclohexan, Tetrachlormethan oder Toluol gelöst ist. Die Ungenauigkeit der experimentellen Ergebnisse beträgt $3 \cdot 10^{-11}$ $m^2 \cdot s^{-1}$.

Erst kürzlich wurde ein neues Exzess-Gibbs-Energie-Modell mit dem Namen COSMOSPACE vorgestellt. Im Unterschied zu anderen Exzess-Gibbs-Energie-Modellen, wie z.B. der Wilson-Gleichung oder UNIQUAC, ist dieses Modell thermodynamisch konsistent und die Parameter haben eine physikalische Bedeutung. Darüber hinaus können die Wilson-Gleichung und UNIQUAC als Spezialfälle des allgemeineren COSMOSPACE-Ansatzes hergeleitet werden, der auf der a priori Methode COSMO-RS basiert. Die benötigten molekularen Parameter, wie Segmenttypen, -flächen, -volumen, und –wechselwirkungsparameter werden über eine neue Methodik bestimmt. Sogenannte Sigmaprofile, die die Ladungsdichteverteilung auf einer molekularen Oberfläche beschreiben, bilden die Grundlage dieses Ansatzes. Im Unterschied zu COSMO-RS werden die Sigmaprofile jedoch nicht kontinuierlich ausgewertet, sondern in genauso viele Bereiche unterteilt wie Peaks im Profil vorhanden sind. Jeder dieser Peaks beschreibt einen separaten Segmenttyp. Die Segmentfläche und die Segmentladungsdichte werden über die

entsprechende Peakfläche sowie über eine gewichtete Verteilungsfunktion ermittelt. Da die so bestimmten Parameter nur grobe Abschätzungen liefern, wird zusätzlich eine beschränkte 2-Parameter-Optimierungsstrategie entwickelt, um die Vorhersagegenauigkeit des Modells zu verbessern. Bei dieser Methodik wird die negativste Segmentladung von jedem Molekül als Fitparameter verwendet. Um die Elektroneutralität der Molekületoberflächen zu gewährleisten, wird die positivste Segmentladung jedes Moleküls über die Elektroneutralitätsbedingung neu berechnet. Insgesamt werden 91 thermodynamisch konsistente experimentelle Datensätze ausgewertet und die Vorhersagegenauigkeit von COSMOSPACE mit den Ergebnissen der Wilson-Gleichung und des UNIQUAC-Modells verglichen. Bei der Auswahl dieser Datensätze wurde darauf geachtet, ein breites Spektrum der möglichen thermodynamischen Situationen abzudecken. In schwach nichtidealen Systemen ist die Modellgüte der drei Ansätze identisch, während UNIQUAC im Fall von alkoholischen Systemen fehlerhafte Ergebnisse liefert. Ein Vergleich des Wilson-Modells mit COSMOSPACE zeigt, dass Wilson im Mittel bessere Ergebnisse liefert. Andererseits kann der Wilson-Ansatz nicht für Systeme mit Phasenseparation eingesetzt werden, während der Anwendungsbereich von COSMOSPACE nur durch die verfügbaren molekularen Parameter beschränkt ist. Da diese über quantenchemische COSMO-Berechnungen leicht zugängig sind, ist COSMOSPACE ein wertvolles Werkzeug zur Beschreibung von thermodynamischen Stoffeigenschaften.

Auf Basis von Eyrings Absolute Reaction Rate Theory wird ein neues Modell zur Beschreibung von Gemischviskositäten entwickelt. Die Nichtidealitäten der Mischung werden mit Hilfe des COSMOSPACE-Ansatzes berücksichtigt, der bereits erfolgreich bei der Vorausberechnung von Phasengleichgewichten eingesetzt worden ist. Die notwendigen Modell- und Komponentenparameter werden aus den VLE-Berechnungen mit COSMOSPACE übernommen. Für eine verbesserte Vorhersagegenauigkeit des Viskositätsansatzes wird der neuentwickelte, beschränkte Optimierungsalgorithmus eingesetzt. Auf diese Weise können die zwei unbekannten Segmentparameter über einen Datenfit durch Minimierung der Fehlerquadratsumme bestimmt werden, wobei die Parameter ihre physikalische Bedeutung behalten. Experimentelle Datensätze von 49 binären Mischungen werden eingesetzt, um die Vorhersagegenauigkeit des neuen Modellansatzes mit den Ergebnissen des Eyring-UNIQUAC-Modells zu vergleichen. Die Ergebnisse zeigen, das mit einer mittleren relativen Abweichung von 1.21 % der neue Eyring-COSMOSPACE-Ansatz dem oft verwendeten Eyring-UNIQUAC-Modell mit einer Abweichung von 1.41 % zu bevorzugen ist. Auch wenn die Vorhersagequalität nur leicht verbessert werden kann, ist der Vorteil des neuen Ansatzes seine theoretisch konsistente Basis. Wie im Falle der VLE-Berechnungen, ist der COSMOSPACE-Ansatz auch hier gegenüber der UNIQUAC-Methode vor allem in stark nichtideale Systeme zu bevorzugen. Bei solchen Systemen können die berechneten relativen mittleren Abweichungen für einige Systemklassen um den Faktor 2 reduziert werden.

Ein neues Modell für den Maxwell-Stefan-Diffusionskoeffizienten wird ebenfalls auf Basis von Eyrings Absolute Reaction Rate Theory entwickelt. Dieses Modell, eine Erweiterung der Vignes-Gleichung, beschreibt die Konzentrationsabhängigkeit des Diffusionskoeffizienten als Funktion der Diffusionskoeffizienten bei unendlicher Verdünnung und eines zusätzlichen Exzess-Gibbs-Energie-Beitrags. Dieser Anteil ermöglicht die explizite Berücksichtigung von thermodynamischen Nichtidealitäten bei der Modellierung dieses Transportkoeffizienten. Wenn für diesen Anteil und für den thermodynamischen Korrekturfaktor der selbe Satz von Wechselwirkungsparameter eingesetzt wird, der über VLE-Berechnungen ermittelt wurde, ist eine theoretisch konsistente Modellierung von Phasengleichgewichten und Diffusion möglich. Der neue Diffusionsansatz wird ebenfalls in einer modifizierten Form präsentiert, um den Einfluss von Viskositätseffekten zu berücksichtigen. Mit Hilfe dieser beiden Modelle werden der Einfluss von Viskosität und Thermodynamik auf die Vorhersagegenauigkeit von Diffusionskoeffizienten näher untersucht. Das Wilson-Modell, COSMOSPACE und UNIFAC werden für die Beschreibung der Thermodynamik

herangezogen, während die Mischungsviskosität über ein Polynom dritten Grades beschrieben wird, um weitere Ungenauigkeiten bei der Diffusionsberechnung auszuschließen. Insgesamt werden 85 binäre Mischungen aus Alkanen, Cycloalkanen, X-Alkanen, Aromaten, Ketonen und Alkoholen untersucht, um die Qualität der neuen Modellansätze mit den Berechnungsergebnissen der Vignes-Gleichung und des Leffler-Cullinan-Ansatzes zu vergleichen. Da nur für die Hälfte der Diffusionsexperimente zuverlässige VLE-Daten gefunden wurden, wird UNIFAC für eine erste Bewertung für die Berechnung des thermodynamischen Korrekturfaktors eingesetzt. Diese Ergebnisse zeigen, dass der neue Ansatz ohne Viskositätskorrektur besser ist als die anderen untersuchten Modelle. Dieses Ergebnis wird auch durch nachfolgende Untersuchungen bestätigt, bei denen der Einfluss der genaueren thermodynamischen Ansätze untersucht wird. Diese Ergebnisse zeigen eine deutliche Abhängigkeit der Güte der Diffusionsberechnungen von der Genauigkeit der thermodynamischen Modelle. Der neue Diffusionsansatz liefert zusammen mit UNIFAC eine relative mittlere Abweichung von 8.92 %. Im Unterschied hierzu führen die Kombinationen mit COSMOSPACE oder Wilson zu einer Abweichung von 7.9 %, die in Übereinstimmung ist mit anderen Diffusionskoeffizientenmodellen.

Zusammenfassend kan gesagt werden, dass der neue Ansatz die Berechnung von Diffusionskoeffizienten erleichtert. Die Gleichung ist mathematisch einfach und universell einsetzbar. Die Vorhersagequalität des Modells ist genauso gut wie bestehende Ansätze, wobei hier keine zusätzlichen Informationen wie physikalische Stoffeigenschaften der Reinstoffe, Selbstdiffusionskoeffizienten oder Gemischviskositäten benötigt werden.

Mit der Einführung des zusätzlichen Exzess-Gibbs-Energie-Beitrags nimmt der Einfluss der Thermodynamik auf die Vorausberechnung von Diffusionskoeffizienten zu, während der damit verbundene Fehler unbestimmt bleibt. Daher ist es notwendig, das Phasengleichgewicht vor allem in den verdünnten Konzentrationsbereichen so exakt wie möglich zu modellieren. Nur so ist es in Zukunft möglich, die Abweichungen der berechneten Diffusionskoeffizienten von derzeit 7.9 % auf unter 2 % zu reduzieren, einem Wert, der z.B. für die Vorhersagequalität von Gemischviskositätsmodellen typisch ist.

Im Unterschied zu vielen anderen Modellen, kann der Einfluss der Gemischviskosität im hier vorgestellten Modell vernachlässigt werden. Auch wenn die Gemischviskosität bei der Berechnung von Diffusionskoeffizienten nicht mehr benötigt wird, gestatten die hier vorgestellten Modelle eine konsistente Modellierung von Diffusion, Viskosität und Thermodynamik in Flüssigsystemen.

Contents

1 Introduction

1.1 Diffusion

Molecular diffusion describes the relative motion of individual molecules in a mixture induced by their thermal energy causing random, irregular movements. But it may also arise from pressure gradients, temperature gradients, external force fields, and concentration gradients. The resulting net diffusion flux is down the potential gradient, i.e. in the case of a concentration gradient from regions of higher to lower concentration until uniformity of the system is reached.

In an idealised theoretical picture, the diffusing species is considered to travel with a constant velocity along a straight line until it collides with another molecule which results in a change of its velocity in magnitude and direction. These collisions cause the molecules to move in a highly zigzag path and the net diffusion distance is only a fraction of the length of the actual path. Since the number of collisions is a function of the density, diffusion rates in liquids are much smaller than in gases. With decreasing pressure the diffusion rates may increase due to the reduced number of collisions. The same effect may be achieved by an increase in temperature due to the higher molecular velocity.

These small rates in liquid mixtures also explain the importance of diffusion in many chemical engineering processes. Often it is the rate determining step, like in reactive extraction systems. In such systems, for example, mass transfer may be affected by the high ratio of solvent to solute viscosity (Bart 2001). In modelling such unit operations with the rate-based approach (Krishnamurthy and Taylor 1985), accurate knowledge of diffusion coefficients is indispensable in order to compute the required diffusion fluxes.

Previously, diffusion coefficients were deemed unimportant in comparison to other properties like vapour-liquid equilibria or viscosities. The result is that diffusion models are still lacking accuracy, while highly sophisticated models have been derived for the other properties. Only recently the researchers' attitude towards the development of diffusion models has started to change which may be seen in the increasing number of publications in this field.

1.2 Diffusion Coefficients

One of the first names associated with diffusion is Adolf Eugen Fick. In 1855 he developed a phenomenological description of diffusion in binary liquid systems (Fick 1855). This theory states that the diffusion flux of a species is proportional to its concentration gradient times a proportionality constant called the diffusion coefficient. At about the same time another approach was published, known as the Maxwell-Stefan equation (Maxwell 1952). This model derived from the kinetic gas theory and later extended to liquid systems (Standart et al. 1979) describes diffusion fluxes in terms of gradients in activities and Maxwell-Stefan diffusion coefficients. Furthermore, other driving forces such as those aforementioned may also be included. For a binary mixture the two models are related by

$$D = \Gamma Đ \tag{1.1}$$

with $Đ$ as the Maxwell-Stefan diffusivity and D as the Fick diffusivity. The thermodynamic correction factor Γ defined in terms of an excess Gibbs (g^{E}) energy expression accounts for the nonideal behaviour of the mixture.

$$\Gamma = 1 + x_1 \left.\frac{\partial \ln \gamma_1}{\partial x_1}\right|_{x_2,T,P} \tag{1.2}$$

Hence, the problem of modelling diffusion fluxes is shifted towards the accurate determination of diffusion coefficients. With (1.1) the diffusivities can be transformed into one another. Therefore, the Fick model and the Maxwell-Stefan equation may be employed in the description of diffusion fluxes once information on either type of diffusivity is available.

1.3 Experimental Determination of Diffusion Coefficients

Over the last decades several methods have been developed to measure diffusion coefficients in liquid systems. Of the various techniques, which are for example described in detail by Wakeham (Wakeham 1991), the holographic interferometry and the Taylor dispersion are the experimental set-ups mostly used during the last decade. Of these two methods, the Taylor dispersion is often the method of choice for the measurement of diffusion coefficients in binary systems. This method yields results of similar quality compared to the holographic interferometry while keeping the experimental effort and the data processing steps to a minimum. In addition, this technique is also applicable to the measurement of diffusion coefficients at infinite dilution. All measurements can be carried out with standard HPLC-equipment that can be easily automated (Ven-Lucassen et al. 1995).

Measurements in multicomponent systems cannot be easily performed with this technique. The experimental set-up needs to be extended and measurements become more laborious. In addition to this, the data processing also becomes more complex which often results in large uncertainties. Therefore, the holographic interferometry is usually preferred for the measurement of diffusion coefficients in multicomponent systems. Analogue to the measurements in binary systems with this technique, the experimental effort is high and the data processing steps are very time-consuming.

1.4 Modelling Diffusion Coefficients

As the number of diffusion coefficient data published in the literature is limited, the development of diffusivity models is highly desirable. A comparison of the Fick's law and the Maxwell-Stefan equation reveals that expressions for the Maxwell-Stefan diffusivity are to be preferred for several reasons (Taylor and Krishna 1993; Wesselingh and Krishna 2000). One of the reasons is that the Maxwell-Stefan approach separates thermodynamics and mass transfer while the Fick diffusivity accounts for both effects in one coefficient as may be seen from (1.1). This makes the Maxwell-Stefan diffusivity less concentration dependent and, therefore, „simpler“ to model.

Hydrodynamic theories, kinetic theory, statistical mechanics, and absolute reaction rate theory often form the basis for the development of new diffusivity approaches. In these models the Maxwell-Stefan diffusivity is at least a function of composition and the diffusivities at infinite dilution (see for example the models by Vignes (Vignes 1966) and Darken (Darken 1948)). Often, additional parameters and physical properties are employed to improve the prediction accuracy. Examples for such parameters are viscosities, self diffusion coefficients, and association constants as the contributions by various authors show (Leffler and Cullinan 1970; Cussler 1980; Rutten 1992; Li et al. 2001). As these examples demonstrate providing the required parameters may be cumbersome and may, in the worst case, also lead to larger deviations in the desired diffusivities than achieved with the simple interpolation schemes from Vignes or Darken. However, this must be evaluated for each case separately.

The quality of the diffusivity models may be judged from comparisons of predictions with experimental Fick diffusion coefficients. In order to compute Fick diffusivities from a Maxwell-Stefan diffusivity approach, the diffusion coefficients at infinite dilution need to be determined in a first step. This can be done by means of experimental data or some model. The majority of the models are founded on the Stokes-Einstein equation. Within this approach, the diffusivity is related to the solute size and the solvent viscosity. One of the most famous representatives of these models is the Wilke-Chang equation (Wilke and Chang 1955). Though widely accepted, it must be emphasized that this model is, in its original form, not suitable for diffusivity predictions if water is the solute component. However, this situation can be greatly improved by simply applying a different constant for the water correction factor (Kooijman 2002). In this way the maximum error may be reduced from 167 % to 41 %. Only recently another variant of the Stokes-Einstein equation was proposed by Kooijman (Kooijman 2002) with a special focus on the prediction of aqueous systems. It was shown that this model is superior to the Wilke-Chang equation as well as to many other published models. The average deviation with this new method is 10 % for 245 data points including aqueous and organic systems.

However, care must be taken when selecting a limiting diffusivity model. Especially in highly nonideal binary systems, for example, it is often the case that one limiting value may be estimated within these 10 % deviation while the other value deviates more than 30 % from reality. Already in this first step, larger errors may be introduced in the computation of the Fick diffusion coefficients and it is, therefore, advisable to use experimental values whenever possible.

Secondly, a Maxwell-Stefan diffusivity model must be chosen to compute the concentration dependence of this transport property. As already stated, special care must be taken if additional parameters or properties are required. Only with accurate information of these values, can reliable diffusivity data be obtained. Recent developments in this field are presented in Chap. 5.

Finally, a g^E-model must be chosen to compute the thermodynamic correction factor. With all the highly sophisticated thermodynamic models available this step may seem the easiest to accomplish. However, it is also the most important since the results directly influence the diffusivity predictions. Many of the g^E-expressions require interaction parameters which may be obtained from least-squares fits to experimental activity coefficients data or to experimental vapour-liquid equilibrium (VLE) data. Hence, information on the first derivative of a g^E-expression is used to determine the parameters whereas the thermodynamic correction factor, as defined in (1.2), is expressed in terms of the second derivative of this function. From this dependence it is obvious that a unique solution for the shape of the thermodynamic correction factor is difficult to obtain. First, this shape can be influenced by the set of interaction parameters used for the calculation. Multiple sets of interaction parameters exist for a single set of experimental data which all satisfy the convergence criterion of the least-squares fit. While the difference in the description of the VLE data with these parameter sets is negligible, it may have an impact on the shape of the thermodynamic correction factor. As was pointed out by Taylor and Krishna (Taylor and Krishna 1993) and can be seen in Fig. 1.1, the choice of the g^E-model also influences the shape of this function since these models differ in the prediction accuracy of the experimental activity coefficients. Finally, the thermodynamic correction factor is also a function of the experimental

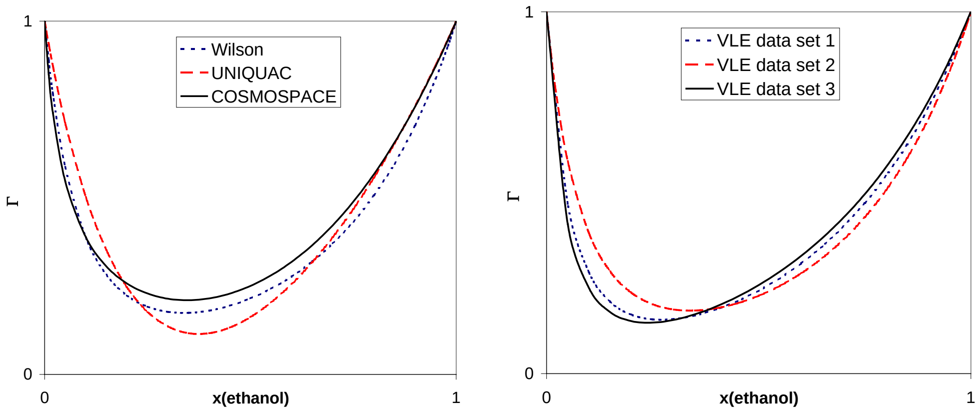

Figure 1.1. Thermodynamic correction factor of ethanol-benzene at 25 °C as a function of the g^E-model chosen (left) and as a function of different VLE-data sets (all measured at 25 °C) computed with the Wilson model (right).

data set used to determine the interaction parameters. Due to the inherent experimental errors, different data sets lead to different results for the correction factor (Fig. 1.1). Unfortunately, the thermodynamic correction factor is experimentally not accessible and it remains ambiguous which of the many curvatures is correct. For that reason it is advisable to obtain the interaction parameters from a simultaneous fit to various carefully selected experimental VLE data sets and finally choose the g^E-model with the smallest deviation from the experimental data.

With all this additional information required, modelling of diffusion coefficient is not an easy task. Current knowledge on diffusion adequately describes diffusion coefficients for ideal and slightly nonideal systems but fails for highly nonideal systems. For such systems the various kinds of molecular interaction are often not appropriately accounted for in the diffusivity model. Chemical theories that were developed for molecular association often lack the required equilibrium constants. Therefore, new models are crucial for the accurate modelling of diffusion coefficients.

1.5 Outline of the Thesis

This thesis deals with the determination of mutual diffusion coefficients in homogeneous binary liquid systems with a special focus on highly nonideal mixtures. Apart from the experimental determination of Fick diffusivities special attention is paid to the theoretical modelling of this transport property. A new Maxwell-Stefan diffusivity approach is presented and thoroughly investigated. Additionally, the performance of some g^E-models and viscosity approaches are also critically assessed since the overall accuracy of the diffusivity prediction strongly depends on these properties.

In Chap. 2 all aspects of the experimental determination of Fick diffusivities are covered. Here, the experimental set-up, a Taylor dispersion unit, and the experimental procedure are explained in detail. Accurate diffusion coefficient data is reported for alcohols in inert and solvating solvents over the whole concentration range at various temperatures.

The performance of current g^E-models is tested in Chap. 3. Besides the well-known Wilson equation (Wilson 1964) and the UNIQUAC-model (Abrams and Prausnitz 1975; Maurer and Prausnitz 1978), a new g^E-expression called COSMOSPACE (Klamt et al. 2002) is also assessed. A new fitting method is employed to determine the required interaction parameters of this approach. In contrast to other fitting strategies used to obtain interaction parameters, the neutrality of the overall surface charge is used as an additional constraint on the optimization procedure to retain the physical significance of the parameters.

On the basis of COSMOSPACE and Eyring's absolute reaction rate theory (Glasstone et al. 1941) a new viscosity model is derived in Chap. 4 and compared to other models published in the literature. Again, the new fitting method is used to derive the interaction parameters from experimental data.

Finally, in Chap. 5 a new Maxwell-Stefan diffusivity model is suggested which also originates from Eyring's absolute reaction rate theory. An alternative form accounting for viscosity effects is also presented. Both versions are critically evaluated in terms of thermodynamics and viscosity influences on the prediction quality of the diffusion coefficients.

1.6 List of Symbols

D	Fick diffusion coefficient ($m^2\ s^{-1}$)
Đ	Maxwell-Stefan diffusion coefficient ($m^2\ s^{-1}$)
P	pressure (Pa)

T	temperature (K)
x_i	mole fraction of component *i* (-)

Greek Symbols

Γ	thermodynamic correction factor (-)
γ_i	activity coefficient of component *i* (-)

1.7 References

Abrams, D. S. and Prausnitz, J. M.: *Statistical Thermodynamics of Liquid Mixtures: A New Expression for the Excess Gibbs Energy of Partly or Completely Miscible Systems*. AIChE J. **21**(1): 116-128 (1975).

Bart, H. J.: Reactive Extraction. in: *Heat and Mass Transfer*. Mewes, D. and Mayinger, F. (Series Eds.). Berlin, Springer (2001).

Cussler, E. L.: *Cluster Diffusion in Liquids*. AIChE J. **26**(1): 43-51 (1980).

Darken, L. S.: *Diffusion, mobility and their interrelation through free energy in binary metallic systems*. Trans. Am. Inst. Mining, Met. Eng. **175**: 184-201 (1948).

Fick, A.: *On Liquid Diffusion*. Phil. Mag. **10**: 30-39 (1855).

Glasstone, S., Laidler, K. and Eyring, H.: The Theory of Rate Processes. McGraw-Hill, New York (1941).

Klamt, A., Krooshof, G. J. P. and Taylor, R.: *COSMOSPACE: Alternative to Conventional Activity-Coefficient Models*. AIChE J. **48**(10): 2332-2349 (2002).

Kooijman, H. A.: *A Modification of the Stokes-Einstein Equation for Diffusivities in Dilute Binary Mixtures*. Ind. Eng. Chem. Res. **41**: 3326-3328 (2002).

Krishnamurthy, R. and Taylor, R.: *A Nonequilibrium Stage Model of Multicomponent Separation Processes*. AIChE J. **31**: 449-456 (1985).

Leffler, J. and Cullinan, H. T.: *Variation of Liquid Diffusion Coefficients with Composition*. Ind. Eng. Chem. Fundam. **9**(1): 84-88 (1970).

Li, J., Liu, H. and Hu, Y.: *A mutual-diffusion-coefficient model based on local composition*. Fluid Phase Equilibria **187-188**: 193-208 (2001).

Maurer, G. and Prausnitz, J. M.: *On the Derivation and Extension of the UNIQUAC Equation*. Fluid Phase Equilibria **2**: 91-99 (1978).

Maxwell, J. C.: *The Scientific Papers of James Clerk Maxwell*. Niven, W. D. (Ed.), New York, Dover (1952).

Rutten, P. W. M.: Diffusion in Liquids. Delft University Press, Delft (1992).

Standart, G. L., Taylor, R. and Krishna, R.: *The Maxwell-Stefan Formulation of Irreversible Thermodynamics for Simultaneous Heat and Mass Transfer*. Chem. Eng. Commun. **3**: 277-289 (1979).

Taylor, R. and Krishna, R.: Multicomponent Mass Transfer. John Wiley & Sons, New York (1993).

Ven-Lucassen, I. M. J. J. v. d., Kieviet, F. G. and Kerkhof, P. J. A. M.: *Fast and convenient implementation of the Taylor dispersion method*. J. Chem. Eng. Data **40**(2): 407-411 (1995).

Vignes, A.: *Diffusion in Binary Solutions*. Ind. Eng. Chem. Fundam. **5**(2): 189-199 (1966).

Wakeham, W. A.: Measurement of the transport properties of fluids. Oxford, Blackwell Scientific (1991).

Wesselingh, J. A. and Krishna, R.: Mass Transfer in Multicomponent Mixtures. Delft University Press, Delft (2000).

Wilke, C. R. and Chang, P.: *Correlation of Diffusion Coefficients in Dilute Solutions*. AIChE J. **1**(2): 264-270 (1955).

Wilson, G. M.: *Vapor-Liquid Equilibrium. XI. A New Expression for the Excess Free Energy of Mixing*. J. Am. Chem. Soc. **86**: 127-130 (1964).

2 Measurement of Diffusion Coefficients in Thermodynamically Nonideal Systems

Accurate diffusion coefficient data are reported for highly nonideal binary mixtures. The mixtures consist of an alcohol (ethanol, 1-propanol, 1-butanol) dissolved in hexane, cyclohexane, carbon tetrachloride, or toluene. All measurements have been conducted over the whole concentration range at various temperatures, (25, 30, and 35) °C, by means of the Taylor dispersion technique. The uncertainty of the reported data is estimated to be within $3 \cdot 10^{-11}$ m^2s^{-1}.

2.1 Introduction

With the increasing use of the nonequilibrium model (Krishnamurthy and Taylor 1985; Taylor and Krishna 1993) in the design of chemical processes a thorough knowledge of many physical properties is required. One of the important transport coefficients is the diffusion coefficient since this type of mass transfer is often the rate determining step. In contrast to other properties like viscosity or density, the number of reliable reported diffusion coefficients is limited, especially for highly nonideal binary mixtures. Therefore, diffusion coefficient measurements were conducted for several binary alcohol-solvent systems over the whole concentration range as a function of the temperature. The experimental set-up used in this study is a Taylor dispersion unit, well known for its accuracy and rapidity (Pratt and Wakeham 1974; Harris et al. 1993; Ven-Lucassen et al. 1995).

2.2 Experimental Set-Up and Data Processing

In a Taylor dispersion experiment a pulse is rapidly injected into a fluid (eluent) of a different composition flowing slowly through a narrow capillary. Due to the superposition of a laminar flow profile (which pulls the pulse apart) and the radially induced molecular diffusion (which narrows the pulse) the pulse is dispersed. In the ideal case of a binary mixture does this lead to a Gaussian distribution. A mathematical description of the dispersion process and of the concentration profile at the end of the capillary was derived by Taylor (Taylor 1953, 1954). The resulting expression was used within the data processing step. A formal derivation of the equation and the underlying assumptions may be found elsewhere (Alizadeh et al. 1980; Baldauf and Knapp 1983; Rutten 1992; Bollen 1999).

The experimental set-up of a Taylor dispersion apparatus consists of standard HPLC-equipment, see Figure 2.1. For details on the design of such an apparatus the reader is referred to the literature (Rutten 1992; Ven-Lucassen et al. 1995; Bollen 1999). To prepare the eluent and injection solutions, a glass flask was placed on a balance (Mettler model A200, precision of 0.001 g) and the components were weighed in order of increasing volatility. The eluent was stored in a 500 mL glass flask while the samples were transferred from 10 mL glass flasks to clear crimp vials. All chemicals were obtained from Merck Eurolab (analytical grade) and used without further purification. During an experiment the helium purged eluent flowed through a membrane degasser to a quaternary dual piston pump (HP model 1050). The feed pump was connected to an autosampler (Spark Midas) equipped with a six-port sample injection valve (Rheodyne type 7739) and a sample loop volume of 20 μL. To avoid extra dispersion, dead volume connectors were used to connect the PEEK capillary directly to the injection valve. The 23.42 m long capillary with an inner diameter of $d = 0.53$ mm was helically coiled with a coiling diameter of $d_c = 0.8$ m. In this way the arrangement matches the assumption $d_c >> d$ to avoid secondary flow in the capillary. Therefore, (2.1)-(2.5) can

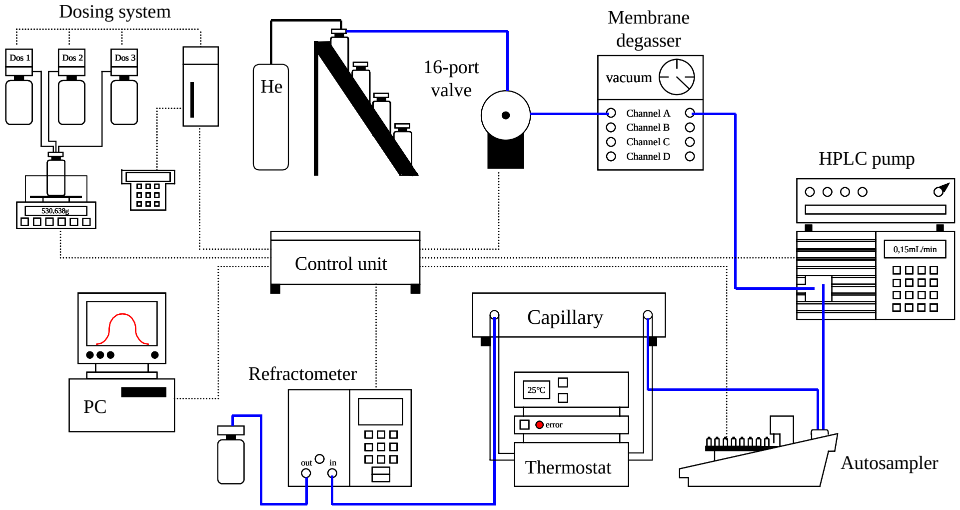

Figure 2.1. Experimental set-up of the Taylor dispersion unit.

be applied for further data processing. For temperature control, the capillary was placed in a water bath connected to a thermostat. The outlet of the capillary was linked to a differential refractometer (Waters model R-403) using dead volume connectors. Since only small composition differences were measured, the eluent was always taken as the reference fluid. Additionally, the refractometer cell was thermostated at a slightly higher temperature than the water bath of the capillary to reduce the noise in the detector signal. This was recorded by a PC which also fully controlled the whole apparatus. Prior to carrying out measurements with a new eluent composition, the apparatus was initially purged with the new eluent mixture at a flowrate of 1 mL/min for about 10 min and afterwards at the experimental flowrate of 0.15 mL/min for several hours. Typical residence times obtained at this flowrate are around 31 min.

A least-squares fitting strategy was applied for the data processing of the detector signals since the moment's method, an alternative procedure, was deemed less accurate (Leaist 1991; Ven-Lucassen et al. 1995). Following the recommendation of Bollen (Bollen 1999) the data processing was done in two steps. In the first step, data points which clearly belong to the baseline were selected from both sides of the peak and a polynomial function (mostly of degree three) was then fitted to the selection. This function was then subtracted from the original peak to obtain a baseline corrected peak, i.e. to account for baseline drifting of the detector output. In the second step a three parameter form of Taylor's equation was then fitted to the corrected peak as was also mentioned by other researchers (Rutten 1992; Ven-Lucassen et al. 1995).

$$\Delta y_1(t) = \frac{P_1}{\sqrt{P_2 t}} \exp\left(-\frac{L^2 \left(1 - t/P_3\right)^2}{4 P_2 t} \right) \tag{2.1}$$

Here, Δy_1 denotes the computed value of the detector signal, t the time and L the length of the capillary while the three parameters are defined by

$$P_1 = \frac{2 s_1 n_1^E}{\pi d^2 \sqrt{\pi}} \tag{2.2}$$

$$P_2 = \frac{u_{\mathrm{av}}^2 d^2}{192 D} \tag{2.3}$$

$$P_3 = \frac{L}{u_{\mathrm{av}}} \tag{2.4}$$

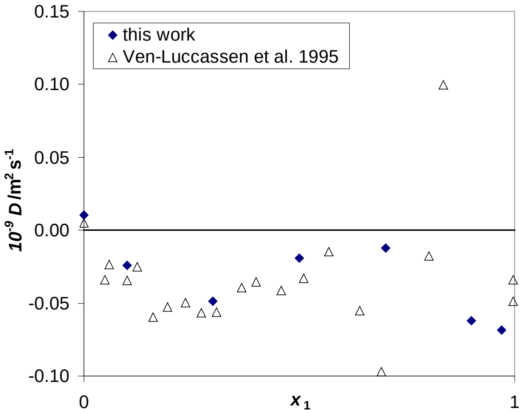

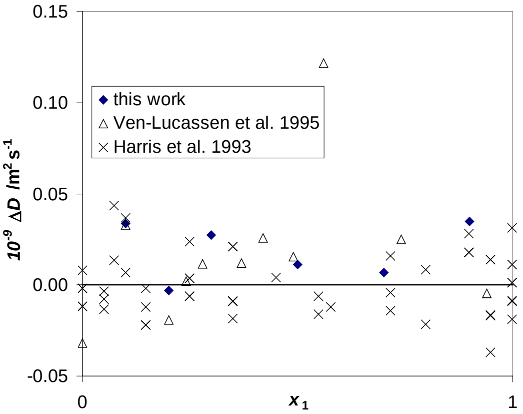

Figure 2.2. Differences Δ*D* between experimental data and orthogonal polynomial function(Harris et al. 1993) for the mixture methanol (1) + water (2) at 25 °C (left).

Figure 2.3. Differences Δ*D* between experimental data and orthogonal polynomial function (Harris et al. 1993) for the mixture ethanol (1) + water (2) at 25 °C (right).

with s_1 as the detector linearity, n_1^{E} as the excess number of tracer moles in the pulse, and u_{av} as the cross-section averaged velocity of the eluent. As may be seen from their definition the parameters P_2 and P_3 represent the dispersion coefficient and the residence time, respectively. The defining equations (2.3) and (2.4) of these parameters also serve to compute the desired diffusion coefficient from:

$$D = \frac{L^2 d^2}{192 P_2 P_3^2} \tag{2.5}$$

The estimated uncertainty in x is 0.01, in *t* it equals 1s and it amounts to $3 \cdot 10^{-11}$ $\mathrm{m^2 s^{-1}}$ in *D*.

2.3 Results

The Taylor dispersion apparatus was tested at (25.0 ± 0.1) °C using the mixtures methanol + water and ethanol + water. Figures 2.2 to 2.3 present the deviations between the measurements of this work and an orthogonal polynomial function determined by Harris et al. (Harris et al. 1993) to test their data against those of other authors. Additionally, results of other researchers are depicted for comparison. The average deviation of the validation experiments is $\pm 3 \cdot 10^{-11}$ $\mathrm{m^2 s^{-1}}$ which is in agreement with the accuracy for this type of set-up and type of systems reported by other researchers (Pratt and Wakeham 1974; Harris et al. 1993; Ven-Lucassen et al. 1995). The measured diffusion coefficients as well as the computed differences of the validation experiments are summarized in Table 2.1. The tabulated *D* values are averages of at least three replicate

Table 2.1. Diffusion coefficients *D* of alcohol (1) + water (2) mixtures, (deviations Δ*D* from orthogonal polynomial function(Harris et al. 1993) given in parenthesis).

		x_1								
		0.0	0.1	0.2	0.3	0.5	0.7	0.9	0.97	1.0
	T/°C	$D/(10^{-9}\ \mathrm{m^2 \cdot s^{-1}})$ and $\Delta D/(10^{-9}\ \mathrm{m^2 \cdot s^{-1}})$								
MeOH	25	1.57	1.22		0.95	1.03	1.37	1.87	2.05	
		(0.01)	(-0.02)		(-0.05)	(-0.02)	(-0.01)	(-0.06)	(-0.07)	
EtOH	25		0.70	0.41	0.38	0.51	0.76	1.08		
			(0.03)	(0.0)	(0.03)	(0.01)	(0.01)	(0.03)		

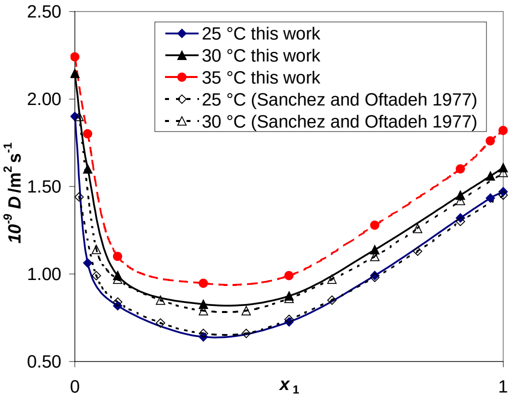

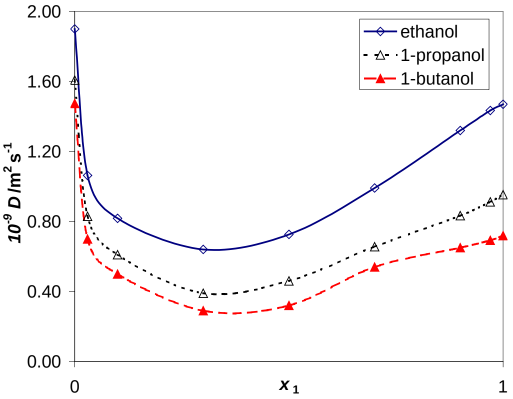

Figure 2.4. Diffusion coefficients *D* of ethanol (1) + carbon tetrachloride (2) mixtures (left).
Figure 2.5. Diffusion coefficients *D* of alcohol (1) + carbon tetrachloride (2) mixtures at 25 °C (right).

measurements.

Diffusion coefficients of several alcohol + solvent systems were measured. In addition to the concentration dependence, the influence of the chain length of the alcohol component, as well as the effect of temperature on the diffusion coefficients, were considered. In total, 9 different binary mixtures at temperatures from (25 to 35) °C were studied over the whole concentration range. For the alcohol ethanol (EtOH), 1-propanol (1-PropOH) and 1-butanol (1-BuOH) were chosen while for the solvent hexane, cyclohexane, toluene, and carbon tetrachloride were taken. The experimentally measured diffusion coefficients are presented in the Tables of the Appendix.

Figure 2.4 shows the *D* values for the ethanol + carbon tetrachloride system at various temperatures. The results of holographic interferometry measurements by Sanchez and Oftadeh (Sanchez and Oftadeh 1977) are also depicted. The lines presented serve only as a visual aid. As can be seen from the graph the findings of this work and of the research by Sanchez and Oftadeh (Sanchez and Oftadeh 1977) are in excellent agreement. This graph also reveals a strong concentration dependence of the *D* values and, as expected from theory, they are also strongly related to the temperature. With increasing temperature, the mobility of the molecules is enhanced due to a decrease in the liquid viscosity.

The influence of the molecular chain length on the diffusion coefficient has also been investigated as the results in Figure 2.5 show. Here, the diffusion coefficients of alcohol + carbon tetrachloride mixtures are presented at 25 °C. As is evident from the graph an increase in the chain length causes a decrease in the diffusion coefficient. This behaviour which lowers the *D* values from ethanol to 1-butanol can be explained by the lower mobility of the larger alcohol molecules.

2.4 Summary

In this work a fully automated Taylor dispersion apparatus was used to determine diffusion coefficients of 9 binary alcohol-solvent mixtures. As expected for thermodynamically nonideal mixtures the reported data points show a strong concentration dependence. Additionally, the *D* values are also a strong function of temperature. The uncertainty of the reported data is estimated to be within $3\cdot10^{-11}$ m^{2}s^{-1}.

2.5 Symbols

D molecular diffusion coefficient (m^2 s^{-1})

L	length of the capillary (m)
$P_{1\ldots3}$	fitting parameters (-)
d	diameter of the capillary (m)
n^{E}	excess number of tracer moles in the pulse (-)
s	detector linearity (-)
t	time (s)
u_{sup}	superficial velocity (m s^{-1})
Δy	computed detector signal (-)

2.6 References

Alizadeh, A., Nieto de Castro, C. A., and Wakeham, W. A.: *The theory of the Taylor dispersion technique for liquid diffusivity measurements*. Int. J. Thermophysics **1**(3): 243-284 (1980).

Baldauf, W. and Knapp, H.: *Measurements of diffusivities in liquids by the dispersion method*. Chem. Eng. Sci. **38**(7): 1031-1037 (1983).

Bollen, A. M.: *Collected Tales on Mass Transfer in Liquids*. Dissertation. University Groningen, Groningen (1999).

Harris, K. R., Goscinska, T., and Lam, H. N.: *Mutual Diffusion Coefficients for the Systems Water-Ethanol and Water-Propan-1-ol at 25 °C*. J. Chem. Soc. Faraday Trans. **89**(12): 1969-1974 (1993).

Krishnamurthy, R. and Taylor, R.: *A Nonequilibrium Stage Model of Multicomponent Separation Processes*. AIChE **31**: 449-456 (1985).

Leaist, D. G.: *Ternary diffusion coefficients of 18-Crown-6 Ether-KCl-Water by direct least-squares analysis of Taylor dispersion measurements*. J. Chem. Soc. Faraday Trans. **87**(4): 597-601 (1991).

Pratt, K. C. and Wakeham, W. A.: *The mutual diffusion coefficient of ethanol-water mixtures: determination by a rapid, new method*. Proc. R. Soc. London, Series A **336**: 363-406 (1974).

Rutten, P. W. M.: Diffusion in Liquids. Delft University Press, Delft (1992).

Sanchez, V. and Oftadeh, H.: *Restricted Diffusion in Binary Organic Liquid Mixtures*. J. Chem. Eng. Data **22**(2): 123-125 (1977).

Taylor, G.: *Dispersion of soluble matter in solvent flowing slowly through a tube*. Proc. R. Soc. London, Series A **219**: 186-203 (1953).

Taylor, G.: *Conditions under which dispersion of a solute in a stream of solvent can be used to measure molecular diffusion*. Proc. R. Soc. London, Series A **225**: 473-477 (1954).

Taylor, R. and Krishna, R.: Multicomponent Mass Transfer. John Wiley & Sons, New York (1993).

Ven-Lucassen, I. M. J. J. v. d., Kieviet, F. G., and Kerkhof, P. J. A. M.: *Fast and convenient implementation of the Taylor dispersion method*. J. Chem. Eng. Data **40**(2): 407-411 (1995).

Appendix

A Experimental Results of the Taylor Dispersion Experiments

The following Tables contain the experimental results obtained from Taylor dispersion experiments. Only the average *D* values are reported. The mole fractions given in the Tables refer to the alcohol component.

Table A1. Diffusion coefficients *D* of alcohol (1) + carbon tetrachloride (2) mixtures.

		x_1								
		0.0	0.03	0.1	0.3	0.5	0.7	0.9	0.97	1.0
	T/°C	$D/(10^{-9}\,m^2s^{-1})$								
EtOH	25	1.90	1.06	0.82	0.64	0.73	0.99	1.32	1.43	1.47
	30	2.15	1.60	0.99	0.83	0.87	1.14	1.45	1.56	1.61
	35	2.24	1.80	1.10	0.95	0.99	1.28	1.60	1.76	1.82
1-PropOH	25	1.61	0.83	0.61	0.39	0.46	0.66	0.83	0.91	0.95
1-ButOH	25	1.47	0.7	0.50	0.29	0.32	0.54	0.65	0.69	0.72
	35	1.74	0.93	0.71	0.52	0.56	0.65	0.80	0.89	0.94

Table A2. Diffusion coefficients *D* of alcohol (1) + toluene (2) mixtures.

		x_1								
		0.0	0.03	0.1	0.3	0.5	0.7	0.9	0.97	1.0
	T/°C	$D/(10^{-9}\,m^2s^{-1})$								
EtOH	25	3.12	2.94	2.41	1.22	0.98	1.16	1.55	1.70	1.74
	35	3.61	3.40	2.90	1.70	1.35	1.59	1.89	2.04	2.11
1-PropOH	25	2.67	2.37	1.81	1.00	0.85	1.01	1.28	1.40	1.46

Table A3. Diffusion coefficients *D* of alcohol (1) + hexane mixtures.

		x_1								
		0.0	0.03	0.1	0.3	0.5	0.7	0.9	0.97	1.0
	T/°C	$D/(10^{-9}\,m^2s^{-1})$								
EtOH	25	5.74	4.07	2.41	1.54	1.30	1.30	1.43	1.54	1.60
1-PropOH	25	5.20	3.37	2.17	1.38	1.15	1.08	1.09	1.03	1.02

Table A4. Diffusion coefficients *D* of alcohol (1) + cyclohexane (2) mixtures.

		x_1								
		0.0	0.03	0.1	0.3	0.5	0.7	0.9	0.97	1.0
	T/°C	$D/(10^{-9}\,m^2s^{-1})$								
EtOH	25		0.99	0.77	0.43	0.46	0.73	1.23	1.41	
1-PropOH	25		0.83	0.66	0.39	0.42	0.65	1.00	1.15	

3 Binary Vapour-Liquid-Equilibrium Predictions with COSMOSPACE

The applicability of COSMOSPACE to binary VLE predictions is thoroughly investigated. For this purpose a new method is developed to determine the required molecular parameters such as segment types, areas, volumes, and interaction parameters. So-called sigma profiles form the basis of this approach which describe the screening charge densities appearing on a molecule's surface. To improve the prediction results a constrained two-parameter fitting strategy is also developed. These approaches are crucial to guarantee the physical significance of the segment parameters. Finally, the prediction quality of this approach is compared to the findings of the Wilson model, UNIQUAC, and the a priori predictive method COSMO-RS for a broad range of thermodynamic situations. The results show that COSMOSPACE yields results of similar quality compared to the Wilson model, while both perform much better than UNIQUAC and COSMO-RS.

3.1 Introduction

Synthesis, design, and optimization of the various processes in the chemical engineering world are usually done with process simulation tools. During such simulations, mass and energy balances must be solved simultaneously and the accuracy of such calculations mainly depends on the proper choice of sophisticated models for pure component and mixture properties. One of the major issues in the design of thermal separation processes is the accurate representation of vapour-liquid equilibria (VLE). At pressures which are not too high, vapour phase nonidealities may be omitted, and the problem of phase equilibrium calculations using the γ-ϕ-concept may be reduced to the determination of activity coefficients γ_i also neglecting the Poynting correction.

$$x_i \gamma_i P_i^0 = y_i P \tag{3.1}$$

To solve the stated problem many theories of the liquid state were developed. Guggenheim's quasi-chemical approximation (Guggenheim 1952) is one such theoretical picture. In this theory a fluid mixture may be regarded as a regular lattice with all lattice sites occupied by single hard core molecules, which interact with their entire surface with the next nearest neighbours. These interactions cause the molecules to preferably order themselves with respect to their adjacent neighbours on the lattice, which results in a deviation between macroscopic (overall) and microscopic (local) composition. Famous excess Gibbs energy models, which originate from this concept are the Wilson equation (Wilson 1964), the NRTL model (Renon and Prausnitz 1968), UNIQUAC (Abrams and Prausnitz 1975; Maurer and Prausnitz 1978), UNIFAC (Fredenslund et al. 1975), or its modified forms (Gmehling and Weidlich 1986; Larsen et al. 1987; Weidlich and Gmehling 1987).

Guggenheim's idea was refined by Barker (Barker 1952), who divided the molecular surface area into as many contact sites as there are nearest neighbours and introduced the concept of functional groups, which are directly related to the contact sites. Kehiaian et al. (Kehiaian et al. 1978), for example, used this concept to derive their DISQUAC model.

A further refinement was recently proposed with the GEQUAC model (Egner et al. 1997, 1999; Ehlker and Pfennig 2002), a group contribution method for polar and associating liquid mixtures. Here, the carbonyl group and the hydroxyl group are divided into donor and acceptor surface parts to account for chemical interaction effects such as hydrogen bonding in a more detailed way. The numerous parameters for the enthalpic and entropic contributions to the interaction parameters, as well as the surface areas of the different functional groups, were fitted to a large VLE database. In the present form this method is only suitable for alkane systems with ketones or alcohols as second component.

With the increasing performance of computers a new generation of models has become more popular. A priori predictive methods such as COSMO-RS (Klamt 1995; Klamt and Eckert 2000; Eckert and Klamt 2002), or its slight modification COSMO-SAC (Lin and Sandler 2002), are based on quantum chemical COSMO calculations to obtain screening charges of a molecule in a perfect conductor. Then, a statistical thermodynamic model is applied to the screening charge density function, called a sigma profile, to compute e.g. activity coefficients. In this theory it is assumed that molecules may be regarded as a collection of surface segments, which results in an ensemble of pairwise interacting surface pieces with type-specific surface charges. Hence, an even more realistic picture of association effects such as hydrogen bonding can be drawn.

On the basis of COSMO-RS a multicomponent activity coefficient model called COSMOSPACE (Klamt et al. 2002) was developed, which may be used independently of its origin. In the original COSMOSPACE article by Klamt et al. (Klamt et al. 2002) it is shown that this model yields excellent agreement with lattice Monte Carlo simulations, whereas lattice models such as UNIQUAC fail. Additionally, it is explained by means of some examples how this model may be used to predict VLE of binary mixtures.

In the present communication a critical assessment of this new g^E-expression is conducted. The next section provides the underlying theory of this model, followed by an explanation of how the model and molecular parameters are determined. Then the COSMOSPACE results obtained for several phase equilibrium calculations are compared with those from the Wilson model and UNIQUAC. Furthermore, the results of COSMO-RS calculation are also given to allow a comparison between COSMOSPACE and its theoretical basis. Finally, some concluding remarks are given.

3.2 The COSMOSPACE Model

Likewise to the UNIQUAC or the GEQUAC model, two parts contribute in the COSMOSPACE model to the activity coefficients γ_i of a species *i*.

$$\ln\gamma_i = \ln\gamma_i^C + \ln\gamma_i^R \tag{3.2}$$

For the entropic part which accounts for geometrical restraints the Staverman-Guggenheim expression is used in a modified form[1] as is applied in Mod. UNIFAC (Gmehling and Weidlich 1986; Weidlich and Gmehling 1987)

$$\ln\gamma_i^C = 1 - \phi_i^{'} + \ln\phi_i^{'} - \frac{z}{2}q_i\left(1 - \frac{\phi_i}{\theta_i} + \ln\frac{\phi_i}{\theta_i}\right) \tag{3.3}$$

whereas the variables x_i, ϕ_i, $\phi_i^{'}$, and θ_i denote the mole fraction, the two volume fractions and the surface area fraction of component *i* in the mixture, and *z* is the coordination number of the lattice. The volume and surface area fractions are defined with respect to the relative volume r_i and surface area q_i and with c_{comb} as an adjustable parameter.

---

[1] In the article by Klamt et al. (Klamt et al. 2002) the original Staverman-Guggenheim approach is used which may be obtained by setting c_{comb}=1 in (3.4).

$$\phi_i' = \frac{x_i r_i^{c_{\text{comb}}}}{\sum_j x_j r_j^{c_{\text{comb}}}} \qquad \phi_i = \frac{x_i r_i}{\sum_j x_j r_j} \qquad \Theta_i = \frac{x_i q_i}{\sum_j x_j q_j} \tag{3.4}$$

For the derivation of the second contribution of (3.2), the assumption is made that molecular interactions may be computed from the partition sum of an ensemble of pairwise interacting surface segments, which leads to an expression similar to that used in UNIFAC.

$$\ln \gamma_i^R = \sum_\nu n_i^\nu \left(\ln \gamma^\nu - \ln \gamma_i^\nu \right) \tag{3.5}$$

The residual activity coefficient γ_i^R is now a function of n_i^ν, the number of segments of type ν on molecule *i*, γ^ν, the segment activity coefficient of type ν in the mixture, and γ_i^ν, the segment activity coefficient of type ν in pure liquid *i*. In contrast to UNIFAC, the segment activity coefficients are computed by an iterative procedure, which may be easily solved by repeated substitution. Starting with all segment activity coefficients set to unity on the right-hand side of (3.6), the final result automatically satisfies the Gibbs-Duhem equation.

$$\frac{1}{\gamma^\nu} = \sum_\mu \tau_{\mu\nu} \theta^\mu \gamma^\mu \tag{3.6}$$

For physical consistency the interaction parameter $\tau_{\mu\nu}$ is given by a symmetric matrix whose elements are defined as

$$\tau_{\mu\nu} = \exp\left[-\frac{u_{\mu\nu} - 1/2\left(u_{\mu\mu} + u_{\nu\nu}\right)}{RT} \right] \tag{3.7}$$

$u_{\mu\nu}$ refers to the segment interaction energy of types μ and ν. The relative number of segments of type ν is defined by

$$\theta^\nu = \frac{n^\nu}{n} \tag{3.8}$$

with

$$n^\nu = \sum_i N_i n_i^\nu \tag{3.9}$$

as the number of segments of type ν and

$$n = \sum_i N_i n_i \tag{3.10}$$

as the total number of segments in the mixture. The number of molecules of species i in the system is $N_i = N x_i$, and the total number of surface segments on a molecule i is given by

$$n_i = \sum_\nu n_i^\nu = \frac{A_i}{a_{\text{eff}}} \tag{3.11}$$

A_i equals the total surface area of molecule i, and a_{eff} is an effective contact area, which must be considered as an adjustable parameter.

For the special case of a binary mixture the model equations can be simplified. If in a binary mixture each molecule consists only of one type of segment (which equals the idea of UNIQUAC) or both molecules are composed of the same two types of segments, (3.6) may be solved algebraically. Klamt et al. (Klamt et al. 2002) referred to these special cases as the *Homogeneous Double-Binary COSMOSPACE* model and the *Nonhomogeneous Double-Binary COSMOSPACE* model, respectively.

The derivatives of (3.6), which may be used for the computation of, e.g., the excess enthalpy or thermodynamic correction factors, may be calculated from a set of linear equations.

$$0 = b_\nu + \sum_\mu C^*_{\nu\mu} d_\mu \tag{3.12}$$

The elements of the symmetric matrix $C^*_{\nu\mu}$ and the vectors b_ν and d_ν are defined according to the following equations:

$$C^*_{\nu\mu} = \begin{cases} 1 + C_{\nu\mu} & \forall \quad \nu = \mu \\ C_{\nu\mu} & \forall \quad \nu \neq \mu \end{cases} \tag{3.13}$$

$$C_{\nu\mu} = \sqrt{\theta^\nu}\gamma^\nu \tau_{\nu\mu} \gamma^\mu \sqrt{\theta^\mu} \tag{3.14}$$

$$b_\nu = \sqrt{\theta^\nu}\gamma^\nu \sum_\mu \gamma^\mu \tau_{\nu\mu} \partial\theta^\mu + \sqrt{\theta^\nu}\gamma^\nu \sum_\mu \gamma^\mu \theta^\mu \partial\tau_{\nu\mu} \tag{3.15}$$

$$d_\nu = \sqrt{\theta^\nu}\,\partial \ln \gamma^\nu \tag{3.16}$$

Note that the derivatives in b_ν are directly available and that d_ν contains the desired derivatives of the segment activity coefficients, from which the derivatives of γ_i may be deduced. A formal derivation of this technique may be found in Appendix D of the COSMOSPACE article (Klamt et al. 2002).

The aforementioned model equations suggest that the theoretical derivation of COSMOSPACE is superior to other excess Gibbs energy models. First of all, COSMOSPACE is thermodynamically consistent which is in contrast to models like the Wilson equation or UNIQUAC. Second, these equations may be derived as special cases of the more general COSMOSPACE approach. And, last but not least, the COSMOSPACE model parameters may also retain their physical significance if determined appropriately.

3.3 Estimation of Model and Component Parameters

One alternative to determine the required COSMOSPACE model parameters is to follow the approaches other excess Gibbs energy models used to obtain their parameters. In principle, r_i and q_i may be obtained from van der Waals cavities or computed from UNIFAC groups (Fredenslund et al. 1975). z may be assumed to be 10 and a_{eff}, n_i^ν, and $u_{\mu\nu}$ (or the resulting interaction parameter $\tau_{\mu\nu}$) may be fitted to experimental data. In this way, for example, a new, theoretically consistent group contribution method may be developed. However, at this point one question arises: How many and what kinds of segment types belong to a specific molecule? This question may be answered by applying the functional group concept as is done in UNIFAC or by making use of sigma profiles, which form the basis of the calculations in the a priori predictive methods COSMO-RS and COSMO-SAC. Sigma profiles may be explained best in terms of the distribution function, $p(\sigma)$, which describes the amount of surface in the ensemble, having a screening charge density between σ and $\sigma + \mathrm{d}\sigma$. Since interaction effects between surface parts of molecules are mainly caused by attraction and repulsion forces, which depend on the local polarities and electron

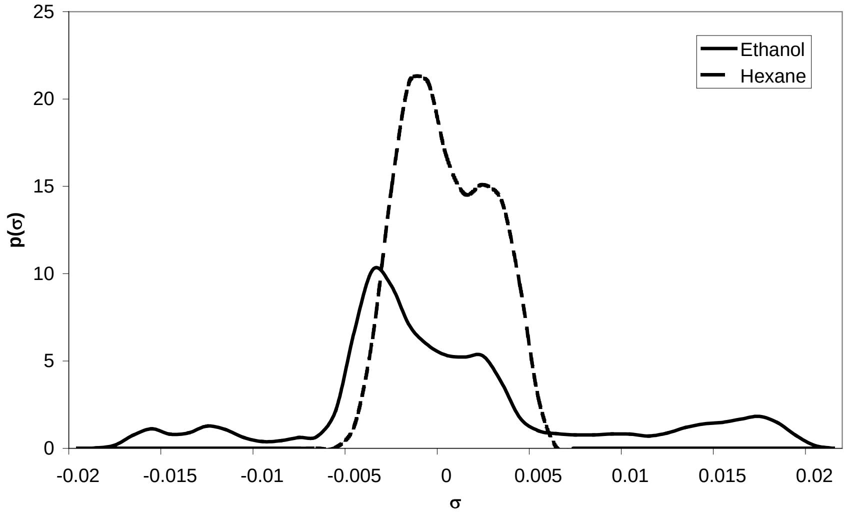

Figure 3.1. Sigma profiles of ethanol and hexane.

densities, the concept of the screening charge densities is to be preferred throughout this work. In the following it is, therefore, explained in detail how the desired molecular parameters may be derived from such profiles. Note that this technique is not restricted to binary mixtures but also can be used to determine the parameters of multicomponent systems. Further explanations and more examples on the interpretation of sigma profiles may be found elsewhere (Klamt and Eckert 2000; Eckert and Klamt 2002).

In Figure 3.1 the sigma profiles of an ethanol and a hexane molecule are depicted. Note that positive polarities of a molecule cause negative screening charges, while negative polarities cause positive screening charges. As may be seen from the graph the hexane molecule consists of two peaks, one slightly negative and one slightly positive alkyl peak separated at $\sigma = 0$. These peaks are caused by the difference in electronegativity of the composing atoms C and H. Instead, ethanol shows four peaks. Two of them result from the hydroxyl group of the alcohol molecule, one donor peak at $\sigma = -0.015$ e Å^{-2} and one acceptor peak at $\sigma = 0.015$ e Å^{-2}. The other two peaks around $\sigma = 0$ e Å^{-2} are attributed to the screening charges of the alkyl group and are, compared to the hexane peaks, slightly shifted toward the negative side due to the additional polarization by the neighbouring hydroxyl group. The sigma profiles of the two components, therefore, suggest to model hexane by two and ethanol by four segment types. Each of these segment types is unequivocally characterized by its segment area and its corresponding averaged screening charge. Since the integral of the $p_i(\sigma)$-function yields the total molecular surface area A_i of species i, the area under a single peak bounded by σ_{lb} and σ_{ub} provides the surface area A_i^ν of that kind of segment.

$$A_i^\nu = \sum\nolimits_{\sigma_{\text{lb}}}^{\sigma_{\text{ub}}} p_i(\sigma) \tag{3.17}$$

The averaged screening charge σ_i^ν corresponding to this peak may be computed from a weighted distribution function.

$$\sigma_i^\nu = \frac{1}{A_i^\nu} \sum\nolimits_{\sigma_{\text{lb}}}^{\sigma_{\text{ub}}} \sigma\, p_i(\sigma) \tag{3.18}$$

In total the sigma profiles of 26 chemical species were evaluated. The final results can be found in Table 3.1.

Table 3.1. Segment parameters of chemical species.

Components	Molecular parameters		Segment parameters							
	area	volume	sigma	area	lb	ub	sigma	area	lb	ub
	[A^2]	[A^3]	[e/A^2]	[A^2]	[e/A^2]	[e/A^2]	[e/A^2]	[A^2]	[e/A^2]	[e/A^2]
Alkanes										
Pentane	137.165	124.395	-1.697E-03	72.7330	-0.006	0	1.915E-03	64.4320	0	0.006
Hexane	156.896	145.683	-1.733E-03	83.8220	-0.006	0	1.987E-03	73.0740	0	0.006
Heptane	176.891	167.634	-1.864E-03	94.6940	-0.006	0	2.147E-03	82.1970	0	0.006
Octane	196.840	189.543	-2.695E-08	105.5480	-0.006	0	3.116E-08	91.2920	0	0.006
Nonane	216.795	211.314	-1.793E-03	116.5120	-0.006	0	2.083E-03	100.2830	0	0.006
Decane	236.775	233.315	-1.774E-03	127.4465	-0.006	0	2.068E-03	109.3285	0	0.006
Undecane	257.076	255.973	-1.761E-03	138.3480	-0.006	0	2.052E-03	118.7280	0	0.006
Dodecane	276.641	276.831	-1.750E-03	149.2100	-0.006	0	2.049E-03	127.4310	0	0.006
Hexadecane	356.856	366.403	-1.715E-03	192.7925	-0.006	0	2.015E-03	164.0635	0	0.006
Cycloalkanes										
Cyclohexane	131.487	126.302	-2.114E-03	70.0380	-0.006	0.000	2.410E-03	61.4490	0.000	0.006
X-Alkanes										
CCl4	134.206	128.392	-3.124E-03	49.6150	-0.01	0	1.832E-03	84.5910	0	0.007
Alcohols										
Methanol	67.561	48.427	-1.295E-02	7.6180	-0.019	-0.01	-2.652E-03	34.5860	-0.009	0
			1.361E-03	13.6320	0	0.01	1.466E-02	11.7250	0.011	0.021
Ethanol	88.110	69.985	-1.391E-02	7.1210	-0.019	-0.01	-3.257E-03	45.7730	-0.009	0
			3.005E-03	23.7050	0	0.01	1.537E-02	11.5110	0.011	0.021
Propanol	108.046	91.830	-1.275E-02	7.1430	-0.019	-0.01	-3.212E-03	57.0480	-0.009	0
			3.346E-03	32.4620	0	0.01	1.455E-02	11.3930	0.011	0.021
1-Butanol	128.142	113.948	-1.167E-02	7.0820	-0.019	-0.01	-3.471E-03	69.1950	-0.009	0
			4.070E-03	40.3950	0	0.01	1.381E-02	11.4700	0.011	0.021
Pentanol	148.200	135.482	-1.423E-02	7.4780	-0.019	-0.01	-2.369E-03	80.2435	-0.009	0
			2.456E-03	49.0835	0	0.01	1.544E-02	11.3950	0.011	0.021
Hexanol	168.311	157.799	-1.425E-02	7.4830	-0.019	-0.01	-2.269E-03	91.3260	-0.009	0
			2.367E-03	58.1060	0	0.01	1.547E-02	11.3960	0.011	0.021
Heptanol	188.174	179.441	-1.423E-02	7.4750	-0.019	-0.01	-2.194E-03	102.3580	-0.009	0
			2.316E-03	66.9450	0	0.01	1.544E-02	11.3960	0.011	0.021
Octanol	208.123	201.441	-1.423E-02	7.4840	-0.019	-0.01	-2.137E-03	113.1400	-0.009	0
			2.265E-03	76.1010	0	0.01	1.544E-02	11.3980	0.011	0.021
2-Propanol	106.438	91.697	-1.378E-02	6.8360	-0.019	-0.01	-3.070E-03	55.2805	-0.009	0
			2.947E-03	34.1955	0	0.013	1.611E-02	10.1260	0.013	0.022
2-Butanol	125.819	113.839	-1.384E-02	6.8020	-0.019	-0.01	-2.744E-03	64.8765	-0.009	0
			2.880E-03	45.2625	0	0.013	1.597E-02	8.8780	0.013	0.022
Ketones										
Acetone	102.682	86.349	-5.152E-03	50.4870	-0.009	-0.002	-8.835E-04	15.7060	-0.002	0
			6.680E-03	29.4885	0	0.005	1.100E-02	7.0000	0.005	0.019
Aromatics										
Benzene	121.371	109.980	-4.100E-03	59.7980	-0.009	0	3.982E-03	61.5730	0	0.008
Toluene	140.550	131.815	-5.532E-03	36.7495	-0.009	-0.004	-2.238E-03	34.3500	-0.004	0
			1.990E-03	33.9655	0	0.004	5.991E-03	35.4850	0.004	0.01
o-Xylene	156.113	152.381	-4.824E-03	51.0140	-0.009	-0.003	-1.642E-03	29.1585	-0.003	0
			1.869E-03	41.4425	0	0.004	6.276E-03	34.4980	0.004	0.01
p-Xylene	159.576	153.546	-4.740E-03	50.3760	-0.009	-0.003	-1.693E-03	31.5245	-0.003	0
			1.918E-03	44.1055	0	0.004	6.182E-03	33.5700	0.004	0.01

To compute the interaction parameters $\tau_{\mu\nu}$ from the averaged sigma values, the interaction energy concept of COSMO-RS (Klamt and Eckert 2000) may be consulted. In this concept, electrostatic interactions $u_{\mu\nu}^{\text{misfit}}$ (called “misfit energy” by the authors) and hydrogen-bonding interactions $u_{\mu\nu}^{\text{hb}}$ contribute to the pair interaction energy $u_{\mu\nu}$, which is used in (3.7) for the calculation of $\tau_{\mu\nu}$.

$$\begin{aligned} u_{\mu\nu} &= u_{\mu\nu}^{\text{misfit}} + u_{\mu\nu}^{\text{hb}} \\ &= a_{\text{eff}} \frac{\alpha'}{2} (\sigma_\mu + \sigma_\nu)^2 + a_{\text{eff}} c_{\text{hb}} \max[0, \sigma_{\text{acc}} - \sigma_{\text{hb}}] \min[0, \sigma_{\text{don}} + \sigma_{\text{hb}}] \end{aligned} \tag{3.19}$$

α' is a constant for the misfit energy, c_{hb} is a strength coefficient, and σ_{hb} is a cutoff value for hydrogen bonding. σ_{acc} and σ_{don} refer to the larger and smaller value of σ_{μ} and σ_{ν}, respectively. Once the model parameters are defined this method readily allows the computation of activity coefficients without any molecular fitting parameters. Since the sigma profiles of many species were approximated by only two or four peaks, the resulting activity coefficients show larger deviations than the core model COSMO-RS or other well-established methods. Nevertheless, this method readily gives rough estimates of the thermodynamic behaviour of fluid systems. To improve the prediction quality the following fitting strategy was developed.

From simple consideration it is obvious that the segment types with the most negative or positive screening charges largely contribute to the overall interactions in a system. Therefore, the most negative sigma value of each component was chosen as an adjustable parameter, which yields two fitting parameters for a binary mixture. The parameters were constrained by the lower and upper screening charges σ_{lb} and σ_{ub} by which the corresponding peak is limited. An additional constraint was imposed on the optimization procedure by the electroneutrality condition of the overall surface charge of a molecule i.

$$\sum_{\nu} \sigma_i^{\nu} A_i^{\nu} = 0 \tag{3.20}$$

A change in the most negative screening charge affects at least one other screening charge on that particular molecule to fulfill this condition. From the same consideration as aforementioned it was decided to recalculate the value of the segment type with the most positive screening charge on molecule i by means of (3.20), also making use of the lower and upper bounds on that peak. To clarify this treatment consider ethanol as an example molecule. As was previously stated the donor-OH group causes the most negative peak of this molecule. The value of the average screening charge of this type of segment is given in Table 3.1 to be –0.01391 e A^{-2}, which serves as an initial guess for the optimization routine. The lower and upper sigma constraints are –0.019 e A^{-2} and –0.01 e A^{-2}, respectively. According to the defined treatment a change in the sigma-value of the donor-OH group causes a change in the sigma-value of the acceptor-OH group, the most positive segment type of the ethanol molecule whose value has to be recalculated from (3.20), obeying the upper and lower sigma-bounds of that segment type. The original sigma-value is 0.01537 e A^{-2}, and the values of the corresponding lower and upper limits are 0.011 e A^{-2} and 0.021 e A^{-2}, respectively. In the same way the hexane molecule may be modeled. Here, the surface charge of the negatively polarized alkyl segment serves as a fitting parameter, while the charge of the positively polarized alkyl segment must be recalculated to fulfill the electroneutrality constraint.

In principle, the technique presented here is not limited to just one single fitting parameter per molecule. For the ethanol molecule, for example, two fitting parameters are also considerable, i.e., the values of the two segment types with the negative surface charges. To obey (3.20) at least one of the two positive screening charge values needs to be adjusted. For a single molecule the maximum number of adjustable parameters is given by the total number of segment types minus one.

For a consistent use of the molecular parameters within the combinatorial and the residual part, the values of r_i and q_i must be calculated from the surface area A_i and the volume V_i of molecule i as obtained from COSMO-RS. Values for A_i and V_i are also provided in Table 3.1. The reference values for the surface area and the volume were adopted from COSMO-SAC with A_{ref} =55.6973 Å^2 and V_{ref} =37.7471 Å^3.

Finally, the model parameters were taken from COSMO-RS as initial guesses and further adjusted from an overall fitting of all sets of VLE-data considered in this work. For a_{eff}, c_{hb}, and c_{comb} new values were obtained, and the others remain unchanged. The effective contact area a_{eff}

is 7.7 Å^2, the electrostatic misfit energy α' equals 6635 kJ mol^{-1} Å^2 e^{-2}, the value for the strength coefficient for hydrogen bonding c_{hb} is 500 kJ mol^{-1} Å^2 e^{-2}, the cutoff value for hydrogen bonding is still σ_{hb} =0.0084 e Å^{-2}, the constant in the combinatorial part amounts to c_{comb} =0.2, and z =10 is the value for the coordination number.

3.4 Choice of VLE Data

A broad range of chemical mixtures is considered reflecting the various types of thermodynamic behaviour, i.e., ideal state to highly nonideal state including also association effects. The main focus of this work is on binary mixtures consisting of alkanes, cycloalkanes, halogenated alkanes (X-alkanes), aromatics, ketones, and alcohols. All experimental data sets were exclusively taken from the DECHEMA data series. Only binary isothermal Pxy data passing the thermodynamic consistency tests proposed by Redlich and Kister (Redlich and Kister 1948), Herington (Herington 1947), and van Ness et al. (van Ness et al. 1973) were used to compare the results of the COSMOSPACE model with the findings of UNIQUAC, the Wilson equation, and the quantum-chemical approach COSMO-RS. The vapour-liquid equilibria were computed according to (3.1) with vapour pressures calculated from the Antoine equation with parameters provided by the DECHEMA data series. The required interaction parameters were fitted to the experimental data in a least-squares analysis using the sum of relative deviations in the activity coefficients as objective function

$$F = \sum_{i=1}^{2} \sum_{j=1}^{N} \left(\frac{\gamma_{i,j}^{\exp} - \gamma_{i,j}^{\mathrm{calc}}}{\gamma_{i,j}^{\exp}} \right)^2 \tag{3.21}$$

with N as the number of experimental data points. Systems with more than one data set were fitted simultaneously to obtain a unique set of interaction parameters. The COSMO-RS calculations were performed with the COSMOTherm software package (Eckert and Klamt 2003). The sum of relative deviations in the vapour mole fractions was finally used as the criterion to assess the various g$^{\mathrm{E}}$-expressions

$$\mathrm{dev}/\% = 100 \sum_{j=1}^{N} \left| \frac{y_{1,j}^{\exp} - y_{1,j}^{\mathrm{calc}}}{y_{1,j}^{\exp}} \right| \tag{3.22}$$

whereas 1 refers to the first component in the mixture.

3.5 Results

In total 91 data sets with 1202 data points were investigated. Figure 3.2 provides an overview of all systems under consideration. The numbers in brackets following the mixture type refer to the total number of systems in this group and the total number of data points, respectively. An additional asterisk means that some of the data sets in this group were fitted simultaneously. To allow a better visual comparison of the models, relative deviations larger than 6 % as were computed with COSMO-RS, are omitted in this figure. The detailed results are summarized in the Appendix. A number in brackets in the first column of that table indicates the number of data sets used for this case. The last four columns provide the relative mean deviations in the vapour phase mole fractions, as were computed with the Wilson equation, UNIQUAC, COSMOSPACE, and COSMO-RS. For systems with more than one data set, only the average values of all sets are displayed there.

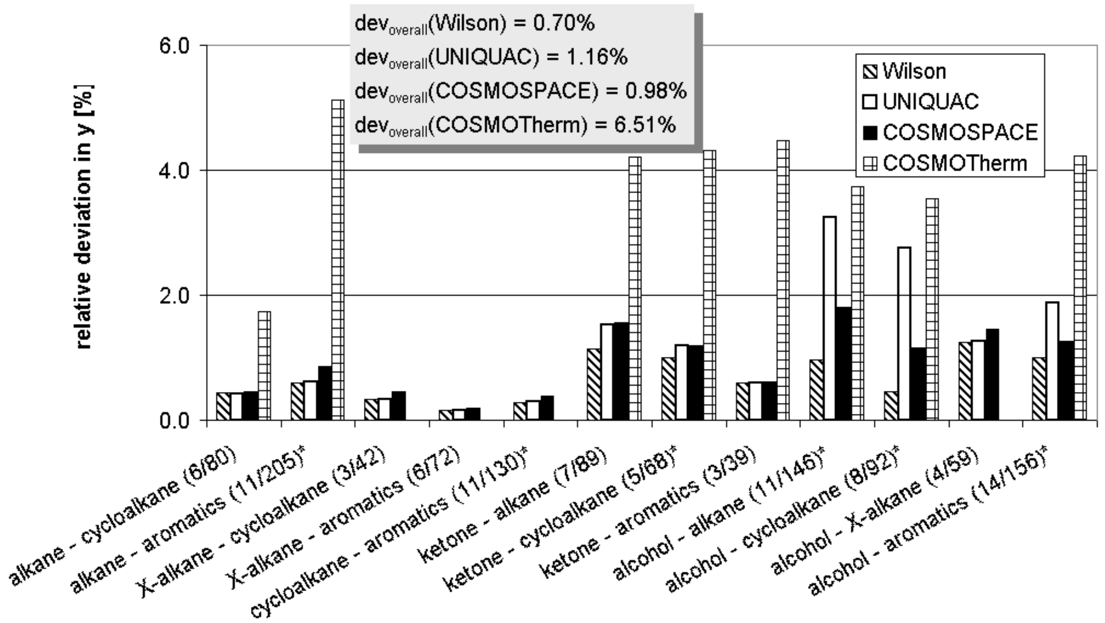

Figure 3.2. Relative deviations in y for all mixture classes investigated.

As may be seen from the graph, the semiempirical approaches' maximum relative deviation is below 3.5 %, and the average relative deviation is around 1 %. In contrast, the average relative deviation of the COSMO-RS model is 6.51 % which can be considered good for a quantum-chemical approach. As expected, systems consisting of nonpolar or only slightly polar, nonassociating components show the lowest deviations with approximately 0.5 % (first five groups) for the semiempirical models. Though the COSMOSPACE results are slightly worse than the Wilson and UNIQUAC predictions, they are still below 1% maximum deviation. Surprisingly, for these mixture types the COSMO-RS approach shows the largest deviations (up to 16 % for the mixture type X-alkane – aromatics). In Figure 3.3 the activity coefficient results and the corresponding phase diagram are exemplarily shown for the system hexane – cyclohexane at 35 °C. All models but COSMO-RS yield excellent agreement between experimental data and predicted values. COSMO-RS shows some deficiencies to predict the slight increase in activity coefficients.

In nonassociating systems with a polar component (ketone systems) the model fits of Wilson, UNIQUAC, and COSMOSPACE result in larger deviations between experimental data and computed values. One reason might be that the phase behaviour is not solely dominated by the

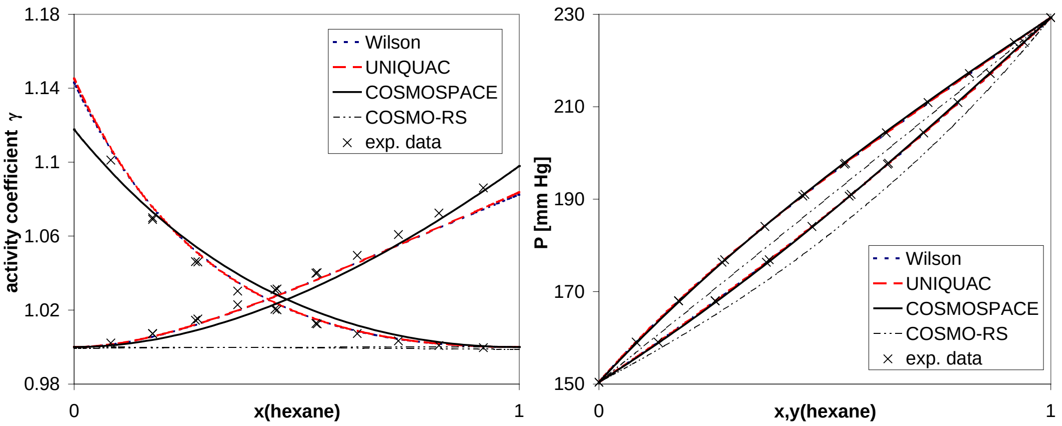

Figure 3.3. Activity coefficient results (left) and phase diagram (right) for the system hexane – cyclohexane at 35 °C.

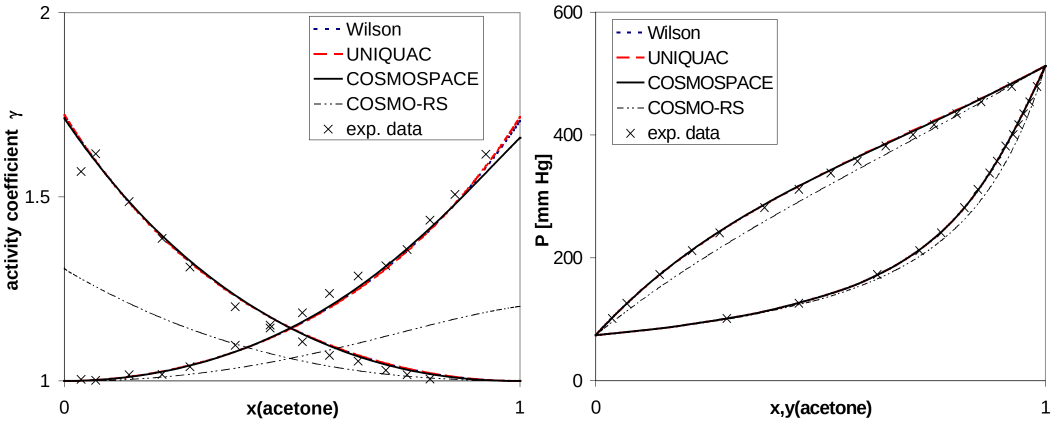

Figure 3.4. Activity coefficient results (left) and phase diagram (right) for the system acetone – toluene at 35 °C.

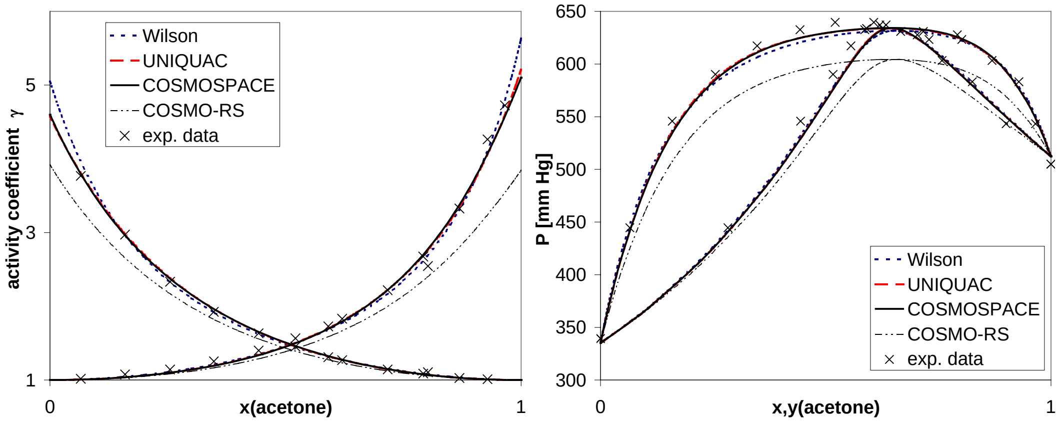

Figure 3.5. Activity coefficient results (left) and phase diagram (right) for the system acetone – hexane at 45 °C.

weak van der Waals interactions but also by some self-associating tendency of acetone due to the strong polarization of the keto-group. Only recently it was, therefore, suggested to model acetone like a self-associating component (von Solms et al. 2004). Both COSMOSPACE and UNIQUAC yield the same prediction accuracy for this mixture class, while the Wilson fits are somewhat better. On average, the predictions are still good as may be judged from the results depicted in the following figures. Figure 3.4 presents the results of the system acetone – toluene at 45 °C. This mixture shows only minor deviations from thermodynamic ideality and can, therefore, be properly reflected by the three semiempirical models. In contrast, the thermodynamics of the other example, acetone – hexane at 45 °C, is characterized by an azeotropic point (see Figure 3.5). Considering the slight scatter in the experimental values qualitatively good results can be obtained, also for the prediction of the azeotrop. COSMO-RS also predicts the azeotrop composition properly but underestimates the corresponding pressure.

The last four classes depicted in Figure 3.2 show the results of thermodynamically highly nonideal binary mixtures, in which association and solvation effects dominate the molecular interactions. As expected for this case, the predictions of the semiempirical approaches show the largest deviations from reality as can also be seen from the final results of the systems hexane – ethanol, ethanol – cyclohexane, and ethanol – benzene displayed in Figures 3.6–3.8. Especially the inaccuracies of the UNIQUAC predictions are striking. As the activity coefficient plots clearly demonstrate, UNIQUAC is incapable of describing the activity coefficients in the diluted alcohol region properly. Instead, these values are largely underestimated, which finally results in incorrect predictions of liquid-liquid phase separations. In contrast, Wilson and COSMOSPACE allow a good representation of the activity coefficient data over the whole concentration range. They differ only slightly in the region of infinite dilution. While the Wilson

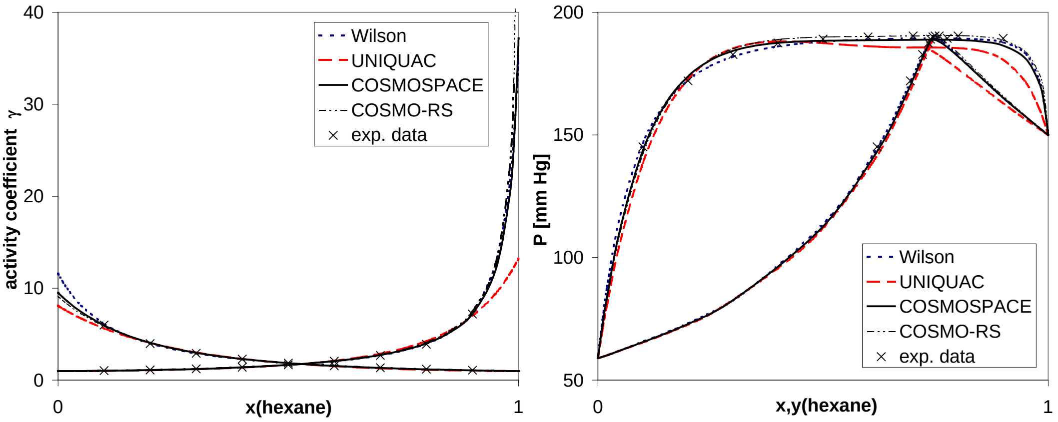

Figure 3.6. Activity coefficient results (left) and phase diagram (right) for the system hexane – ethanol at 25 °C.

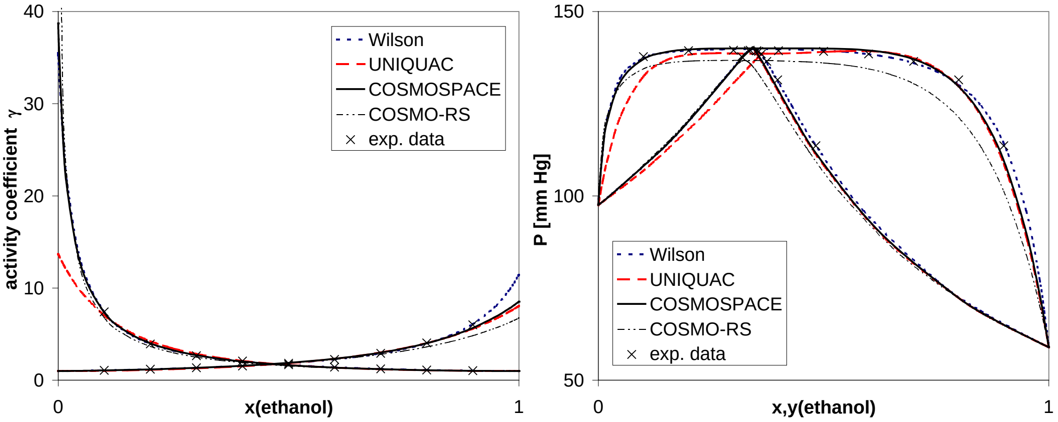

Figure 3.7. Activity coefficient results (left) and phase diagram (right) for the system ethanol – cyclohexane at 25 °C.

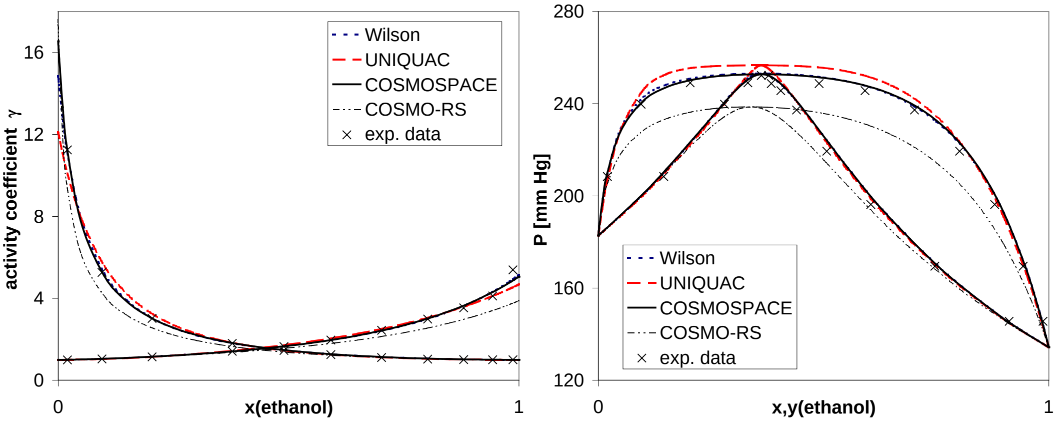

Figure 3.8. Activity coefficient results (left) and phase diagram (right) for the system ethanol – benzene at 40 °C.

predictions are better for the hexane and cyclohexane activity coefficients at infinite dilution, COSMOSPACE is superior to Wilson if the alcohol is infinitely diluted. However, these small differences do not have an impact on the accuracy of the predicted phase behaviour as the Pxy-plots demonstrate. Similar prediction results can be obtained for the other systems investigated. As the figures show, qualitatively good results can also be obtained with the COSMO-RS model. Especially the ethanol – hexane system presented in Figure 3.6 shows high resemblance between the prediction and the experimental data. Again, larger deviations of COSMO-RS can be found for alcohol – X-alkane mixtures.

On average, the Wilson results are significantly better than the UNIQUAC predictions but it must also be kept in mind that the Wilson method cannot be used to predict miscibility gaps, which, therefore, limits its range of applicability. The COSMOSPACE approach is with an average deviation of 1.42 % worse than Wilson but still much better than UNIQUAC. Additionally, the model does not suffer from faulty phase splitting predictions. As expected, with the new fitting strategy presented the COSMOSPACE predictions are much better than those of its theoretical basis, the quantum-chemical COSMO-RS approach.

3.6 Summary

In this work the applicability of COSMOSPACE to binary VLE predictions was thoroughly investigated. This model, which was derived from the a priori predictive method COSMO-RS, describes activity coefficients in terms of two contributions. The entropic part, which accounts for geometrical restraints, is described here by a modified Staverman-Guggenheim approach as is used in Mod. UNIFAC. For the description of the residual part an analytical solution to the statistical thermodynamics of an ensemble of pairwise interacting surfaces is applied.

The required segment parameters were derived from approximations of the individual peaks appearing in so-called sigma profiles. Such profiles, which form the basis of all COSMO-RS calculations, describe the screening charge densities of a molecular surface. By means of this newly introduced concept, interaction effects between surface parts of molecules may be appropriately reflected since such effects are mainly caused by attraction and repulsion forces. Additionally, the resulting parameters also inherit the physical significance of the sigma profiles. Parameters, which were derived in this way, are the segment types of a molecule and the corresponding segment areas and volumes as well as the screening charges appearing on the segment’s areas.

To allow a “fair” comparison of the model accuracy of this approach with the Wilson model and UNIQUAC, a two-parameter fitting strategy was also developed for COSMOSPACE. The most negative screening charge of each molecule was chosen as an adjustable parameter since these charge values largely contribute to the overall interactions in the system. Since a change in one of the screening charges violates the electroneutrality of the molecule’s surface, the most positive screening charge value was recalculated from this constraint. Additionally, the fitting parameters were bounded by the limiting screening charges of the corresponding peaks appearing in the sigma profiles. In this way the parameters retain their physical meaning.

A broad range of chemical mixtures was chosen to fully investigate the applicability of the models to the various thermodynamic situations appearing in reality. For this purpose 91 thermodynamically consistent VLE data sets were collected from the literature. As the results show, in the case of ideal and slightly nonideal systems, the model predictions are almost indistinguishable with relative mean deviations around 0.5 %. With increasing thermodynamic nonidealities the deviations between experimental data and predicted values increase. While Wilson and COSMOSPACE still allow good predictions with deviations around 1 %, the UNIQUAC predictions fail in the case of systems containing an alcohol component due to erroneous predictions of miscibility gaps. A comparison of Wilson and COSMOSPACE reveals that, on average, Wilson performs slightly better. On the other hand, Wilson is incapable of predicting phase splitting, while the range of applicability of COSMOSPACE is only limited by the available molecular parameters. Since these can be easily obtained from quantum chemical COSMO calculations, COSMOSPACE is a valuable tool for the calculation of thermodynamic properties.

3.7 List of Symbols

A	area (Å^2)

C	matrix used to compute derivatives (-)
N	number of molecules, number of experimental data points in objective function (-)
P	pressure (Pa)
R	molar gas constant (8.3144 J mol^{-1} K^{-1})
T	temperature (K)
V	volume (m^{3})
a	area parameter (m^{2})
b	vector used to compute derivatives (-)
c	model parameter (-)
d	vector used to compute derivatives (-)
n	number of segments (-)
p	distribution function (-)
q	relative surface area parameter (-)
r	relative volume parameter (-)
u	segment interaction energy (e Å^{-2})
x	mole fraction of liquid phase (-)
y	mole fraction of vapour phase (-)
z	coordination number (-)

Greek Letters

Θ	surface area fraction (-)
α'	electrostatic misfit energy parameter (kJ mol^{-1} Å^{-2})
ϕ	volume fraction (-)
γ	activity coefficient (-)
μ	segment type (-)
ν	segment type (-)
τ	interaction parameter (-)
σ	screening charge (e Å^{-2})
θ	relative number of segments (-)

Subscripts

acc	acceptor value
don	donor value
eff	effective value
hb	H-bonding
i	component i
lb	lower bound
ref	reference value
ub	upper bound

Superscripts

*	used in the computation of derivatives
0	refers to vapour pressure
C	combinatorial part
R	residual part

3.8 References

Abrams, D. S. and Prausnitz, J. M.: *Statistical Thermodynamics of Liquid Mixtures: A New Expression for the Excess Gibbs Energy of Partly or Completely Miscible Systems*. AIChE J. **21**(1): 116-128 (1975).

Barker, J. A.: *Cooperative orientation in solutions*. J. Chem. Phys. **20**: 1526-1532 (1952).

Eckert, F. and Klamt, A.: *Fast Solvent Screening via Quantum Chemistry: COSMO-RS Approach*. AIChE J. **48**(2): 369-385 (2002).

Eckert, F. and Klamt, A.: COSMOTherm. Leverkusen, Germany, COSMOlogic GmbH & Co. KG (2003).

Egner, K., Gaube, J., and Pfennig, A.: *GEQUAC, an excess Gibbs energy model for simultaneous description of associating and non-associating liquid mixtures*. Ber. Buns. Ges. **101**(2): 209-218 (1997).

Egner, K., Gaube, J., and Pfennig, A.: *GEQUAC, an excess Gibbs energy model describing associating and nonassociating liquid mixtures by a new model concept for functional groups*. Fluid Phase Equilibria **158-160**: 381-389 (1999).

Ehlker, G. H. and Pfennig, A.: *Development of GEQUAC as a new group contribution method for strongly non-ideal mixtures*. Fluid Phase Equilibria **203**(1-2): 53-69 (2002).

Fredenslund, A., Jones, R. L., and Prausnitz, J. M.: *Group-Contribution Estimation of Activity Coefficients in Nonideal Liquid Mixtures*. AIChE J. **21**(6): 1086-1099 (1975).

Gmehling, J. and Weidlich, U.: *Results of a modified UNIFAC method for alkane-alcohol systems*. Fluid Phase Equilibria **27**: 171-180 (1986).

Guggenheim, E. A.: Mixtures. Clarendon Press, Oxford (1952).

Herington, E. F. G.: *A thermodynamic test for the internal consistency of experimental data on volatility ratios*. Nature (London, UK) **160**: 610-611 (1947).

Kehiaian, H. V., Grolier, J. P. E., and Benson, G. C.: *Thermodynamics of organic mixtures. A generalized quasichemical theory in terms of group surface interactions*. J. Chim. Phys. **75**(11-12): 44-61 (1978).

Klamt, A.: *Conductor-like Screening Model for Real Solvents: A New Approach to the Quantitative Calculation of Solvation Phenomena*. J. Phys. Chem. **99**: 2224-2235 (1995).

Klamt, A. and Eckert, F.: *COSMO-RS: a novel and efficient method for the a priori prediction of thermophysical data of liquids*. Fluid Phase Equilibria **172**: 43-72 (2000).

Klamt, A., Krooshof, G. J. P., and Taylor, R.: *COSMOSPACE: Alternative to Conventional Activity-Coefficient Models*. AIChE J. **48**(10): 2332-2349 (2002).

Larsen, B. L., Rasmussen, P., and Fredenslund, A.: *A modified UNIFAC group-contribution model for prediction of phase equilibria and heats of mixing*. Ind. Eng. Chem. Res. **26**(11): 2274-2286 (1987).

Lin, T.-S. and Sandler, S. I.: *A Priori Phase Equilibrium Prediction from a Segment Contribution Solvation Model*. Ind. Eng. Chem. Res. **41**: 899-913 (2002).

Maurer, G. and Prausnitz, J. M.: *On the Derivation and Extension of the UNIQUAC Equation*. Fluid Phase Equilibria **2**: 91-99 (1978).

Redlich, O. and Kister, A. T.: *Algebraic Representation of Thermodynamic Properties and the Classification of Solutions*. Ind. Eng. Chem. **40**(2): 345-348 (1948).

Renon, H. and Prausnitz, J. M.: *Local Compositions in Thermodynamic Excess Functions for Liquid Mixtures*. AIChE J. **14**: 135-144 (1968).

van Ness, H. C., Byer, S. M., and Gibbs, R. E.: *Vapor-liquid equilibrium. I. Appraisal of data reduction methods*. AIChE J. **19**(2): 238-244 (1973).

von Solms, N., Michelsen, M. L., and Kontogeorgis, G. M.: *Applying Association Theories to Polar Fluids*. Ind. Eng. Chem. Res. **43**(7): 1803-1806 (2004).

Weidlich, U. and Gmehling, J.: *A Modified UNIFAC Model. 1. Prediction of VLE, h^E, and γ^{∞}*. Ind. Eng. Chem. Res. **26**: 1372-1381 (1987).

Wilson, G. M.: *Vapor-Liquid Equilibrium. XI. A New Expression for the Excess Free Energy of Mixing*. J. Am. Chem. Soc. **86**: 127-130 (1964).

Appendix

A Detailed Results of all Vapour-Liquid Equilibrium Calculations

Table A presents the detailed results of all vapour-liquid equilibrium calculations. The first column of that table describes the system for which the measurements were conducted. A number in brackets following the mixture type indicates that more than one set of experimental data has been used to determine the parameters. The second column provides the experimental temperature and the third column the number of data points of the experimental data set. The last four columns show the relative mean deviations in *y* as were computed with the Wilson equation, UNIQUAC, COSMOPACE, and the a priori predictive method COSMOS-RS.

Table A. Systems investigated and relative mean deviations in *y* as a function of the g^E-model

System	T/°C	N	relative mean deviations in y/%			
			Wilson	UNIQUAC	COSMOSPACE	COSMO-RS
alkane + alkane						
n-heptane + n-octane	55	14	0.24	0.23	0.73	1.80
n-pentane + n-hexane	25	10	1.45	1.45	2.06	2.26
alkane + cycloalkane						
n-hexane + cyclohexane	25	31	0.31	0.30	0.78	3.51
n-hexane + cyclohexane	35	16	0.32	0.32	0.48	1.97
n-hexane + cyclohexane	70	7	0.77	0.74	0.55	1.34
cyclohexane + n-heptane	25	11	0.35	0.35	0.29	2.72
cyclohexane + n-heptane	40	8	0.33	0.31	0.39	0.34
cyclohexane + n-heptane	60	7	0.54	0.55	0.23	0.52
alkane + aromatics						
n-pentane + benzene	45	16	1.06	1.04	1.13	1.59
n-hexane + benzene (2)	25	61	0.15	0.24	0.87	5.74
n-hexane + benzene	55	14	0.66	0.67	0.75	6.04
benzene + n-heptane	20	22	0.46	0.47	0.42	5.79
benzene + n-heptane	25	14	0.22	0.22	0.51	5.39
benzene + n-heptane	45	15	0.68	0.73	0.87	6.80
benzene + n-heptane	55	13	0.81	0.83	0.86	6.92
n-heptane + toluene	25	27	0.90	0.92	1.06	6.38
n-heptane + toluene	30	10	0.40	0.39	0.37	4.18
n-heptane + toluene	55	13	0.62	0.63	1.76	2.42
x-alkane + cycloalkane						
tetrachloromethane + cyclohexane	40	9	0.29	0.29	0.57	9.83
tetrachloromethane + cyclohexane	60	12	0.55	0.58	0.48	11.52
tetrachloromethane + cyclohexane (2)	70	21	0.14	0.14	0.31	10.98
x-alkane + aromatics						
tetrachloromethane + benzene	20	7	0.17	0.13	0.20	16.27
tetrachloromethane + benzene	30	7	0.14	0.14	0.15	15.74
tetrachloromethane + benzene	40	8	0.31	0.31	0.45	19.09
tetrachloromethane + toluene	35	14	0.17	0.17	0.18	19.71
tetrachloromethane + toluene	40	21	0.09	0.12	0.09	10.01
tetrachloromethane + toluene	45	15	0.07	0.07	0.07	18.35
cycloalkane + aromatics						
benzene + cyclohexane	8	14	0.21	0.28	0.41	12.28
benzene + cyclohexane	10	12	0.28	0.29	0.28	7.49
benzene + cyclohexane	14	14	0.16	0.21	0.31	12.15

System	T/°C	N	relative mean deviations in y/%			
			Wilson	UNIQUAC	COSMOSPACE	COSMO-RS
benzene + cyclohexane	20	14	0.15	0.20	0.33	12.05
benzene + cyclohexane	25	13	0.19	0.20	0.43	8.77
benzene + cyclohexane (3)	40	26	0.41	0.41	0.47	6.15
benzene + cyclohexane	60	12	0.17	0.19	0.21	7.23
benzene + cyclohexane	70	14	0.44	0.44	0.46	5.18
cyclohexane + toluene	25	11	0.52	0.52	0.52	2.19
ketone + alkane						
n-pentane + acetone	25	14	0.57	1.49	1.64	7.69
acetone + n-hexane	-20	10	1.41	1.53	1.77	5.49
acetone + n-hexane	-5	13	0.87	2.04	2.16	4.01
acetone + n-hexane	20	16	0.49	1.19	1.37	3.37
acetone + n-hexane	45	16	1.31	1.42	1.02	2.76
acetone + n-hexane	55	11	1.89	1.68	1.48	3.58
acetone + n-heptane	50	9	1.43	1.36	1.44	2.53
ketone + cycloalkane						
acetone + cyclohexane (2)	25	35	0.69	1.64	1.52	8.09
acetone + cyclohexane	35	11	1.16	1.29	1.37	3.01
acetone + cyclohexane	45	11	1.03	1.00	1.06	3.14
acetone + cyclohexane	55	11	1.13	0.82	0.83	3.03
ketone + aromatics						
acetone + benzene	25	13	0.51	0.49	0.56	4.65
acetone + benzene	45	11	0.71	0.70	0.71	5.45
acetone + toluene	45	15	0.58	0.59	0.56	3.34
alcohol + alkane						
methanol + n-hexane	25	7	0.85	8.33	4.65	12.94
n-hexane + methanol	45	13	1.74	4.4	2.66	6.39
n-hexane + ethanol (2)	25	18	0.46	1.69	0.63	0.87
n-hexane + ethanol	35	11	0.58	1.98	0.84	1.59
n-hexane + ethanol	50	20	1.08	3.06	1.57	3.51
ethanol + n-heptane	40	15	2.01	6.39	3.16	3.16
n-hexane + n-propanol	25	9	0.37	0.81	0.67	1.38
n-hexane + n-propanol	45	5	0.56	1.03	1.01	1.02
n-propanol + n-heptane	60	33	1.73	4.53	2.66	5.52
n-pentane + n-butanol	30	15	0.34	0.20	0.19	0.96
alcohol + x-alkane						
tetrachloromethane + ethanol	45	13	1.06	1.65	1.41	19.37
tetrachloromethane + ethanol	50	10	2.77	1.41	3.26	9.52
tetrachloromethane + ethanol	65	15	0.92	1.54	0.95	14.79
tetrachloromethane + n-butanol	35	21	0.20	0.42	0.19	1.67
alcohol + cycloalkane						
cyclohexane + ethanol	10	19	0.55	2.59	1.06	2.40
cyclohexane + ethanol (2)	20	26	0.55	2.43	0.80	2.56
ethanol + cyclohexane	25	9	0.81	3.85	2.28	5.25
ethanol + cyclohexane	35	9	0.28	3.47	1.50	3.94
ethanol + cyclohexane	50	8	0.29	2.85	1.04	4.02
cyclohexane + n-propanol	25	12	0.54	1.66	0.66	1.98
alcohol + aromatics						
methanol + benzene (2)	25	18	1.39	2.43	1.67	1.64
ethanol + benzene (2)	25	18	1.66	2.45	1.72	4.83
ethanol + benzene	40	11	0.99	2.73	0.83	7.16
ethanol + benzene	45	12	0.80	2.16	0.94	5.53
ethanol + benzene	50	16	1.13	2.64	0.81	6.19
ethanol + benzene	55	9	1.42	2.14	1.27	5.79
ethanol + toluene	35	10	0.49	1.80	0.95	3.79
ethanol + toluene	45	19	0.99	2.19	2.57	4.54
ethanol + toluene	55	10	0.69	1.46	0.75	3.23
benzene + n-propanol	25	9	0.60	0.81	1.62	2.40
benzene + n-propanol	60	15	1.43	1.19	1.52	5.28
benzene + n-butanol	45	9	0.39	0.48	0.42	0.38

B COSMOSPACE Model Parameters and Literature References to VLE Data

Table B presents the COSMOSPACE model parameters as were determined from the constraint least squares-fit. In addition to that, all literature references are given.

Table B. COSMOSPACE model parameters and literature references to VLE data.

Components	Molecular parameters		Segment parameters							
	Area [A^2]	volume [A^3]	sigma [e/A^2]	area [A^2]	lb [e/A^2]	ub [e/A^2]	sigma [e/A^2]	area [A^2]	lb [e/A^2]	ub [e/A^2]
Alkane + Cycloalkane										
Hexane - Cyclohexane at 25 °C										
Ref.: Martin M.L., Youings J.C., Aust. J. Chem. 33, 2133 (1980)										
Hexane	156.895	145.683	-1.367E-03	83.8220	-0.006	0	1.568E-03	73.0740	0	0.006
Cyclohexane	131.486	126.302	-2.972E-03	70.0380	-0.006	0	3.388E-03	61.4490	0	0.006
Hexane - Cyclohexane at 35 °C										
Ref.: Ott J.B., Marsh K.N., Stokes R.H., J. Chem. Thermodyn. 12, 1139 (1980)										
Hexane	156.895	145.683	-1.539E-03	83.8220	-0.006	0	1.765E-03	73.0740	0	0.006
Cyclohexane	131.486	126.302	-2.950E-03	70.0380	-0.006	0	3.362E-03	61.4490	0	0.006
Hexane - Cyclohexane at 70 °C										
Ref.: Susarev M.P., Chen. S.T., Zh. Fiz. Khim. 37, 1739 (1963)										
Hexane	156.895	145.683	-2.053E-03	83.8220	-0.006	0	2.356E-03	73.0740	0	0.006
Cyclohexane	131.486	126.302	-3.186E-03	70.0380	-0.006	0	3.631E-03	61.4490	0	0.006
Cyclohexane - Heptane at 25 °C										
Ref.: Katayama T., Sung E.K., Lightfoot E.N., AICHE J. 11, 924 (1965)										
Cyclohexane	131.486	126.302	-2.928E-03	70.0380	-0.006	0	3.337E-03	61.4490	0	0.006
Heptane	176.891	167.634	-1.403E-03	94.6940	-0.006	0	1.616E-03	82.1970	0	0.006
Cyclohexane - Heptane at 40 °C										
Ref.: Cruetzen J.L., Haase R., Sieg L., Z. Naturforsch. A5, 600 (1950)										
Cyclohexane	131.486	126.302	-2.535E-03	70.0380	-0.006	0	2.889E-03	61.4490	0	0.006
Heptane	176.891	167.634	-1.965E-03	94.6940	-0.006	0	2.264E-03	82.1970	0	0.006
Cyclohexane - Heptane at 60 °C										
Ref.: Cruetzen J.L., Haase R., Sieg L., Z. Naturforsch. A5, 600 (1950)										
Cyclohexane	131.486	126.302	-2.024E-03	70.0380	-0.006	0	2.307E-03	61.4490	0	0.006
Heptane	176.891	167.634	-2.024E-03	94.6940	-0.006	0	2.331E-03	82.1970	0	0.006
Alkane + Aromatics										
Pentane - Benzene at 45 °C										
Ref.: Wang J.L.H., Lu B.C.Y., J. Appl. Chem. Biotechnol. 21, 297 (1971)										
Pentane	137.164	124.395	-1.568E-03	72.7330	-0.006	0	1.770E-03	64.4320	0	0.006
Benzene	121.371	109.980	-4.759E-03	59.7980	-0.009	0	4.622E-03	61.5730	0	0.008
Hexane - Benzene at 25 °C										
Ref.: Harris, Dunlop, 1970, DECHEMA data series 1,6a p. 542										
Ref.: Murray R.S., Martin M.L., J. Chem. Thermodyn. 7, 839 (1975)										
Hexane	156.895	145.683	-1.125E-03	83.8220	-0.006	0	1.291E-03	73.0740	0	0.006
Benzene	121.371	109.980	-4.564E-03	59.7980	-0.009	0	4.432E-03	61.5730	0	0.008
Hexane - Benzene at 55 °C										
Ref.: Yuan K.S., Lu B.C-Y., Ho J.C.K., Keshpande A.K., J. Chem. Eng. Data 8, 549 (1963)										
Hexane	156.895	145.683	-2.114E-03	83.8220	-0.006	0	2.425E-03	73.0740	0	0.006
Benzene	121.371	109.980	-4.982E-03	59.7980	-0.009	0	4.839E-03	61.5730	0	0.008
Benzene - Heptane at 20 °C										
Ref.: Werner, Schuberth, 1966, DECHEMA data series 1,6b p. 157										
Benzene	121.371	109.980	-4.557E-03	59.7980	-0.009	0	4.426E-03	61.5730	0	0.008
Heptane	176.891	167.634	-1.506E-03	94.6940	-0.006	0	1.735E-03	82.1970	0	0.006
Benzene - Heptane at 25 °C										
Ref.: Harris K.R., Dunlop P.J., J. Chem. Thermodyn. 2, 805 (1970)										
Benzene	121.371	109.980	-4.540E-03	59.7980	-0.009	0	4.409E-03	61.5730	0	0.008
Heptane	176.891	167.634	-1.557E-03	94.6940	-0.006	0	1.793E-03	82.1970	0	0.006
Benzene - Heptane at 45 °C										
Ref.: Palmer, Smith, 1972, DECHEMA data series 1,6b p. 145										
Benzene	121.371	109.980	-4.591E-03	59.7980	-0.009	0	4.458E-03	61.5730	0	0.008
Heptane	176.891	167.634	-1.628E-03	94.6940	-0.006	0	1.876E-03	82.1970	0	0.006

Components	Molecular parameters		Segment parameters							
	Area [A^2]	volume [A^3]	sigma [e/A^2]	area [A^2]	lb [e/A^2]	ub [e/A^2]	sigma [e/A^2]	area [A^2]	lb [e/A^2]	ub [e/A^2]
Benzene - Heptane at 55 °C										
Ref.: Kirss H., Kudryavtseva L.S. Eisen Ol, Eesti NSV Tead. Akad. Toim., Keem. Geol. 24, 15 (1975)										
Benzene	121.371	109.980	-4.610E-03	59.7980	-0.009	0	4.477E-03	61.5730	0	0.008
Heptane	176.891	167.634	-1.684E-03	94.6940	-0.006	0	1.940E-03	82.1970	0	0.006
Heptane - Toluene at 25 °C										
Ref.: Surovy J., Heinrich J., Sb. Pr. Chem. Fak. Svst. 201 (1966)										
Heptane	176.891	167.634	-2.127E-04	94.6940	-0.006	0	2.450E-04	82.1970	0	0.006
Toluene	140.550	131.815	-4.785E-03	36.7495	-0.009	-0.004	-2.238E-03	34.3500	-0.004	0.000
			1.990E-03	33.9655	0.000	0.004	5.217E-03	35.4850	0.004	0.010
Heptane - Toluene at 30 °C										
Ref.: Markuzin N.P., Pavlova L.M., Zh. Pril. Khim. (Leningrad) 44, 311 (1971)										
Heptane	176.891	167.634	-4.449E-04	94.6940	-0.006	0	5.125E-04	82.1970	0	0.006
Toluene	140.550	131.815	-4.727E-03	36.7495	-0.009	-0.004	-2.238E-03	34.3500	-0.004	0.000
			1.990E-03	33.9655	0.000	0.004	5.157E-03	35.4850	0.004	0.010
Heptane - Toluene at 55 °C										
Ref.: Kirss H., Kudryavtseva L.S. Eisen Ol, Eesti NSV Tead. Akad. Toim., Keem. Geol. 24, 15 (1975)										
Heptane	176.891	167.634	-2.302E-04	94.6940	-0.006	0	2.653E-04	82.1970	0	0.006
Toluene	140.550	131.815	-4.928E-03	36.7495	-0.009	-0.004	-2.238E-03	34.3500	-0.004	0.000
			1.990E-03	33.9655	0.000	0.004	5.366E-03	35.4850	0.004	0.010
Halogenated Alkane + Cycloalkane										
CCl4 - Cyclohexane at 40 °C										
Ref.: Scatchard G., Wood S.E., Mochel J.M., 1939, DECHEMA data series I,6a, 147										
CCl4	134.206	128.392	-4.105E-03	49.6150	-0.010	0	2.408E-03	84.5910	0	0.007
Cyclohexane	131.486	126.302	-9.910E-04	70.0380	-0.006	0	1.129E-03	61.4490	0	0.006
CCl4 - Cyclohexane at 60 °C										
Ref.: Dvorak K., Boublik T., Collect. Czech. chem. Commun. 28, 1249 (1963)										
CCl4	134.206	128.392	-4.069E-03	49.6150	-0.010	0	2.387E-03	84.5910	0	0.007
Cyclohexane	131.486	126.302	-1.024E-03	70.0380	-0.006	0	1.167E-03	61.4490	0	0.006
CCl4 - Cyclohexane at 70 °C										
Ref.: Scatchard G., Wood S.E., Mochel J.M., 1939, DECHEMA data series I,6a, 148										
Ref.: Brown I., Ewald A.H., Austr. J. Sci. Research A3, 306 (1950)										
CCl4	134.206	128.392	-3.732E-03	49.6150	-0.010	0	2.189E-03	84.5910	0	0.007
Cyclohexane	131.486	126.302	-2.040E-04	70.0380	-0.006	0	2.325E-04	61.4490	0	0.006
Halogenated Alkane + Aromatics										
CCl4 - Benzene at 20 °C										
Ref.: Schulze, 1914, Dechema data series , 1,7 p.47										
CCl4	134.206	128.392	-3.189E-03	49.6150	-0.010	0	1.870E-03	84.5910	0	0.007
Benzene	121.371	109.980	-4.100E-03	59.7980	-0.009	0	3.982E-03	61.5730	0	0.008
CCl4 - Benzene at 30 °C										
Ref.: Schulze, 1914, Dechema data series , 1,7 p.48										
CCl4	134.206	128.392	-3.650E-03	49.6150	-0.010	0	2.141E-03	84.5910	0	0.007
Benzene	121.371	109.980	-4.274E-03	59.7980	-0.009	0	4.150E-03	61.5730	0	0.008
CCl4 - Benzene at 40 °C										
Ref.: G. Scatchard, S.E. Wood, J.M. Mochel, J. Am. Soc., 1939, Vol. 61, 3206-3210										
CCl4	134.206	128.392	-2.567E-03	49.6150	-0.010	0	1.505E-03	84.5910	0	0.007
Benzene	121.371	109.980	-3.624E-03	59.7980	-0.009	0	3.519E-03	61.5730	0	0.008
CCl4 - Toluene at 35 °C										
Ref.: Wang, Boublikova, Lu, 1970, DECHEMA data series 1,7 p. 346										
CCl4	134.206	128.392	-6.893E-03	49.6150	-0.010	0	4.043E-03	84.5910	0	0.007
Toluene	140.550	131.815	-8.391E-03	36.7495	-0.009	-0.004	-2.238E-03	34.3500	-0.004	0.000
			1.990E-03	33.9655	0.000	0.004	8.952E-03	35.4850	0.004	0.010
CCl4 - Toluene at 40 °C										
Ref.: Wang, Boublikova, Lu, 1970, DECHEMA data series 1,7 p. 347										
CCl4	134.206	128.392	-6.858E-03	49.6150	-0.010	0	4.023E-03	84.5910	0	0.007
Toluene	140.550	131.815	-8.349E-03	36.7495	-0.009	-0.004	-2.238E-03	34.3500	-0.004	0.000
			1.990E-03	33.9655	0.000	0.004	8.908E-03	35.4850	0.004	0.010
CCl4 - Toluene at 45 °C										
Ref.: Wang, Boublikova, Lu, 1970, DECHEMA data series 1,7 p. 348										

Components	Molecular parameters		Segment parameters							
	Area [A^2]	volume [A^3]	sigma [e/A^2]	area [A^2]	lb [e/A^2]	ub [e/A^2]	sigma [e/A^2]	area [A^2]	lb [e/A^2]	ub [e/A^2]
CCl4	134.206	128.392	-6.789E-03	49.6150	-0.010	0	3.982E-03	84.5910	0	0.007
Toluene	140.550	131.815	-8.198E-03	36.7495	-0.009	-0.004	-2.238E-03	34.3500	-0.004	0.000
			1.990E-03	33.9655	0.000	0.004	8.751E-03	35.4850	0.004	0.010
Cycloalkane + Aromatics										
Benzene - Cyclohexane at 8 °C										
Ref.: Aim K., Fluid Phase Equilibria 2, 119 (1978)										
Benzene	121.371	109.980	-4.739E-03	59.7980	-0.009	0	4.603E-03	61.5730	0	0.008
Cyclohexane	131.486	126.302	-1.857E-03	70.0380	-0.006	0	2.117E-03	61.4490	0	0.006
Benzene - Cyclohexane at 10 °C										
Ref.: Boublik T., Collect. Czech. Chem. Comun. 28, 1771 (1963)										
Benzene	121.371	109.980	-4.816E-03	59.7980	-0.009	0	4.677E-03	61.5730	0	0.008
Cyclohexane	131.486	126.302	-1.986E-03	70.0380	-0.006	0	2.264E-03	61.4490	0	0.006
Benzene - Cyclohexane at 14 °C										
Ref.: Aim K., Fluid Phase Equilibria 2, 119 (1978)										
Benzene	121.371	109.980	-4.734E-03	59.7980	-0.009	0	4.597E-03	61.5730	0	0.008
Cyclohexane	131.486	126.302	-1.877E-03	70.0380	-0.006	0	2.139E-03	61.4490	0	0.006
Benzene - Cyclohexane at 20 °C										
Ref.: Aim K., Dechema data series 1,6,c, p.217										
Benzene	121.371	109.980	-4.730E-03	59.7980	-0.009	0	4.594E-03	61.5730	0	0.008
Cyclohexane	131.486	126.302	-1.896E-03	70.0380	-0.006	0	2.161E-03	61.4490	0	0.006
Benzene - Cyclohexane at 25 °C										
Ref.: Tasic, Djordjevic, Grozdanic, 1978, DECHEMA data series 1,6a p. 237										
Benzene	121.371	109.980	-4.614E-03	59.7980	-0.009	0	4.481E-03	61.5730	0	0.008
Cyclohexane	131.486	126.302	-1.912E-03	70.0380	-0.006	0	2.179E-03	61.4490	0	0.006
Benzene - Cyclohexane at 40 °C										
Ref.: Friend, Scheller, Weber, 1970, DECHEMA data series 1,6a p. 211										
Ref.: G. Scatchard, S.E. Wood, J.M. Mochel, J. Phys. Chem., 1939, Vol. 43, 119-130										
Ref.: Young, Mentzer, Greenkorn, Chao, 1977, DECHEMA data series 1,6a p. 239										
Benzene	121.371	109.980	-4.551E-03	59.7980	-0.009	0	4.420E-03	61.5730	0	0.008
Cyclohexane	131.486	126.302	-1.691E-03	70.0380	-0.006	0	1.927E-03	61.4490	0	0.006
Benzene - Cyclohexane at 60 °C										
Ref.: Boublik, 1971, DECHEMA data series 1,6a p. 207										
Benzene	121.371	109.980	-4.343E-03	59.7980	-0.009	0	4.218E-03	61.5730	0	0.008
Cyclohexane	131.486	126.302	-1.214E-03	70.0380	-0.006	0	1.384E-03	61.4490	0	0.006
Benzene - Cyclohexane at 70 °C										
Ref.: Pena M.D., Cheda D.r., An. Quim. 66, 721 (1970)										
Benzene	121.371	109.980	-4.712E-03	59.7980	-0.009	0	4.576E-03	61.5730	0	0.008
Cyclohexane	131.486	126.302	-2.068E-03	70.0380	-0.006	0	2.356E-03	61.4490	0	0.006
Cyclohexane - Toluene at 25 °C										
Ref.: Katayama T., Sung E.K., Lightfoot E.N., AICHE J. 11, 924 (1965)										
Cyclohexane	131.486	126.302	-1.416E-03	70.0380	-0.006	0	1.614E-03	61.4490	0	0.006
Toluene	140.550	131.815	-5.474E-03	36.7495	-0.009	-0.004	-2.238E-03	34.3500	-0.004	0.000
			1.990E-03	33.9655	0.000	0.004	5.930E-03	35.4850	0.004	0.010
Ketone + Alkane										
Petane - Acetone at 25 °C										
Ref.: Rall W., Schaefer K., Z. Elektrochem. 63, 1019 (1959)										
Pentane	137.164	124.395	-1.579E-03	72.7330	-0.006	0	1.782E-03	64.4320	0	0.006
Acetone	102.681	86.349	-5.837E-03	50.4870	-0.009	-0.002	-8.835E-04	15.7060	-0.002	0.000
			6.680E-03	29.4885	0.000	0.005	1.594E-02	7.0000	0.005	0.019
Acetone - Hexane at -20 °C										
Ref.: Schaefer K., Rall, W., Z. Elektrochem. 62, 1090 (1958)										
Acetone	102.681	86.349	-5.956E-03	50.4870	-0.009	-0.002	-8.835E-04	15.7060	-0.002	0.000
			6.680E-03	29.4885	0.000	0.005	1.680E-02	7.0000	0.005	0.019
Hexane	156.895	145.683	-1.899E-03	83.8220	-0.006	0	2.179E-03	73.0740	0	0.006
Acetone - Hexane at -5 °C										
Ref.: Schaefer K., Rall, W., Z. Elektrochem. 63, 1019 (1959)										
Acetone	102.681	86.349	-5.831E-03	50.4870	-0.009	-0.002	-8.835E-04	15.7060	-0.002	0.000
			6.680E-03	29.4885	0.000	0.005	1.590E-02	7.0000	0.005	0.019
Hexane	156.895	145.683	-1.647E-03	83.8220	-0.006	0	1.890E-03	73.0740	0	0.006

Components	Molecular parameters		Segment parameters							
	Area [A^2]	volume [A^3]	sigma [e/A^2]	area [A^2]	lb [e/A^2]	ub [e/A^2]	sigma [e/A^2]	area [A^2]	lb [e/A^2]	ub [e/A^2]
Acetone - Hexane at 20 °C										
Ref.: Rall W., Schaefer K., Z. Elektrochem. 63, 1019 (1959)										
Acetone	102.681	86.349	-6.007E-03	50.4870	-0.009	-0.002	-8.835E-04	15.7060	-0.002	0.000
			6.680E-03	29.4885	0.000	0.005	1.717E-02	7.0000	0.005	0.019
Hexane	156.895	145.683	-2.066E-03	83.8220	-0.006	0	2.370E-03	73.0740	0	0.006
Acetone - Hexane at 45 °C										
Ref.: Schaefer K., Rall, W., Z. Elektrochem. 63, 1019 (1959)										
Acetone	102.681	86.349	-5.975E-03	50.4870	-0.009	-0.002	-8.835E-04	15.7060	-0.002	0.000
			6.680E-03	29.4885	0.000	0.005	1.694E-02	7.0000	0.005	0.019
Hexane	156.895	145.683	-2.106E-03	83.8220	-0.006	0	2.416E-03	73.0740	0	0.006
Acetone - Hexane at 55 °C										
Ref.: Kudryavtseva L.S., Susarev M.P., Zh. Prikl.Khim. 36, 1471 (1963)										
Acetone	102.681	86.349	-5.891E-03	50.4870	-0.009	-0.002	-8.835E-04	15.7060	-0.002	0.000
			6.680E-03	29.4885	0.000	0.005	1.633E-02	7.0000	0.005	0.019
Hexane	156.895	145.683	-1.892E-03	83.8220	-0.006	0	2.170E-03	73.0740	0	0.006
Acetone - Heptane at 50 °C										
Ref.: Schaefer K., Rall W., Wirth-Lindemann F.C., Z. Phys. Chem. (Frankfurt) 14, 197 (1958)										
Acetone	102.681	86.349	-6.098E-03	50.4870	-0.009	-0.002	-8.835E-04	15.7060	-0.002	0.000
			6.680E-03	29.4885	0.000	0.005	1.782E-02	7.0000	0.005	0.019
Heptane	176.891	167.634	-2.312E-03	94.6940	-0.006	0	2.664E-03	82.1970	0	0.006
Ketone + Cycloalkane										
Acetone - Cylcohexane at 25 °C										
Ref.: Tasic, Djordjevic, Grozdanic, 1978, DECHEMA data series 1,3/4 p. 216										
Ref.: Puri P.S., Polak J., Ruether J.A., 1974, DECHEMA data series 1,3/4 p. 214										
Acetone	102.681	86.349	-6.186E-03	50.4870	-0.009	-0.002	-8.835E-04	15.7060	-0.002	0.000
			6.680E-03	29.4885	0.000	0.005	1.846E-02	7.0000	0.005	0.019
Cyclohexane	131.486	126.302	-1.811E-03	70.0380	-0.006	0	2.064E-03	61.4490	0	0.006
Acetone - Cylcohexane at 35 °C										
Ref.: Marinichev A.N., Susarev M.P. Zh. Prikl. Khim. 38, 378 (1965)										
Acetone	102.681	86.349	-6.039E-03	50.4870	-0.009	-0.002	-8.835E-04	15.7060	-0.002	0.000
			6.680E-03	29.4885	0.000	0.005	1.740E-02	7.0000	0.005	0.019
Cyclohexane	131.486	126.302	-1.867E-03	70.0380	-0.006	0	2.128E-03	61.4490	0	0.006
Acetone - Cyclohexane at 45 °C										
Ref.: Marinichev A.N., Susarev M.P. Zh. Prikl. Khim. 38, 378 (1965)										
Acetone	102.681	86.349	-6.151E-03	50.4870	-0.009	-0.002	-8.835E-04	15.7060	-0.002	0.000
			6.680E-03	29.4885	0.000	0.005	1.821E-02	7.0000	0.005	0.019
Cyclohexane	131.486	126.302	-2.069E-03	70.0380	-0.006	0	2.358E-03	61.4490	0	0.006
Acetone - Cyclohexane at 55 °C										
Ref.: Marinichev A.N., Susarev M.P. Zh. Prikl. Khim. 38, 378 (1965)										
Acetone	102.681	86.349	-6.355E-03	50.4870	-0.009	-0.002	-8.835E-04	15.7060	-0.002	0.000
			6.680E-03	29.4885	0.000	0.005	1.968E-02	7.0000	0.005	0.019
Cyclohexane	131.486	126.302	-2.374E-03	70.0380	-0.006	0	2.705E-03	61.4490	0	0.006
Ketone + Aromatics										
Acetone - Benzene at 25 °C										
Ref.: Tasic, Djordjevic, Grozdanic, 1978, DECHEMA data series ? p. 208										
Acetone	102.681	86.349	-5.842E-03	50.4870	-0.009	-0.002	-8.835E-04	15.7060	-0.002	0.000
			6.680E-03	29.4885	0.000	0.005	1.598E-02	7.0000	0.005	0.019
Benzene	121.371	109.980	-4.164E-03	59.7980	-0.009	0	4.044E-03	61.5730	0	0.008
Acetone - Benzene at 45 °C										
Ref.: Brown I., Smith F., Austr. J. Chem. 10, 423 (1957)										
Acetone	102.681	86.349	-5.830E-03	50.4870	-0.009	-0.002	-8.835E-04	15.7060	-0.002	0.000
			6.680E-03	29.4885	0.000	0.005	1.589E-02	7.0000	0.005	0.019
Benzene	121.371	109.980	-4.210E-03	59.7980	-0.009	0	4.088E-03	61.5730	0	0.008
Acetone - Toluene at 45 °C										
Ref.: Kraus, Linek, 1971, DECHEMA data series ? p. 233										
Acetone	102.681	86.349	-6.076E-03	50.4870	-0.009	-0.002	-8.835E-04	15.7060	-0.002	0.000
			6.680E-03	29.4885	0.000	0.005	1.766E-02	7.0000	0.005	0.019
Toluene	140.550	131.815	-5.373E-03	36.7495	-0.009	-0.004	-2.238E-03	34.3500	-0.004	0.000
			1.990E-03	33.9655	0.000	0.004	5.826E-03	35.4850	0.004	0.010

Components	Molecular parameters		Segment parameters							
	Area [A^2]	volume [A^3]	sigma [e/A^2]	area [A^2]	lb [e/A^2]	ub [e/A^2]	sigma [e/A^2]	area [A^2]	lb [e/A^2]	ub [e/A^2]
Alcohol + Alkane										
Methanol - Hexane at 25 °C										
Ref.: Iguchi A., Kagaku Sochi 20, 66 (1978)										
Methanol	67.561	48.427	-1.771E-02	7.6180	-0.019	-0.01	-2.652E-03	34.5860	-0.009	0.000
			1.361E-03	13.6320	0.000	0.01	1.775E-02	11.7250	0.011	0.021
Hexane	156.895	145.683	-2.282E-03	83.8220	-0.006	0	2.618E-03	73.0740	0	0.006
Hexane - Methanol at 45 °C										
Ref.: Ferguson J.B., Z. Phys. Chem. 36, 1123 (1932)										
Hexane	156.895	145.683	-2.125E-03	83.8220	-0.006	0	2.438E-03	73.0740	0	0.006
Methanol	67.561	48.427	-1.721E-02	7.6180	-0.019	-0.01	-2.652E-03	34.5860	-0.009	0.000
			1.361E-03	13.6320	0.000	0.01	1.742E-02	11.7250	0.011	0.021
Hexane - Ethanol at 25 °C										
Ref.: Smith V.C., Robinson R.L.Jr., J. Chem. Eng. Data 15, 391 (1970)										
Ref.: Iguchi A., Kagaku Sochi 20, 66 (1978)										
Hexane	156.895	145.683	-1.703E-03	83.8220	-0.006	0	1.954E-03	73.0740	0	0.006
Ethanol	88.110	69.985	-1.709E-02	7.1210	-0.019	-0.01	-3.257E-03	45.7730	-0.009	0.000
			3.005E-03	23.7050	0.000	0.01	1.733E-02	11.5110	0.011	0.021
Hexane - Ethanol at 35 °C										
Ref.: Kudryavtseva L.S., Susarev M.P., Zh. Prikl. Khim. 36, 1471 (1963)										
Hexane	156.895	145.683	-2.204E-03	83.8220	-0.006	0	2.528E-03	73.0740	0	0.006
Ethanol	88.110	69.985	-1.900E-02	7.1210	-0.019	-0.01	-3.257E-03	45.7730	-0.009	0.000
			3.005E-03	23.7050	0.000	0.01	1.852E-02	11.5110	0.011	0.021
Hexane - Ethanol at 50 °C										
Ref.: Pena M.D., Cheda D.R., An. Quim. 66, 721 (1970)										
Hexane	156.895	145.683	-2.455E-12	83.8220	-0.006	0	2.816E-12	73.0740	0	0.006
Ethanol	88.110	69.985	-1.523E-02	7.1210	-0.019	-0.01	-3.257E-03	45.7730	-0.009	0.000
			3.005E-03	23.7050	0.000	0.01	1.618E-02	11.5110	0.011	0.021
Ethanol - Heptane at 40 °C										
Ref.: Pena M.D., Cheda D.R., An. Quim. 66, 737 (1970)										
Ethanol	88.110	69.985	-1.786E-02	7.1210	-0.019	-0.01	-3.257E-03	45.7730	-0.009	0.000
			3.005E-03	23.7050	0.000	0.01	1.781E-02	11.5110	0.011	0.021
Heptane	176.891	167.634	-2.156E-03	94.6940	-0.006	0	2.484E-03	82.1970	0	0.006
Hexane - Propanol at 25 °C										
Ref.: Iguchi A., Kagaku Sochi 20, 66 (1978)										
Hexane	156.895	145.683	-2.220E-14	83.8220	-0.006	0	2.547E-14	73.0740	0	0.006
Propanol	108.046	91.830	-1.599E-02	7.1430	-0.019	-0.01	-3.212E-03	57.0480	-0.009	0.000
			3.346E-03	32.4620	0.000	0.01	1.657E-02	11.3930	0.011	0.021
Hexane - Propanol at 45 °C										
Ref.: Brown I., Fock, W., Smith F., J. Chem. Thermodyn. 1, 273 (1969)										
Hexane	156.895	145.683	-2.262E-14	83.8220	-0.006	0	2.595E-14	73.0740	0	0.006
Propanol	108.046	91.830	-1.604E-02	7.1430	-0.019	-0.01	-3.212E-03	57.0480	-0.009	0.000
			3.346E-03	32.4620	0.000	0.01	1.660E-02	11.3930	0.011	0.021
Propanol - Heptane at 60 °C										
Ref.: Pena M.D., Cheda D.R., An. Quim. 66, 747 (1970)										
Propanol	108.046	91.830	-1.594E-02	7.1430	-0.019	-0.01	-3.212E-03	57.0480	-0.009	0.000
			3.346E-03	32.4620	0.000	0.01	1.654E-02	11.3930	0.011	0.021
Heptane	176.891	167.634	-1.166E-03	94.6940	-0.006	0	1.343E-03	82.1970	0	0.006
Pentane - Butanol at 30 °C										
Ref.: Ronc M., Ratcliff G.R., Can. J. Chem. Eng. 54, 326 (1976)										
Pentane	137.164	124.395	-1.084E-03	72.7330	-0.006	0	1.224E-03	64.4320	0	0.006
Butanol	128.142	113.948	-1.603E-02	7.0820	-0.019	-0.01	-3.471E-03	69.1950	-0.009	0.000
			4.070E-03	40.3950	0.000	0.01	1.650E-02	11.4700	0.011	0.021
Alcohol + Cycloalkane										
Cyclohexane - Ethanol at 10 °C										
Ref.: Nagai, J. Isii, N. (1935) from DECHEMA data series 1 2a p. 432										
Cyclohexane	131.486	126.302	-3.365E-09	70.0380	-0.006	0	3.835E-09	61.4490	0	0.006
Ethanol	88.110	69.985	-1.573E-02	7.1210	-0.019	-0.01	-3.257E-03	45.7730	-0.009	0.000
			3.005E-03	23.7050	0.000	0.01	1.650E-02	11.5110	0.011	0.021
Cyclohexane - Ethanol at 20 °C										
Ref.: Nagai, J. Isii, N. (1935) from DECHEMA data series 1 2a p. 433										

Components	Molecular parameters		Segment parameters							
	Area [A^2]	volume [A^3]	sigma [e/A^2]	area [A^2]	lb [e/A^2]	ub [e/A^2]	sigma [e/A^2]	area [A^2]	lb [e/A^2]	ub [e/A^2]
Ref.: Scatchard G., Satkiewicz F.G., J. Amer. Chem. Soc. 86, 130 (1964)										
Cyclohexane	131.486	126.302	-5.120E-04	70.0380	-0.006	0	5.836E-04	61.4490	0	0.006
Ethanol	88.110	69.985	-1.631E-02	7.1210	-0.019	-0.01	-3.257E-03	45.7730	-0.009	0.000
			3.005E-03	23.7050	0.000	0.01	1.685E-02	11.5110	0.011	0.021
Ethanol - Cyclohexane at 25 °C										
Ref.: Iguchi, Dechema data series 1,2,c p.413										
Ethanol	88.110	69.985	-1.607E-02	7.1210	-0.019	-0.01	-3.257E-03	45.7730	-0.009	0.000
			3.005E-03	23.7050	0.000	0.01	1.671E-02	11.5110	0.011	0.021
Cyclohexane	131.486	126.302	-2.221E-14	70.0380	-0.006	0	2.531E-14	61.4490	0	0.006
Ethanol - Cyclohexane at 35 °C										
Ref.: Scatchard G., Satkiewicz F.G., J. Amer. Chem. Soc. 86, 130 (1964)										
Ethanol	88.110	69.985	-1.651E-02	7.1210	-0.019	-0.01	-3.257E-03	45.7730	-0.009	0.000
			3.005E-03	23.7050	0.000	0.01	1.698E-02	11.5110	0.011	0.021
Cyclohexane	131.486	126.302	-6.331E-04	70.0380	-0.006	0	7.216E-04	61.4490	0	0.006
Ethanol - Cyclohexane at 50 °C										
Ref.: Scatchard G., Satkiewicz F.G., J. Amer. Chem. Soc. 86, 130 (1964)										
Ethanol	88.110	69.985	-1.676E-02	7.1210	-0.019	-0.01	-3.257E-03	45.7730	-0.009	0.000
			3.005E-03	23.7050	0.000	0.01	1.713E-02	11.5110	0.011	0.021
Cyclohexane	131.486	126.302	-8.898E-04	70.0380	-0.006	0	1.014E-03	61.4490	0	0.006
Ethanol - Cyclohexane at 65 °C										
Ref.: Scatchard G., Satkiewicz F.G., J. Amer. Chem. Soc. 86, 130 (1964)										
Ethanol	88.110	69.985	-1.706E-02	7.1210	-0.019	-0.01	-3.257E-03	45.7730	-0.009	0.000
			3.005E-03	23.7050	0.000	0.01	1.732E-02	11.5110	0.011	0.021
Cyclohexane	131.486	126.302	-1.107E-03	70.0380	-0.006	0	1.262E-03	61.4490	0	0.006
Cyclohexane - Propanol at 25 °C										
Ref.: Smirnova N.A., 1969, DECHEMA data series , 544										
Cyclohexane	131.486	126.302	-1.349E-04	70.0380	-0.006	0	1.537E-04	61.4490	0	0.006
Propanol	108.046	91.830	-1.656E-02	7.1430	-0.019	-0.01	-3.212E-03	57.0480	-0.009	0.000
			3.346E-03	32.4620	0.000	0.01	1.693E-02	11.3930	0.011	0.021
Alcohol + Halogenated Alkane										
CCl4 - Ethanol at 45 °C										
Ref.: Barker J.A., Brown J. Smith F., Disc. Faraday Soc. 15, 142 (1953)										
CCl4	134.206	128.392	-4.223E-03	49.6150	-0.010	0	2.477E-03	84.5910	0	0.007
Ethanol	88.110	69.985	-1.900E-02	7.1210	-0.019	-0.01	-3.257E-03	45.7730	-0.009	0.000
			3.005E-03	23.7050	0.000	0.01	1.852E-02	11.5110	0.011	0.021
CCl4 - Ethanol at 50 °C										
Ref.: Litvinov N.D., Zh. Fiz. Khim. 26, 1405 (1952).										
CCl4	134.206	128.392	-4.116E-03	49.6150	-0.010	0	2.414E-03	84.5910	0	0.007
Ethanol	88.110	69.985	-1.900E-02	7.1210	-0.019	-0.01	-3.257E-03	45.7730	-0.009	0.000
			3.005E-03	23.7050	0.000	0.01	1.852E-02	11.5110	0.011	0.021
CCl4 - Ethanol at 65 °C										
Ref.: Barker J.A., Brown J. Smith F., Disc. Faraday Soc. 15, 142 (1953)										
CCl4	134.206	128.392	-4.350E-03	49.6150	-0.010	0	2.551E-03	84.5910	0	0.007
Ethanol	88.110	69.985	-1.884E-02	7.1210	-0.019	-0.01	-3.257E-03	45.7730	-0.009	0.000
			3.005E-03	23.7050	0.000	0.01	1.842E-02	11.5110	0.011	0.021
CCl4 - Butanol at 35 °C										
Ref.: Paraskevopoulos, Missen,1962,Dechema data series 1,2,d p.146										
CCl4	134.206	128.392	-3.592E-03	49.6150	-0.010	0	2.107E-03	84.5910	0	0.007
Butanol	128.142	113.948	-1.818E-02	7.0820	-0.019	-0.01	-3.471E-03	69.1950	-0.009	0.000
			4.070E-03	40.3950	0.000	0.01	1.783E-02	11.4700	0.011	0.021
Alcohol + Aromatics										
Methanol - Benzene at 25 °C										
Ref.: Iguchi, Dechema data series 1,2,c p188										
Ref.: S-C. Hwang, P.L. Robinson, J. Chem. Eng. Data, 1977, Vol. 22, 319-325										
Methanol	67.561	48.427	-1.848E-02	7.6180	-0.019	-0.01	-2.652E-03	34.5860	-0.009	0.000
			1.361E-03	13.6320	0.000	0.01	1.825E-02	11.7250	0.011	0.021
Benzene	121.371	109.980	-3.729E-03	59.7980	-0.009	0	3.622E-03	61.5730	0	0.008
Ethanol - Benzene at 25 °C										
Ref.: Iguchi A., Dechema data series 1,2,c, p.389										
Ref.: Smith, Robinson, Dechema data series, 1,2,a p415										

Components	Molecular parameters		Segment parameters							
	Area [A^2]	volume [A^3]	sigma [e/A^2]	area [A^2]	lb [e/A^2]	ub [e/A^2]	sigma [e/A^2]	area [A^2]	lb [e/A^2]	ub [e/A^2]
Ethanol	88.110	69.985	-1.542E-02	7.1210	-0.019	-0.01	-3.257E-03	45.7730	-0.009	0.000
			3.005E-03	23.7050	0.000	0.01	1.630E-02	11.5110	0.011	0.021
Benzene	121.371	109.980	-1.799E-03	59.7980	-0.009	0	1.747E-03	61.5730	0	0.008
Ethanol - Benzene at 40 °C										
Ref.: Udovenko, Fatkulina, Dechema data series , 1,2,a p417										
Ethanol	88.110	69.985	-1.574E-02	7.1210	-0.019	-0.01	-3.257E-03	45.7730	-0.009	0.000
			3.005E-03	23.7050	0.000	0.01	1.650E-02	11.5110	0.011	0.021
Benzene	121.371	109.980	-1.701E-03	59.7980	-0.009	0	1.652E-03	61.5730	0	0.008
Ethanol - Benzene at 45 °C										
Ref.: Brown I., Smith F. Austr. J. Chem. 7, 264 (1954)										
Ethanol	88.110	69.985	-1.643E-02	7.1210	-0.019	-0.01	-3.257E-03	45.7730	-0.009	0.000
			3.005E-03	23.7050	0.000	0.01	1.693E-02	11.5110	0.011	0.021
Benzene	121.371	109.980	-2.292E-03	59.7980	-0.009	0	2.226E-03	61.5730	0	0.008
Ethanol - Benzene at 50 °C										
Ref.: Zharov V.T., Morachevsky A.G., Zh. Prikl. Khim. 36, 2397 (1963)										
Ethanol	88.110	69.985	-1.576E-02	7.1210	-0.019	-0.01	-3.257E-03	45.7730	-0.009	0.000
			3.005E-03	23.7050	0.000	0.01	1.651E-02	11.5110	0.011	0.021
Benzene	121.371	109.980	-2.062E-03	59.7980	-0.009	0	2.003E-03	61.5730	0	0.008
Ethanol - Benzene at 55 °C										
Ref.: J. C. K. Ho, B. C.Y. Lu, J. Chem. Eng. Data, 1963, Vol. 8, 553-558										
Ethanol	88.110	69.985	-1.724E-02	7.1210	-0.019	-0.01	-3.257E-03	45.7730	-0.009	0.000
			3.005E-03	23.7050	0.000	0.01	1.743E-02	11.5110	0.011	0.021
Benzene	121.371	109.980	-2.689E-03	59.7980	-0.009	0	2.611E-03	61.5730	0	0.008
Ethanol - Toluene at 35 °C										
Ref.: Kretschmer C.B., Wiebe R. J. Amer. Chem. Soc. 71, 1793 (1949)										
Ethanol	88.110	69.985	-1.845E-02	7.1210	-0.019	-0.01	-3.257E-03	45.7730	-0.009	0.000
			3.005E-03	23.7050	0.000	0.01	1.818E-02	11.5110	0.011	0.021
Toluene	140.550	131.815	-4.000E-03	36.7495	-0.009	-0.004	-2.238E-03	34.3500	-0.004	0.000
			1.990E-03	33.9655	0.000	0.004	4.404E-03	35.4850	0.004	0.010
Ethanol - Toluene at 45 °C										
Ref.: Van Ness H.C., Soczek C.A., Peloquin G.L. Machado R.L., J. Chem. Eng. Data 12, 217 (1967)										
Ethanol	88.110	69.985	-1.771E-02	7.1210	-0.019	-0.01	-3.257E-03	45.7730	-0.009	0.000
			3.005E-03	23.7050	0.000	0.01	1.772E-02	11.5110	0.011	0.021
Toluene	140.550	131.815	-4.000E-03	36.7495	-0.009	-0.004	-2.238E-03	34.3500	-0.004	0.000
			1.990E-03	33.9655	0.000	0.004	4.404E-03	35.4850	0.004	0.010
Ethanol - Toluene at 55 °C										
Ref.: Kretschmer C.B., Wiebe R. J. Amer. Chem. Soc. 71, 1793 (1949)										
Ethanol	88.110	69.985	-1.804E-02	7.1210	-0.019	-0.01	-3.257E-03	45.7730	-0.009	0.000
			3.005E-03	23.7050	0.000	0.01	1.792E-02	11.5110	0.011	0.021
Toluene	140.550	131.815	-4.000E-03	36.7495	-0.009	-0.004	-2.238E-03	34.3500	-0.004	0.000
			1.990E-03	33.9655	0.000	0.004	4.404E-03	35.4850	0.004	0.010
Benzene - Propanol at 25 °C										
Ref.: Iguchi A., 1978, DECHEMA data series, 535										
Benzene	121.371	109.980	-3.904E-08	59.7980	-0.009	0	3.792E-08	61.5730	0	0.008
Propanol	108.046	91.830	-1.406E-02	7.1430	-0.019	-0.01	-3.212E-03	57.0480	-0.009	0.000
			3.346E-03	32.4620	0.000	0.01	1.536E-02	11.3930	0.011	0.021
Benzene - Propanol at 60 °C										
Ref.: Udovenko V.V., Maranko T.F., IZV. VYSSh. Ucheb. zaved. Khim. Khim. Tekhnol. 15, 1654 (1972)										
Benzene	121.371	109.980	-2.131E-07	59.7980	-0.009	0	2.070E-07	61.5730	0	0.008
Propanol	108.046	91.830	-1.453E-02	7.1430	-0.019	-0.01	-3.212E-03	57.0480	-0.009	0.000
			3.346E-03	32.4620	0.000	0.01	1.566E-02	11.3930	0.011	0.021
Benzene - Butanol at 45 °C										
Ref.: Brown I. Smith F., 1959, DECHEMA data series , 177										
Benzene	121.371	109.980	-1.295E-03	59.7980	-0.009	0	1.257E-03	61.5730	0	0.008
Butanol	128.142	113.948	-1.439E-02	7.0820	-0.019	-0.01	-3.471E-03	69.1950	-0.009	0.000
			4.070E-03	40.3950	0.000	0.01	1.549E-02	11.4700	0.011	0.021

4 Viscosity Calculations on the Basis of Eyring's Absolute Reaction Rate Theory and COSMOSPACE

On the basis of Eyring's absolute reaction rate theory a new mixture viscosity model has been developed. The nonidealities of the mixture are accounted for with the thermodynamically consistent COSMOSPACE approach. The required model and component parameters are derived from sigma-profiles, which form the basis of the a priori predictive method COSMO-RS. To improve the model performance two segment parameters are determined from a least-squares analysis to experimental viscosity data, whereas a constraint optimisation procedure is applied. In this way the parameters retain their physical meaning. Finally, the viscosity calculations of this approach are compared to the findings of the Eyring-UNIQUAC model for a broad range of chemical mixtures. These results show that the new Eyring-COSMOSPACE approach is superior to the frequently employed Eyring-UNIQUAC method.

4.1 Introduction

Viscosity holds a place alongside properties such as density, molecular weight, and heat capacity as one of the basic properties of any substance. Its applications are vast, including areas such as design of fluid flow, heat transfer, separation processes, and reaction engineering. Since it is infeasible to determine the viscosity by experiment for every imaginable temperature, pressure, and composition, the calculation of viscosity from theory is highly desirable.

Many of the viscosity models published in the literature were reviewed by Irving (Irving 1977b, a), Poling et al. (Poling et al. 2001), and more recently by Monnery et al. (Monnery et al. 1995) and Mehrotra et al. (Mehrotra et al. 1996). Most of these equations are based on the principle of corresponding state and Eyring's absolute reaction rate theory (Glasstone et al. 1941). Since any excess Gibbs (g^{E}) energy model can be plugged into Eyring's theory to account for the nonidealities of the mixture, this approach was used more frequently in the past. In this context, especially UNIQUAC (Abrams and Prausnitz 1975; Maurer and Prausnitz 1978) and its group-contribution method UNIFAC (Fredenslund et al. 1975) were in the focus of several researchers.

Wu (Wu 1986) used UNIFAC to develop a group-contribution viscosity prediction method, whereas the required group interaction parameters appearing in UNIFAC were fitted to experimental viscosity data. A similar approach was conducted by Chevalier et al. (Chevalier et al. 1988) and Gaston-Bonhomme et al. (Gaston-Bonhomme et al. 1994) who also adapted the UNIFAC approach to be applicable to viscosity modelling. This method was successfully applied to systems consisting of molecules that differ appreciably in size. The average absolute deviation of 13 ternary alkane systems is reported to be 2.6 % and 3.6 % for 4 quaternary mixtures. Cao et al. (Cao et al. 1993) used the same framework to develop their GC-UNIMOD method yielding an average mean relative standard deviation (MRSD) of 4.1 %. In an earlier work (Cao et al. 1992) they presented a model on the basis of UNIQUAC and Eyring's absolute reaction rate theory. Within this approach they achieved overall average MRSD values of 0.8 % for binary systems and 2.9 % for multicomponent systems when fitting the interaction parameters to experimental viscosity data. Only recently Martins et al. (Martins et al. 2000) also used UNIQUAC as the starting point for their model. With an average MRSD value of 1.2 % of more than 350 binary systems, the model performance is similar to the results of other approaches published in the literature. In a subsequent work (Martins et al. 2001) they also investigated the model performance for multicomponent mixtures with an overall MRSD value of 2.95 % for 48 ternary and 3 quaternary mixtures.

However, the success and wide application of UNIQUAC and UNIFAC are based on thermodynamic inconsistencies as was pointed out by Klamt et al. (Klamt et al. 2002). In their paper they compared UNIQUAC with the newly derived COSMOSPACE model. It was shown that UNIQUAC is only a special case of the more general COSMOSPACE approach, which is an analytical solution to the statistical thermodynamics of the pairwise interacting surface model COSMO-RS (Klamt and Eckert 2000; Eckert and Klamt 2002). Furthermore, due to the assumptions made in the derivation of UNIQUAC, it fails when the performance is tested against lattice Monte Carlo simulations (Wu et al. 1998; Klamt et al. 2002). In contrast, the COSMOSPACE approach perfectly describes the simulation data. Only recently the applicability of COSMOSPACE to the prediction of VLE data was thoroughly examined and the final results of this new approach were also superior to those of UNIQUAC (Bosse and Bart 2005).

These results suggest that viscosity calculations may also be enhanced when applying a more accurate g^E-model within the Eyring approach. It is, therefore, the purpose of this communication to investigate the applicability of the COSMOSPACE solution to viscosity modelling.

In the following the underlying theory of this new approach is introduced. Afterwards, the determination of the required model and component parameters is discussed before the model performance of the new Eyring-COSMOSPACE viscosity model is tested against the Eyring-UNIQUAC approach.

4.2 The Eyring-COSMOSPACE Model

According to Eyring's absolute reaction rate theory the viscosity of any system may be expressed as

$$\eta = \frac{hN}{V}\frac{\Omega}{\Omega^+}\exp\left(\frac{\varepsilon_0}{k_\mathrm{B}T}\right) \tag{4.1}$$

with h as the Planck constant, N the Avogadro number, V the molar volume of the system, Ω and Ω^+ the partition sums of the system in standard and activated state, ε_0 the activation energy at 0 K, k_B the Boltzmann constant and T as the temperature. It is further assumed that the molecules in standard state and activated state are in equilibrium.

$$K^+ = \frac{\Omega^+}{\Omega}\exp\left(-\frac{\varepsilon_0}{k_\mathrm{B}T}\right) \tag{4.2}$$

Following classical thermodynamics this equilibrium constant K^+ may also be defined as

$$K^+ = \exp\left(-\frac{\Delta g^+}{RT}\right) \tag{4.3}$$

with Δg^+ as the standard free energy of activation per mole and R as the molar gas constant. Now (4.1) may be rewritten to give

$$\eta = \frac{hN}{V}\exp\left(\frac{\Delta g^+}{RT}\right) \tag{4.4}$$

For mixtures Δg^+ is evaluated as a function of composition and the free energy of activation of the constituents in the mixture. In the case of an ideal binary system the following mixing rule may apply

$$\Delta g^{+} = x_1 \Delta g_1^{+} + x_2 \Delta g_2^{+} \tag{4.5}$$

with Δg_i^{+} as the free energy of activation in pure species i. Combining this equation with (4.4) leads to an expression for the mixture viscosity.

$$\eta = \frac{hN}{V} \exp\left(\frac{x_1 \Delta g_1^{+} + x_2 \Delta g_2^{+}}{RT} \right) \tag{4.6}$$

If (4.4) is also used to describe pure component viscosities by

$$\eta_i = \frac{hN}{V_i} \exp\left(\frac{\Delta g_i^{+}}{RT} \right) \tag{4.7}$$

(4.6) may be rewritten as

$$\ln(\eta V) = x_1 \ln(\eta_1 V_1) + x_2 \ln(\eta_2 V_2) \tag{4.8}$$

As Eyring pointed out this equation holds only in the case of ideal binary mixtures while it overestimates the mixture viscosities of thermodynamically nonideal systems by a factor g^{E}/cRT. Therefore, (4.5) may be corrected as

$$\Delta g^{+} = x_1 \Delta g_1^{+} + x_2 \Delta g_2^{+} - g^{\mathrm{E}}/c \tag{4.9}$$

with g^{E} as the free excess energy of the system and c some constant value. Finally, the dynamic mixture viscosity is given by

$$\ln(\eta V) = x_1 \ln(\eta_1 V_1) + x_2 \ln(\eta_2 V_2) - \frac{g^{\mathrm{E}}}{\mathrm{cRT}} \tag{4.10}$$

Considering the relation between the dynamic viscosity, the kinematic viscosity, ν, and the density, ρ,

$$\nu = \frac{\eta}{\rho} \tag{4.11}$$

(4.10) can be written to yield an equation for ν

$$\ln(\nu M) = x_1 \ln(\nu_1 M_1) + x_2 \ln(\nu_2 M_2) - \frac{g^{\mathrm{E}}}{\mathrm{cRT}} \tag{4.12}$$

with M and M_i as the molar mass in the mixture and of the pure components, respectively.

In order to compute the excess Gibbs energy contribution, the COSMOSPACE approach is consulted. In this model two parts contribute to the activity coefficient γ_i of a component i

$$\ln \gamma_i = \ln \gamma_i^C + \ln \gamma_i^R \tag{4.13}$$

The combinatorial part is expressed in terms of a modified Staverman-Guggenheim expression as is used in mod. UNIFAC (Gmehling and Weidlich 1986; Weidlich and Gmehling 1987)

$$\ln \gamma_i^C = 1 - \phi_i^{'} + \ln \phi_i^{'} - \frac{z}{2} q_i \left(1 - \frac{\phi_i}{\Theta_i} + \ln \frac{\phi_i}{\Theta_i} \right) \tag{4.14}$$

with ϕ_i and $\phi_i^{'}$ as the two volume fractions and Θ_i as the surface area fraction of component i in the mixture. z denotes the coordination number of the lattice. The volume and surface area fractions are defined with respect to the relative volume r_i and surface area q_i and with x_i as the mole fraction of component i and c_{comb} as an adjustable parameter.

$$\phi_i' = \frac{x_i r_i^{c_{\text{comb}}}}{\sum_j x_j r_j^{c_{\text{comb}}}} \qquad \phi_i = \frac{x_i r_i}{\sum_j x_j r_j} \qquad \Theta_i = \frac{x_i q_i}{\sum_j x_j q_j} \tag{4.15}$$

The residual part was derived from the partition sum of an ensemble of pairwise interacting surface segments.

$$\ln \gamma_i^R = \sum_\nu n_i^\nu \left(\ln \gamma^\nu - \ln \gamma_i^\nu \right) \tag{4.16}$$

Here, γ_i^R denotes the residual activity coefficient, n_i^ν the number of segments of type ν on molecule i, γ^ν the segment activity coefficient of type ν in the mixture and γ_i^ν the segment activity coefficient of type ν in pure liquid i. The segment activity coefficients are given by the following expression, which may be easily solved by repeated substitution starting with all segment activity coefficients set to unity on the right-hand side of this equation.

$$\frac{1}{\gamma^\nu} = \sum_\mu \tau_{\mu\nu} \theta^\mu \gamma^\mu \tag{4.17}$$

Note that the final result automatically satisfies the Gibbs-Duhem equation. For physical consistency the interaction parameter $\tau_{\mu\nu}$ is given by a symmetric matrix whose elements are defined by

$$\tau_{\mu\nu} = \exp\left[-\frac{u_{\mu\nu} - 1/2\left(u_{\mu\mu} + u_{\nu\nu}\right)}{RT} \right] \tag{4.18}$$

with $u_{\mu\nu}$ as the segment interaction energy of types μ and ν. The relative number of segments of type ν is defined by

$$\theta^\nu = \frac{n^\nu}{n} \tag{4.19}$$

with

$$n^\nu = \sum_i N_i n_i^\nu \tag{4.20}$$

as the number of segments of type ν and

$$n = \sum_i N_i n_i \tag{4.21}$$

as the total number of segments in the mixture. The number of molecules of species i in the system is $N_i = N x_i$ and the total number of surface segments on a molecule i is given by

$$n_i = \sum_\nu n_i^\nu = \frac{A_i}{a_{\text{eff}}} \tag{4.22}$$

A_i equals the total surface area of molecule i and a_{eff} is an effective contact area, which must be considered as an adjustable parameter. Once the activity coefficients of all species i are computed, the dimensionless excess Gibbs energy may be computed from

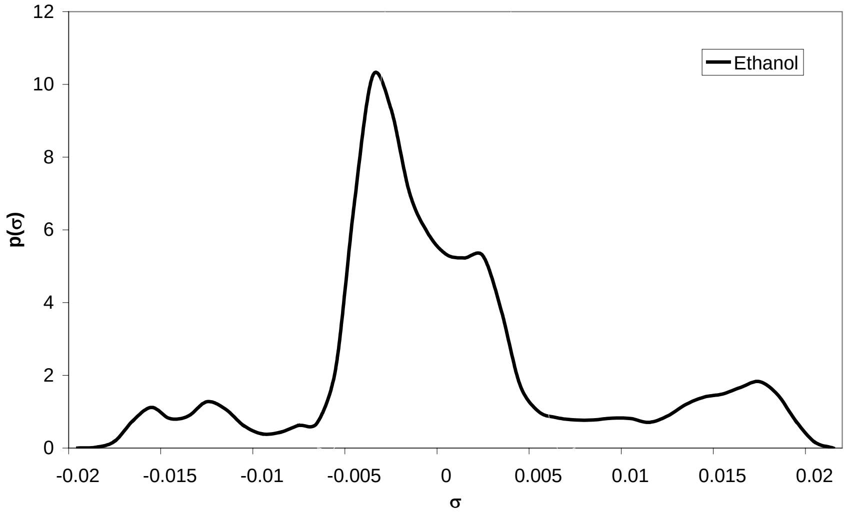

Figure 4.1. Sigma profile of ethanol.

$$\frac{g^{\mathrm{E}}}{RT} = \sum_i x_i \ln \gamma_i \tag{4.23}$$

4.3 Estimation of Model and Component Parameters

Following the recommendations of Bosse and Bart (Bosse and Bart 2005) the energy concept of COSMO-RS (Klamt and Eckert 2000; Eckert and Klamt 2002) is adopted to determine the values for the required model and component parameters of COSMOSPACE. This concept is based on so-called sigma profiles, which may be explained best in terms of the distribution function $p(\sigma)$. This function describes the amount of surface in the ensemble, having a screening charge density between σ and $\sigma + \mathrm{d}\sigma$. In Fig. 4.1 the sigma profile of ethanol is exemplarily depicted. Note that positive polarities cause negative screening charges while negative polarities cause positive screening charges. As can be seen from the graph the ethanol profile consists of four peaks. Two of them result from the hydroxyl group, one donor peak at $\sigma = -0.015$ e Å^{-2} and one acceptor peak at $\sigma = 0.015$ e Å^{-2}. The other two peaks around $\sigma = 0$ e Å^{-2} describe the screening charges of the alkyl group. The profile, therefore, suggests to model ethanol with four different segment types. The required segment areas A_i^{ν} and average screening charges σ_i^{ν} may also be derived from this profile. A_i^{ν} equals the surface area under the corresponding peak while σ_i^{ν} may be computed from a weighted distribution function of this peak. In this way, Bosse and Bart (Bosse and Bart 2005) evaluated the sigma profiles of 26 chemical species. The results of all components used throughout this work are summarised in Table 4.1. This table also provides information on the components' molecular volumes, which were adopted from COSMO-RS as well as the values for the lower and upper screening charges, which bound the corresponding segment type.

The pair interaction energy $u_{\mu\nu}$ used in (4.18) to compute $\tau_{\mu\nu}$ is calculated from

$$\begin{aligned} u_{\mu\nu} &= u_{\mu\nu}^{\mathrm{misfit}} + u_{\mu\nu}^{\mathrm{hb}} \\ &= a_{\mathrm{eff}} \frac{\alpha'}{2} (\sigma_\mu + \sigma_\nu)^2 + a_{\mathrm{eff}} c_{\mathrm{hb}} \max[0, \sigma_{\mathrm{acc}} - \sigma_{\mathrm{hb}}] \min[0, \sigma_{\mathrm{don}} + \sigma_{\mathrm{hb}}] \end{aligned} \tag{4.24}$$

Table 4.1. Segment parameters of chemical species.

Components	Molecular parameters		Segment parameters							
	area [A^2]	volume [A^3]	sigma [e/A^2]	area [A^2]	lb [e/A^2]	ub [e/A^2]	sigma [e/A^2]	area [A^2]	lb [e/A^2]	ub [e/A^2]
Alkanes										
Hexane	156.896	145.683	-1.733E-03	83.8220	-0.006	0	1.987E-03	73.0740	0	0.006
Heptane	176.891	167.634	-1.864E-03	94.6940	-0.006	0	2.147E-03	82.1970	0	0.006
Nonane	216.795	211.314	-1.793E-03	116.5120	-0.006	0	2.083E-03	100.2830	0	0.006
Decane	236.775	233.315	-1.774E-03	127.4465	-0.006	0	2.068E-03	109.3285	0	0.006
Hexadecane	356.856	366.403	-1.715E-03	192.7925	-0.006	0	2.015E-03	164.0635	0	0.006
Cycloalkanes										
Cyclohexane	131.487	126.302	-2.114E-03	70.0380	-0.006	0.000	2.410E-03	61.4490	0.000	0.006
X-Alkanes										
CCl4	134.206	128.392	-3.124E-03	49.6150	-0.01	0	1.832E-03	84.5910	0	0.007
Alcohols										
Methanol	67.561	48.427	-1.295E-02	7.6180	-0.019	-0.01	-2.652E-03	34.5860	-0.009	0
			1.361E-03	13.6320	0	0.01	1.466E-02	11.7250	0.011	0.021
Ethanol	88.110	69.985	-1.391E-02	7.1210	-0.019	-0.01	-3.257E-03	45.7730	-0.009	0
			3.005E-03	23.7050	0	0.01	1.537E-02	11.5110	0.011	0.021
Propanol	108.046	91.830	-1.275E-02	7.1430	-0.019	-0.01	-3.212E-03	57.0480	-0.009	0
			3.346E-03	32.4620	0	0.01	1.455E-02	11.3930	0.011	0.021
1-Butanol	128.142	113.948	-1.167E-02	7.0820	-0.019	-0.01	-3.471E-03	69.1950	-0.009	0
			4.070E-03	40.3950	0	0.01	1.381E-02	11.4700	0.011	0.021
Ketones										
Acetone	102.682	86.349	-5.152E-03	50.4870	-0.009	-0.002	-8.835E-04	15.7060	-0.002	0
			6.680E-03	29.4885	0	0.005	1.100E-02	7.0000	0.005	0.019
Aromatics										
Benzene	121.371	109.980	-4.100E-03	59.7980	-0.009	0	3.982E-03	61.5730	0	0.008
Toluene	140.550	131.815	-5.532E-03	36.7495	-0.009	-0.004	-2.238E-03	34.3500	-0.004	0
			1.990E-03	33.9655	0	0.004	5.991E-03	35.4850	0.004	0.01

with α' as a constant for the misfit energy, c_{hb} the strength coefficient and σ_{hb} a cutoff value for hydrogen bonding. σ_{acc} and σ_{don} are the larger and smaller value of σ_{μ} and σ_{ν}, respectively.

The average segment screening charges σ_i^{ν} provided in Table 4.1 serve as initial guesses for the fitting strategy recently developed by Bosse and Bart (Bosse and Bart 2005). In this method the most negative screening charge of each component is used as a fitting parameter which results in two adjustable parameters for the case of a binary mixture. These parameters are bounded by the corresponding lower and upper screening charge values. Additionally, the electroneutrality condition of the overall surface charge of a molecule i is imposed on the optimisation procedure.

$$\sum_{\nu} \sigma_i^{\nu} A_i^{\nu} = 0 \tag{4.25}$$

To fulfil this constraint a change in the most negative screening charge requires a recalculation of the value of the most positive screening charge, making also use of the lower and upper bounds on that peak. A detailed description of this technique, as well as a more specific analysis of sigma profiles, is given in the literature (Bosse and Bart 2005).

The values of all model parameters were adopted from Bosse and Bart (Bosse and Bart 2005). The effective contact area a_{eff} equals 7.7 Å^2, the electrostatic misfit energy α' is 6635 kJ mol^{-1} Å^2 e^{-2}, the value for the strength coefficient for hydrogen bonding c_{hb} is 500 kJ mol^{-1} Å^2 e^{-2}, the cutoff value for hydrogen bonding σ_{hb} is 0.0084 e Å^{-2}, the constant in the combinatorial part c_{comb} amounts to 0.2, and the coordination number z equals 10. The reference values for the surface area and the volume required to allow a consistent use of the molecular parameters r_i and q_i within the combinatorial and the residual part are A_{ref} =55.6973 Å^2 and V_{ref} =37.7471 Å^3.

4.4 Choice of Experimental Data

A broad range of chemical mixtures is considered reflecting the various types of thermodynamic behaviour, i.e., ideal state to highly nonideal state including also association effects. The main focus of this work is on binary mixtures consisting of alkanes, cycloalkanes, X-alkanes, aromatics, ketones, and alcohols. The majority of the experimental data sets were taken from Martins et al. (Martins et al. 2000) who provide an extensive list of references to experimental viscosity data. In order to determine the adjustable segment screening charges, σ_i^ν, the following fitting strategy was used. The mixture volume, *V*, and the mixture molar mass, *M*, appearing in the working equations (4.10) and (4.12) were computed from the following equations:

$$M = \sum_i x_i M_i \qquad V = \sum_i x_i V_i \tag{4.26}$$

For the pure component viscosities experimental values were taken to minimise the prediction errors. Finally, the σ_i^ν-values were fitted to experimental viscosity data in a least-squares analysis using the sum of relative deviations in the mixture viscosity as objective function.

$$F = \sum_i \left(\frac{\eta_i^{\text{exp}} - \eta_i^{\text{calc}}}{\eta_i^{\text{exp}}} \right)^2 \tag{4.27}$$

In order to assess the quality of the two models, the relative deviation of the calculated values from the experimental viscosity data was used as the criterion.

$$\text{dev}/\% = \frac{100}{N-2} \sum_{i=1}^{N} \left| \frac{\eta_i^{\text{exp}} - \eta_i^{\text{calc}}}{\eta_i^{\text{exp}}} \right| \tag{4.28}$$

Here, N refers to the number of experimental data points and the total sum is divided by the number of independent data points. Since the pure component viscosities are used within the calculation this number equals $N-2$.

4.5 Results

In total, 49 data sets with 560 data points were investigated. Figure 4.2 provides an overview of all systems considered. The numbers in brackets following the mixture type refer to the total number of systems in this group and the total number of data points, respectively. An additional asterisk means that some of the data sets in this group were fitted simultaneously. The detailed results of all systems as well as the references to the literature sources can be found in the Appendix.

As may be seen from Figure 4.2, the average relative deviation for the Eyring-COSMOSPACE model is 1.21 %. Eyring-UNIQUAC performs slightly worse with an average relative deviation of 1.41 %. In many cases both models yield similar results but there are also marked differences in the final results. To get a feeling for the quality of the prediction results, as well as for these deviations, results of the systems with larger errors are presented in the following departure plots.

Figure 4.3 shows the predicted deviations of the system acetone – cyclohexane at 25 °C. In this case the Eyring-UNIQUAC model shows some deficiencies. In the lower acetone concentration range it overpredicts the mixture viscosity while in the higher concentration range the model yields values too low. Instead, Eyring-COSMOSPACE allows a good representation of the experimental data. A similar result can be seen in Fig. 4.4 in which the model results of the n-butanol – n-hexane-system are depicted. Again the Eyring-COSMOSPACE prediction is superior to the Eyring-UNIQUAC findings.

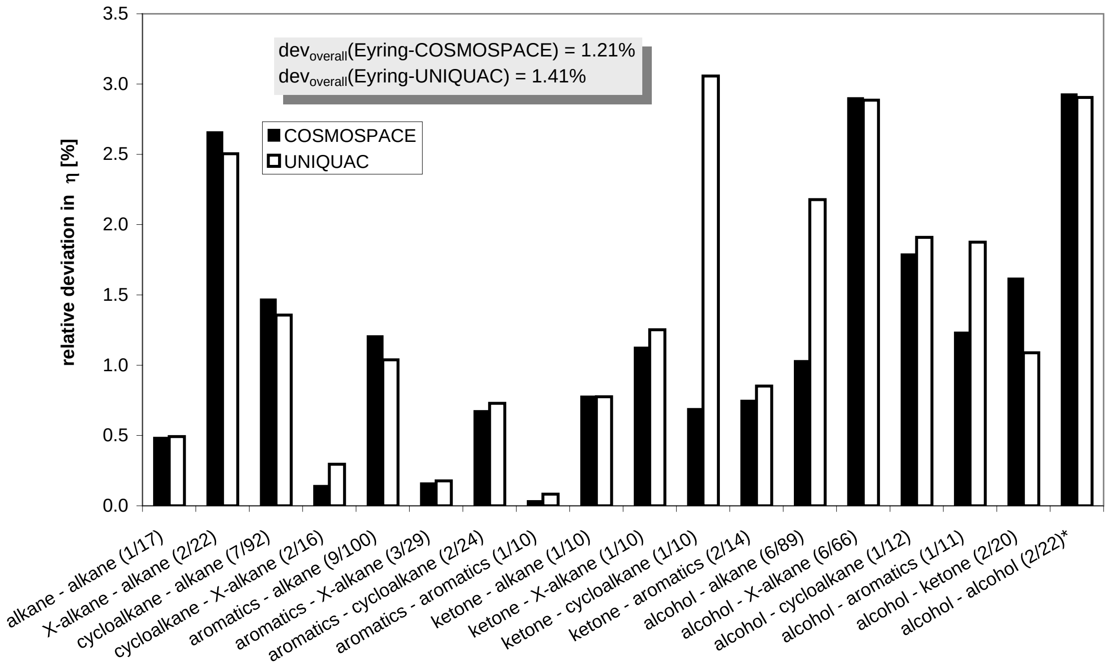

Figure 4.2. Relative deviations in η for all mixture classes investigated.

As the results in Fig. 4.5 demonstrate for the system acetone – ethanol at 25 °C, Eyring-COSMOSPACE is not always superior. However, this inaccuracy is due to the constraint optimisation procedure used to determine the segment screening charges. Here, one of the fitting parameters equals the lower bound. Despite this limitation the prediction result is satisfactory.

Less accurate results are obtained for the systems carbon tetrachloride - hexane (see Fig. 4.6) and ethanol – carbon tetrachloride (Fig. 4.7). While both models are able to predict the concentration dependence of the first system qualitatively, they fail in the second case. Here the shape of the mixture viscosity shows a minimum-maximum curvature. In contrast, an almost identical monotonous shape is computed with both model combinations which, ultimately, leads to the same model deviations (see Fig. 4.7).

To overcome this deficiency, future investigations should target on optimising the model parameters for the Eyring-UNIQUAC model and the Eyring-COSMOSPACE approach to the field of viscosity predictions. If this does not suffice to predict minimum-maximum curvatures, an unconstrained optimisation procedure may also be applied to the Eyring-COSMOSPACE

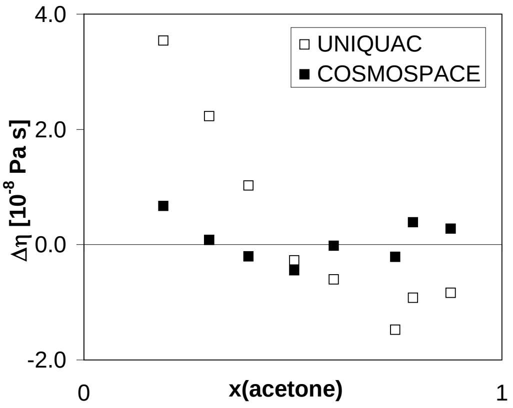

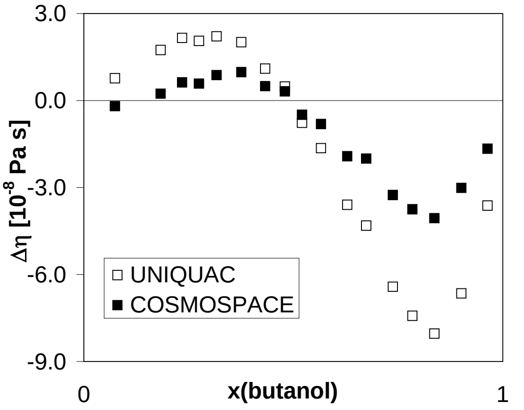

Figure 4.3. Model deviations from experimental data for the system acetone–cyclohexane at 25 °C (left).
Figure 4.4. Model deviations from experimental data for the system n-butanol–n-hexane at 25 °C (right).

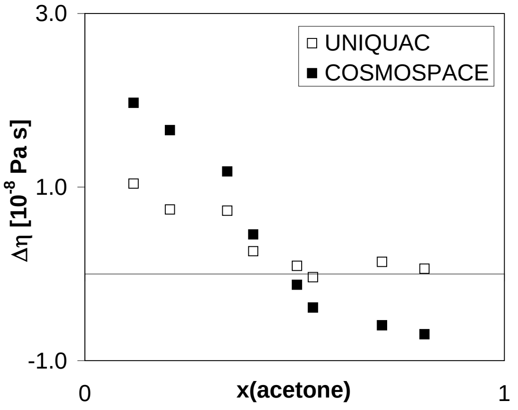

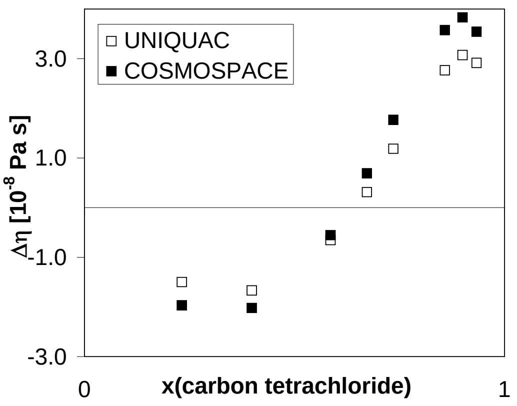

Figure 4.5. Model deviations from experimental data for the system acetone–ethanol at 25 °C (left).
Figure 4.6. Model deviations from experimental data for the system carbon tetrachloride–n-hexane at 25 °C (right).

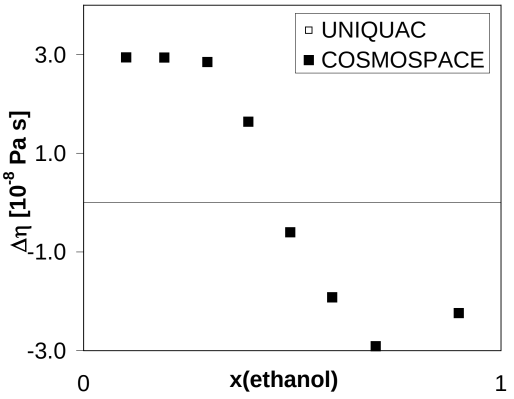

Figure 4.7. Model deviations from experimental data for the system ethanol–carbon tetrachloride at 30 °C.

approach. However, in this way the parameters will not retain their physical significance.

4.6 Summary

In this work a new method for the prediction of mixture viscosities was presented. Like many other viscosity models this approach is based on Eyring's absolute reaction rate theory. The excess Gibbs energy contribution, which accounts for the nonidealities of the mixture is described by the COSMOSPACE approach, an analytical solution to the statistical thermodynamics of a model of pairwise interacting surfaces. Only recently it was shown that this method is superior to UNIQUAC in predicting binary vapour-liquid equilibria. It was, therefore, the aim of this work to investigate the influence of this g^E-expression in respect to predicting mixture viscosities.

Following the recommendations in the literature the required model and component parameters were derived from "so-called" sigma profiles, which describe the amount of surface in an ensemble of molecular segments, having a screening charge density between σ and $\sigma + \mathrm{d}\sigma$. In this way the resulting parameters also inherit the physical significance of the sigma profiles. Parameters which were determined in this way are the segment types of a molecule, the corresponding segment areas and volumes, as well as the screening charges appearing on the segment areas. To improve the prediction quality and to retain the physical significance of the segment screening charges, a constraint optimisation procedure was applied.

In total, 49 experimental data sets were used to assess and compare the prediction quality of the newly developed approach with the Eyring-UNIQUAC model. Especially the systems with larger prediction errors were in the focus of the discussion. It was shown that, except for systems which exhibit a minimum-maximum behaviour for the mixture viscosity qualitatively good results can be achieved. In this other case both models fail.

Summarising it can be said that with an average relative deviation of 1.21 % the Eyring-COSMOSPACE approach is superior to the Eyring-UNIQUAC method with 1.41 %. Further improvements in the prediction quality of this new approach can be achieved by adjusting the model and component parameters to the field of viscosity modelling. In this way it might also be possible to allow the computation of minimum-maximum curvatures in the mixture viscosity.

4.7 List of Symbols

A	area (Å^2)
K	equilibrium constant (-)
F	value of the objective function (-)
M	molar mass (kg m^{-3})
N	number of molecules, number of experimental data points in objective function (-)
N_A	Avogadro constant ($6.022 \cdot 10^{23}$ mol^{-1})
R	molar gas constant (8.3144 J mol^{-1} K^{-1})
T	temperature (K)
V	volume (Å^3)
a	area parameter (Å^2)
c	model parameter (-)
g	Gibbs energy (J mol^{-1})
h	Planck constant ($6.626 \cdot 10^{-34}$ m^2 kg s^{-1})
k_B	Boltzmann constant ($1.38 \cdot 10^{-23}$ m^2 kg s^{-2} K^{-1})
n	number of segments (-)
p	distribution function (-)
q	relative surface area parameter (-)
r	relative volume parameter (-)
u	segment interaction energy (kJ mol^{-1})
x	mole fraction of liquid phase (-)
z	coordination number (-)

Greek Letters

Δg	standard free energy per mole (J mol^{-1})
Θ	surface area fraction (-)
Ω	partition sum (-)
α'	electrostatic misfit energy parameter (kJ mol^{-1} Å^2 e^{-2})
ε_0	activation energy at 0 K (m^2 kg s^{-2})
ϕ	volume fraction (-)
γ	activity coefficient (-)
η	dynamic viscosity (Pa s)
μ, ν	segment type (-)
ν	dynamic viscosity (m^2 s^{-1})
ρ	molar density (kmol m^{-3})

τ	interaction parameter (-)
σ	screening charge (e Å^{-2})
θ	relative number of segments (-)

Subscripts

acc	acceptor value
don	donor value
eff	effective value
hb	H-bonding
i	component i
lb	lower bound
ref	reference value
ub	upper bound

Superscripts

+	activated state
C	combinatorial part
E	excess
R	residual part
calc	calculated value
exp	experimental value
hb	H-bonding
misfit	refers to misfit energy

4.8 References

Abrams, D. S. and Prausnitz, J. M.: *Statistical Thermodynamics of Liquid Mixtures: A New Expression for the Excess Gibbs Energy of Partly or Completely Miscible Systems*. AIChE J. **21**(1): 116-128 (1975).

Bosse, D. and Bart, H. J.: *Binary Vapor-Liquid Equilibrium Predictions with COSMOSPACE*. Ind. Eng. Chem. Res. **44**(23): 8873-8882 (2005).

Cao, W., Fredenslund, A., and Rasmussen, P.: *Statistical Thermodynamic Model for Viscosity of Pure Liquids and Liquid Mixtures*. Ind. Eng. Chem. Res. **31**(11): 2603-2619 (1992).

Cao, W., Knudsen, K., Fredenslund, A., and Rasmussen, P.: *Group-Contribution Viscosity Predictions of Liquid Mixtures Using UNIFAC-VLE Parameters*. Ind. Eng. Chem. Res. **32**(9): 2088-2092 (1993).

Chevalier, J. L., Petrino, P., and Gaston-Bonhomme, Y.: *Estimation Method for the Kinematic Viscosity of a Liquid-Phase Mixture*. Chem. Eng. Sci. **43**(6): 1303-1309 (1988).

Eckert, F. and Klamt, A.: *Fast Solvent Screening via Quantum Chemistry: COSMO-RS Approach*. AIChE J. **48**(2): 369-385 (2002).

Fredenslund, A., Jones, R. L., and Prausnitz, J. M.: *Group-Contribution Estimation of Activity Coefficients in Nonideal Liquid Mixtures*. AIChE J. **21**(6): 1086-1099 (1975).

Gaston-Bonhomme, Y., Petrino, P., and Chevalier, J. L.: *UNIFAC-VISCO Group Contribution Method for Predicting Kinematic Viscosity: Extension And Temperature Dependence*. Chem. Eng. Sci. **49**(11): 1799-1806 (1994).

Glasstone, S., Laidler, K., and Eyring, H.: The Theory of Rate Processes. McGraw-Hill, New York (1941).

Gmehling, J. and Weidlich, U.: *Results of a modified UNIFAC method for alkane-alcohol systems*. Fluid Phase Equilibria **27**: 171-180 (1986).

Irving, J. B.: Viscosities of Binary Liquid Mixtures: A Survey of Mixture Equation. Glasgow, Scotland, National Engineering Laboratory, East Kilbridge (1977a).

Irving, J. B.: Viscosities of Binary Liquid Mixtures: The Effectiveness of Mixture Equations. Glasgow, Scotland, National Engineering Laboratory, East Kilbridge (1977b).

Klamt, A. and Eckert, F.: *COSMO-RS: a novel and efficient method for the a priori prediction of thermophysical data of liquids*. Fluid Phase Equilibria **172**: 43-72 (2000).

Klamt, A., Krooshof, G. J. P., and Taylor, R.: *COSMOSPACE: Alternative to Conventional Activity-Coefficient Models*. AIChE J. **48**(10): 2332-2349 (2002).

Martins, R. J., de M. Cardoso, M. J. E., and Barcia, O. E.: *Excess Gibbs Free Energy Model for Calculating the Viscosity of Binary Liquid Mixtures*. Ind. Eng. Chem. Res. **39**: 849-854 (2000).

Martins, R. J., de M. Cardoso, M. J. E., and Barcia, O. E.: *Calculation of Viscosity of Ternary and Quaternary Liquid Mixtures*. Ind. Eng. Chem. Res. **40**: 1271-1275 (2001).

Maurer, G. and Prausnitz, J. M.: *On the Derivation and Extension of the UNIQUAC Equation*. Fluid Phase Equilibria **2**: 91-99 (1978).

Mehrotra, A. N., Monnery, W. D., and Svrcek, W. Y.: *A review of practical calculation methods for the viscosity of liquid hydrocarbons and their mixtures*. Fluid Phase Equilibria **117**(1-2): 344-355 (1996).

Monnery, W. D., Svrcek, W. Y., and Mehrotra, A. N.: *Viscosity: A Critical Review of Practical Predictive and Correlative Methods*. Can. J. Chem. Eng. **73**: 3-40 (1995).

Poling, B. E., Prausnitz, J. M., and O'Connell, J. P.: The Properties of Gases & Liquids. McGraw Hill (2001).

Weidlich, U. and Gmehling, J.: *A Modified UNIFAC Model. 1. Prediction of VLE, h^E, and γ^{∞}*. Ind. Eng. Chem. Res. **26**: 1372-1381 (1987).

Wu, D. T.: *Prediction of Viscosities of Liquid Mixtures by a Group Contribution Method*. Fluid Phase Equilibria **30**: 149-156 (1986).

Wu, D.-W., Cui, Y., and Donohue, M. D.: *Local Composition Models for Lattice Mixtures*. Ind. Eng. Chem. Res. **37**: 2936-2946 (1998).

Appendix

A Detailed Results of the Viscosity Calculations

Table A provides the detailed results of the viscosity calculations. The last two columns of that table provide the relative mean deviations in the mixture viscosity as were computed from the Eyring-COSMOSPACE and the Eyring-UNIQUAC model. For systems with more than one data set, only the average values of all sets are displayed there. The number of simultaneously fitted data sets is displayed in the first column.

Table A. Systems investigated and relative mean deviations in η. An additional asterisk indicates that more than one system has been fitted.

System	T/°C	N	relative mean deviations in η /%	
			Eyring-COSMOSPACE	Eyring-UNIQUAC
alkane + alkane				
n-heptane – n-hexane	25	17	0.4868	0.4921
X-alkane + alkane				
carbon tetrachloride – n-hexane	25	10	4.2414	3.3193
n-hexadecane – carbon tetrachloride	25	12	1.0764	1.6902
alkane + cycloalkane				
n-hexane – cyclohexane	25	10	1.9928	1.9177
cyclohexane – n-hexane	25	14	1.3218	1.3218

System	T/°C	N	relative mean deviations in η /%	
			Eyring-COSMOSPACE	Eyring-UNIQUAC
cyclohexane – n-heptane	25	14	1.2589	1.0071
n-heptane – cyclohexane	25	12	1.1838	1.0982
cyclohexane – n-nonane	25	14	1.8989	1.7918
cyclohexane – n-decane	25	14	1.0441	1.0065
X-alkane + cycloalkane				
carbon tetrachloride – cyclohexane	25	9	0.1237	0.3517
carbon tetrachloride – cyclohexane	45	7	0.1629	0.2411
alkane + aromatics				
benzene – n-hexane	25	12	1.1383	0.4007
n-hexane – benzene	35	7	2.2241	2.3496
n-hexane – benzene	50	7	2.4713	2.4034
n-heptane – benzene	25	13	1.0079	0.5561
toluene – n-hexane	25	17	0.5851	0.4242
n-hexane – toluene	25	9	1.0525	0.8505
n-hexane – toluene	35	9	0.9686	2.3313
n-hexane – toluene	50	9	1.3038	2.3439
n-heptane – toluene	25	17	0.1031	0.0823
x-alkane + aromatics				
carbon tetrachloride – benzene	20	11	0.294	0.2757
carbon tetrachloride – benzene	25	11	0.0991	0.154
carbon tetrachloride – benzene	45	7	0.0931	0.1029
cycloalkane + aromatics				
benzene – cyclohexane	20	11	0.9627	0.6781
cyclohexane – benzene	25	13	0.3887	0.7798
aromatics + aromatics				
benzene – toluene	25	10	0.0348	0.0825
ketone + alkane				
acetone – n-hexane	25	10	0.779	0.7757
ketone + X-alkane				
acetone – carbon tetrachloride	25	10	1.1274	1.2526
ketone + cycloalkane				
acetone – cyclohexane	25	10	0.6896	3.058
ketone + aromatics				
acetone – benzene	25	7	0.2793	0.5128
acetone – toluene	25	7	1.2198	1.1911
alcohol + alkane				
n-hexane – ethanol	25	13	1.2926	1.9555
n-heptane – ethanol	25	13	1.7518	1.9769
n-hexane – n-propanol	25	13	0.6931	2.5145
n-heptane – n-propanol	25	13	0.6943	2.2858
n-butanol – n-hexane	25	19	1.4878	3.5855
n-butanol – h-heptane	25	18	0.2737	0.7545
alcohol + x-alkane				
ethanol – carbon tetrachloride	25	11	3.2873	3.3059
ethanol – carbon tetrachloride	30	11	2.6702	2.6817
ethanol – carbon tetrachloride	35	11	2.7262	2.7069
ethanol – carbon tetrachloride	35	11	3.0085	3.0073
ethanol – carbon tetrachloride	40	11	2.8477	2.7974
ethanol – carbon tetrachloride	40	11	2.87	2.8183
alcohol + cycloalkane				
cyclohexane – ethanol	25	12	1.7901	1.9099
alcohol + aromatics				
benzene – ethanol	25	11	1.2344	1.8752
alcohol + ketone				
acetone – methanol	25	10	1.6625	1.5551
acetone – ethanol	25	10	1.5759	0.622
alcohol + alcohol				
methanol – ethanol (2)*	25	22	2.9296	2.9047

B Literature References to Viscosity Data

Abdul-Fattah, A.A., Dullien, F.A.L., J. Chem. Eng. Data, **26**: 312-316 (1981).

Aminabhavi, T.M., Patel, R.C., Bridger, K., Jayadevappa, E.S., Prasad, B.R., J. Chem. Eng. Data, **27**: 125-128 (1982).

Aminabhavi, T.M., Aminabhavi, V.A., Balundgi, R.H., Ind. Eng. Chem. Res., **29**: 2106-2122 (1990)

Awwad, A.M., Salman, M.A., Fluid Phase Equilibria, **25**: 195-208 (1986).

Canosa, J., Rodríguez, A., Tojo, J., J. Chem. Eng. Data, **43**: 417-421 (1998).

Heric, E.L., Brewer, J.G., J. Chem. Eng. Data, **12**: 574-583 (1967).

Kouris, S., Panayiotou, C., J. Chem. Eng. Data, **34**: 200-203 (1989).

Pandey, J.D., Vyas, V., Can. J. Chemistry, **72**: 2486-2492 (1994).

Manjeshwar, L.S, Aminabhavi, T.M., J. Chem. Eng. Data, **32**: 409-420 (1987).

Nath, J., Pandey, J.G., J. Chem. Eng Data, **42**: 1133-1136 (1997).

Pandey, J.D., Vyas, V., Can. J. Chemistry, **72**: 2486-2492 (1994).

Petrino, P.J., Gaston-Bonhomme, Y.H., Chevalier, J.L.E., J. Chem. Eng. Data, **40**: 136-140 (1995).

Papioannou, D., Panayiotou, C., J. Chem. Eng. Data, **39**: 463-466 (1994).

Papaioannou, D., Evangelou, T., Panayiotou, C., J. Chem. Eng. Data, **36**: 43-46 (1991).

Teja, A.S., Rice, P., Chem. Eng. Science, **36**: 7-10 (1981).

Wei, I., Rowley, R.L., J. Chem. Eng. Data, **29**: 332-356 (1984).

5 Prediction of Diffusion Coefficients in Liquid Systems

Based on Eyring's absolute reaction rate theory a new model for the Maxwell-Stefan diffusivity has been developed. This model, an extension of the Vignes equation, describes the concentration dependence of the diffusion coefficient in terms of the diffusivities at infinite dilution and an additional excess Gibbs energy contribution. This energy part allows the explicit consideration of thermodynamic nonidealities within the modelling of this transport property. If the same set of interaction parameters, which has been derived from VLE data, is applied for this part and for the thermodynamic correction, a theoretically sound modelling of VLE and diffusion can be achieved. The influence of viscosity and thermodynamics on the model accuracy is thoroughly investigated. For this purpose diffusivities of 85 binary mixtures consisting of alkanes, cycloalkanes, halogenated alkanes, aromatics, ketones, and alcohols are computed. The average relative deviation between experimental data and computed values is approximately 8 % depending on the choice of the g^E-model. These results indicate that this model is superior to some widely used methods.

5.1 Introduction

Diffusion plays an important role in all kinds of separation processes, e.g. distillation or absorption. With the increasing use of nonequilibrium (NEQ) stage modelling (Krishnamurthy and Taylor 1985) a deeper insight into mass transfer has become more important in order to allow accurate and reliable predictions of, e.g., concentration profiles in any kind of equipment. Therefore, fundamental knowledge of various physical and thermodynamic properties, e.g. diffusion coefficients, is required. Especially in highly nonideal systems, thermodynamics strongly influence the diffusional behaviour. Even for binary systems, usually these effects result in large deviations between experimental data and predicted values.

Diffusion problems are tackled with the Fick's law or the Maxwell-Stefan (MS) equation. The relation between the two has been given by Taylor and Krishna (Taylor and Krishna 1993). For a binary mixture this yields:

$$D_{12} = \Gamma Đ_{12} \tag{5.1}$$

As can be seen from this equation, the Fick diffusivity D_{12} equals the MS-diffusion coefficient $Đ_{12}$ times the thermodynamic correction factor Γ

$$\Gamma = 1 + x_1 \left. \frac{\partial \ln \gamma_1}{\partial x_1} \right|_{T,P,x_2} \tag{5.2}$$

with T as the temperature, P the pressure and x_i as the mole fraction of species i. The main difference between both models is that the MS-approach separates diffusional effects from thermodynamic nonidealities. In contrast, the Fick diffusion coefficients must also account for the nonidealities in the mixture.

In recent years several new models have been published in the literature to describe the concentration dependence of diffusion coefficients as a function of the diffusivities at infinite dilution. Often, other physical properties are used as well. Many of these models are based on Eyring's absolute reaction rate theory (Glasstone et al. 1941) though one of the basic assumption does not hold for the liquid state (Tyrrell and Harris 1984).

He (He 1995), for example, combined this approach with the two-liquid theory to obtain an expression for $Đ_{12}$. To avoid the necessity of computing Γ he developed another model to compute the Fick diffusion coefficient directly. Additional basic properties like acentric factors or dipole moments are crucial for the diffusivity calculations. The models perform generally well. They are not recommended for associating systems but alcohol-alcohol mixtures.

Three years later, Fei and Bart (Fei and Bart 1998; Fei and Bart 2001) published a group contribution method on the basis of Eyrings' theory to predict the MS-diffusion coefficient. The distance parameter and the free volume are simultaneously estimated by the diffusional areas of the composing groups of the mixture. In a similar way, the activation energy is approximated. Group parameters of technical relevant systems, like sulfolane systems, were determined as well. The average deviation is reported to be 5 %.

In the same year Hsu and Chen (Hsu and Chen 1998) combined Eyring's theory with the statistical thermodynamics to obtain their UNIDIF-model, an approach to compute Fick diffusion coefficients directly. A combinatorial and a residual part are used to model the diffusion coefficient. The temperature independent interaction parameters, which are used in the residual part, must be fitted to experimental data. The overall absolute deviation for this method is within 2.3 %. In a subsequent paper (Hsu et al. 2000) this method was extended to the group contribution method GC-UNIMOD with satisfactory results.

A completely different concept was followed by Li et al. (Li et al. 2001) who derived a MS-diffusivity approach on the basis of Darken's equation (Darken 1948), the local-composition concept (Wilson 1964) and the cluster theory (Cussler 1980). Besides the diffusivities at infinite dilution, pure component physical properties, self diffusion coefficients, and mixture viscosities are mandatory. The Wilson model (Wilson 1964) is used to account for the thermodynamics. The average relative deviation is estimated to be 6.0 % for 45 binary systems.

As can be seen from the reported deviations, the Fick diffusivity models seem superior to the MS-D approaches. However, this benefit vanishes within the NEQ modelling. Here, mass transfer is described in terms of the MS-equation. If a Fickian approach is applied within this theory, the thermodynamic correction factor, which has been avoided initially, must be cited to calculate the MS-diffusion coefficients. Therefore, it is straightforward to model $Đ_{12}$ directly. Another weakness of some of the models presented here is the extensive use of additional physical properties. In this way the general applicability is limited. Additionally, the model accuracy depends strongly on the reliability of the available approaches for these properties. Therefore, the main goal of this work is to develop a mathematically simple but universally applicable MS-D approach. Furthermore, additional physical properties, which are required to describe the diffusional behaviour properly, must be readily available and founded on an extensive, reliable database.

In the following the underlying theory of the new diffusivity approach is presented. Afterwards, the main criteria are presented which were used to set up a reliable experimental database. Within the results section the model performance is thoroughly investigated. The influence of viscosity and thermodynamics on the diffusivity prediction is discussed and the model performance is compared to the results obtained with other diffusivity approaches commonly used. Finally, all findings are summarised.

5.2 Theory

The new diffusion coefficient approach is based on Eyring's Absolute Reaction Rate Theory (Glasstone et al. 1941). This theory states that diffusional processes may be modelled analogously to chemical reactions, i.e. a sufficient high initial energy is crucial for a diffusional process to overcome the energy barrier between the position of the molecule considered and an adjacent, vacant lattice site. For the case of a concentrated binary liquid, the mutual diffusivity may be expressed as

$$D = D^{\mathrm{id}}\Gamma \tag{5.3}$$

with D^{id} as the diffusion coefficient in an ideal system. Comparing (5.1) and (5.3) reveals that the Maxwell-Stefan diffusivity equals the ideal diffusivity

$$D^{\mathrm{id}} = Đ_{12} \tag{5.4}$$

which is defined as

$$D^{\mathrm{id}} = \lambda^2 k \tag{5.5}$$

λ represents the distance between two successive equilibrium positions. The rate constant k may be determined in terms of an equilibrium constant K^+ which relates the molecules in the standard and the activated state

$$k = \frac{k_{\mathrm{B}}T}{h}\frac{\Omega^+}{\Omega}\exp\left(-\frac{\varepsilon_0}{k_{\mathrm{B}}T}\right) = \frac{k_{\mathrm{B}}T}{h}K^+ \tag{5.6}$$

with k_{B} and h as the Boltzmann and Planck constant, Ω and Ω^+ as the partition sums in the standard and the activated state, and ε_0 as the activation energy per molecule at 0 °K. K^+ may also be computed from the change in the Gibbs energy

$$K^+ = \exp\left(-\frac{\Delta g_{ij}}{RT}\right) \tag{5.7}$$

whereas Δg_{ij} refers to the net activation energy for the diffusion process and R to the molar gas constant. Combining (5.5), (5.6), and (5.7) leads to an expression for the mutual diffusion coefficient in the mixture.

$$Đ_{ij} = \frac{\lambda^2 k_{\mathrm{B}}T}{h}\exp\left(-\frac{\Delta g_{ij}}{RT}\right) \tag{5.8}$$

The diffusivities at infinite dilution may be obtained from the limits of (5.8).

$$Đ_{ij}^{\infty} = \frac{\lambda^2 k_{\mathrm{B}}T}{h}\exp\left(-\frac{\Delta g_{ij}^{\infty}}{RT}\right) \qquad Đ_{ji}^{\infty} = \frac{\lambda^2 k_{\mathrm{B}}T}{h}\exp\left(-\frac{\Delta g_{ji}^{\infty}}{RT}\right) \tag{5.9}$$

In order to express $Đ_{ij}$ as a function of the diffusivities at infinite dilution a mixing rule for Δg_{ij} must be employed. Cullinan (Cullinan 1966), for example, used

$$\Delta g_{ij} = x_j \Delta g_{ij}^{\infty} + x_i \Delta g_{ji}^{\infty} \tag{5.10}$$

in the derivation of the Vignes model (Vignes 1966). Here, a linear dependence of the net activation energy is assumed which is only valid in the case of an ideal system. In nonideal systems this approach leads to diffusivity values much too small for $Đ_{ij}$. To compensate for this effect the mixing rule can be extended to give

$$\Delta g_{ij} = x_j \Delta g_{ij}^{\infty} + x_i \Delta g_{ji}^{\infty} + g^{\mathrm{E}} \tag{5.11}$$

which has been successfully applied in the modelling of viscosities (Martins et al. 2000, 2001; Bosse and Bart 2005b). The values for the excess Gibbs energy g^{E} are directly assessable from the activity coefficient model employed in the calculation of the thermodynamic correction factor. Assuming constant λ-values, the concentration dependence of the Maxwell-Stefan diffusion coefficient may be calculated from (5.8), (5.9) and (5.11).

$$Đ_{ij} = \left(Đ_{ij}^{\infty}\right)^{x_j} \left(Đ_{ji}^{\infty}\right)^{x_i} \exp\left(-\frac{g^{\mathrm{E}}}{RT}\right) \tag{5.12}$$

This equation reduces to the Vignes model for the case of an ideal system (as it should). Since theory states that the transport properties diffusion and viscosity are inversely related, several authors tried to improve the accuracy of the diffusivity models by introducing viscosity coefficients into the equations. In this way Leffler and Cullinan (Leffler and Cullinan 1970), for example, modified the Vignes equation. The same technique can be applied to (5.12) which results in

$$\eta Đ_{ij} = \left(\eta_j Đ_{ij}^{\infty}\right)^{x_j} \left(\eta_i Đ_{ji}^{\infty}\right)^{x_i} \exp\left(-\frac{g^{\mathrm{E}}}{RT}\right) \tag{5.13}$$

with η_i and η as the pure component and mixture viscosity, respectively. (5.12) and (5.13) are the final equations. In the following, they will be referred to as the Bosse model and the Bosse-LVS model.

5.3 Choice of Experimental Data

A broad range of chemical mixtures is considered reflecting the various types of thermodynamic behaviour, i.e. ideal state to highly nonideal state including also association effects. The main focus of this work is on binary mixtures consisting of alkanes, cycloalkanes, halogenated alkanes (X-alkanes), aromatics, ketones, and alcohols. Since the models presented here are a function of the diffusivities at infinite dilution, special attention must be paid to this property within the choice of the experimental data. Therefore, only those systems were considered for which experimental values of the boundaries are available. In this way the overall prediction error can be minimized and an influence of erroneous boundary values on the computation of D in the concentrated liquid also excluded.

Besides the proper choice of a MS-diffusivity model, the reliability of diffusion coefficient predictions depends strongly on the accuracy of the thermodynamic correction factor. This factor is not just a function of the g^{E}-model chosen but also of the VLE data set which serves as the basis for the fitting of the interaction parameters used in the thermodynamic model. To reduce these effects to a minimum, only thermodynamically consistent Pxy-data are applied which match the temperature of the diffusion coefficient measurements. Information on the applied fitting strategy to obtain the required interaction parameters is given elsewhere (Bosse and Bart 2005a).

Finally, a mixture viscosity model is required. In order not to introduce additional inaccuracies into the diffusivity calculation, a polynomial function of degree 3 is fitted to experimental data sets which, again, must match the temperature of the diffusivity experiments.

With this information at hand the performance of the models can be validated. The relative deviation between experimental diffusion coefficients and predicted values is used as the criterion to assess the prediction quality of the new models and to compare the results with the findings of other diffusivity approaches.

$$\Delta D_{\mathrm{rel}} / \% = \frac{100}{N-2} \sum_{j=1}^{N} \left| \frac{D_{12}^{\mathrm{exp}} - D_{12}^{\mathrm{calc}}}{D_{12}^{\mathrm{exp}}} \right| \tag{5.14}$$

Here, N refers to the number of experimental data points and the total sum is divided by the number of independent data points. Since the diffusivities at infinite dilution are used within this calculation, this number equals $N-2$.

A list of references to the experimental diffusion data can be found in the Appendix of this chapter. References to the viscosity data are given in the Appendix of Chapter 4 and references to the VLE data are made in the Appendix of Chapter 3.

5.4 Results

For a first assessment of the new models the thermodynamic correction factor is calculated with UNIFAC (using VLE-parameters) (Fredenslund et al. 1975), and the Vignes equation and the Bosse correlation are applied as MS-diffusivity models. The average relative deviation for 85 data sets with 734 data points is 12.90 % for the combination UNIFAC-Vignes and 8.21 % for UNIFAC-Bosse. The alcohol systems show the largest deviations with maximum values above 40 % for UNIFAC-Vignes which is caused by inaccuracies in the VLE-prediction.

Figure 5.1 provides an overview of the spectrum of systems investigated. Here, the relative mean deviation of D is plotted as a function of the MS-diffusivity model vs. the mixture classes. The Vignes equation, the model of Leffler and Cullinan, the Bosse and Bosse-LVS correlations are chosen as diffusivity models. In this way, the influence of the additional energy term of the new correlations can be explored since the models Bosse and Bosse-LVS differ from the other two only in the g^E/RT-part. Furthermore, the influence of the mixture viscosity can be tested on the new correlation. Again, UNIFAC is applied for the thermodynamics. From the initial 85 data sets, viscosity data of only 36 systems (326 data points) could be gathered from the literature. A comparison of the predictions with Leffler-Cullinan and Vignes reveals the positive influence of the viscosity correction on the accuracy of the diffusivity prediction (see also Rutten (Rutten 1992)). In this way the relative deviation can be reduced from 12.78 % to 10.39 %. In contrast, the additional consideration of the mixture viscosity in Bosse-LVS shows a negative influence in comparison to the Bosse model. This is caused by an overcorrection of *Đ* by the factors g^E/RT and

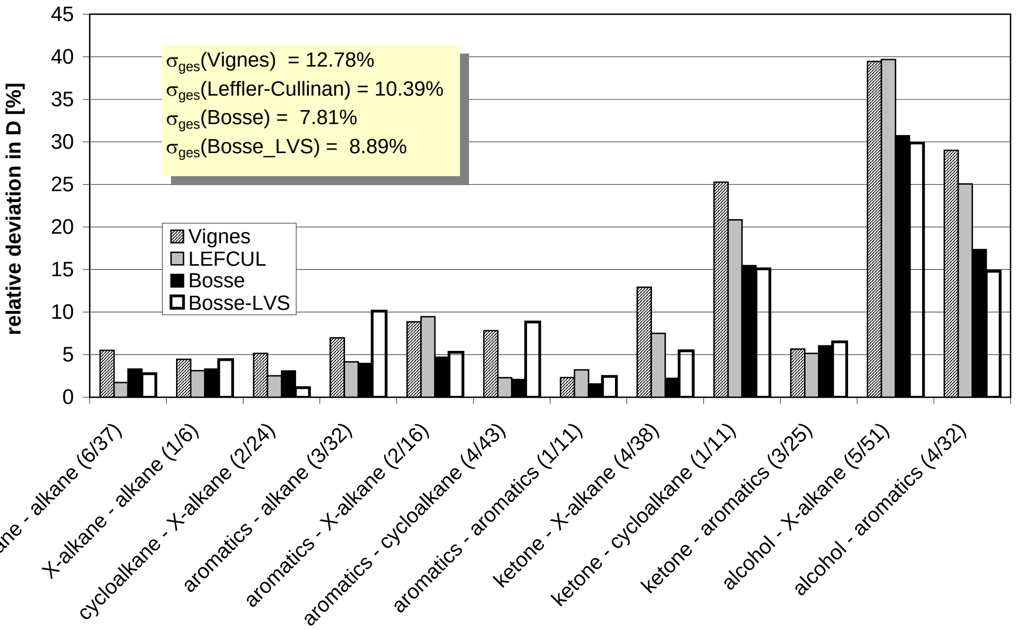

Figure 5.1. Relative deviations of diffusivity calculations in % with various MS-diffusivity models and UNIFAC for the thermodynamic correction factor.

$1/\eta$ which both provide corrections into the same direction for most of the systems. Only for systems with larger deviations, i.e. alcohol systems, the viscosity correction helps to improve the accuracy. However, this behaviour may be regarded as an artefact of an inaccurate description of the thermodynamics. An overall comparison reveals that the Bosse model yields the lowest average deviation with 7.81 % followed by Bosse-LVS with 8.89 %. At this point it must be emphasized that within the calculations with the Bosse model solely information on the vapour-liquid equilibrium is crucial which is a prerequisite for the computation of the thermodynamic correction factor anyway.

The importance of this additional correction term can also be seen in the Figs. 5.2–5.5. Here, the results of the Bosse model and the Vignes equation are depicted. Again, UNIFAC is applied to account for the thermodynamics. For all cases the Bosse model is superior to the Vignes equation. By means of this new correction term the relative mean deviations can be reduced by (39–71) % compared to the deviations of the Vignes model.

Thus far, the influence of the thermodynamics on the diffusion coefficient calculation has been considered with the UNIFAC model. Now, the Wilson model (Wilson 1964), the COSMOSPACE approach (Klamt et al. 2002; Bosse and Bart 2005a), and UNIFAC (Fredenslund et al. 1975) are applied for the thermodynamics to explore the influence of the chosen g^E-model. As aforementioned the required interaction parameters of the first two models were fitted to thermodynamically consistent Pxy-data. Only the diffusivity model with the highest accuracy of the previous examination, the Bosse model, is applied in the following. The final results of these calculations are summarised in Fig. 5.6. Detailed results of these calculations are given in the

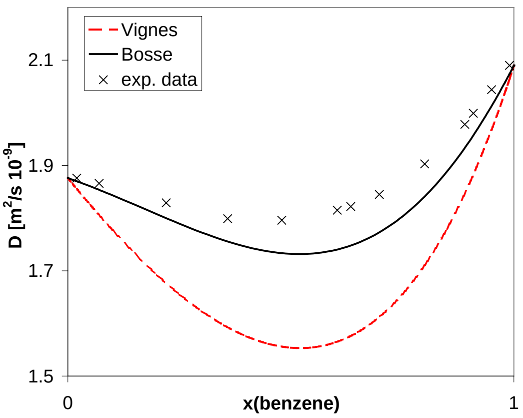

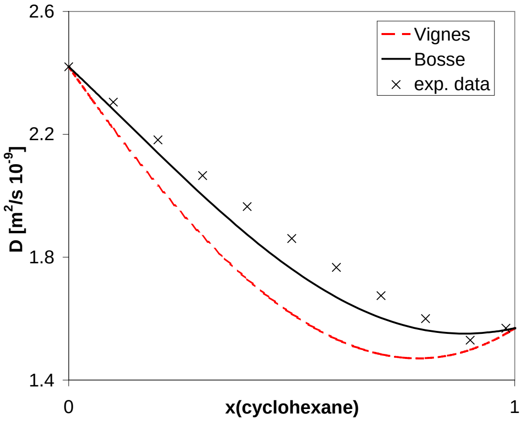

Figure 5.2. Prediction results with UNIFAC + Bosse and Vignes for the system benzene-cyclohexane at 25 °C (left).
Figure 5.3. Prediction results with UNIFAC + Bosse and Vignes for the system cyclohexane-toluene at 25 °C (right).

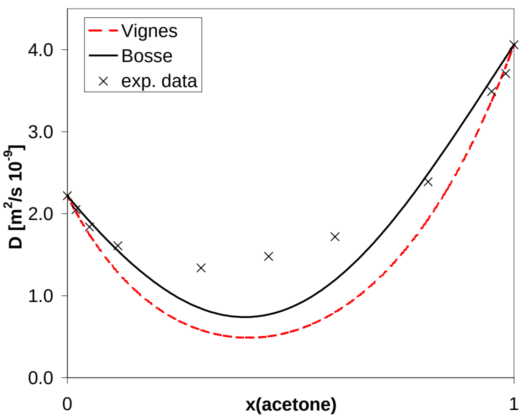

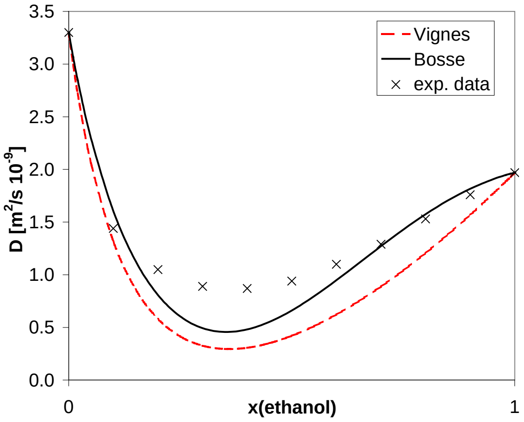

Figure 5.4. Prediction results with UNIFAC + Bosse and Vignes for the system acetone-cyclohexane at 25 °C (left).
Figure 5.5. Prediction results with UNIFAC + Bosse and Vignes for the system ethanol-benzene at 25 °C (right).

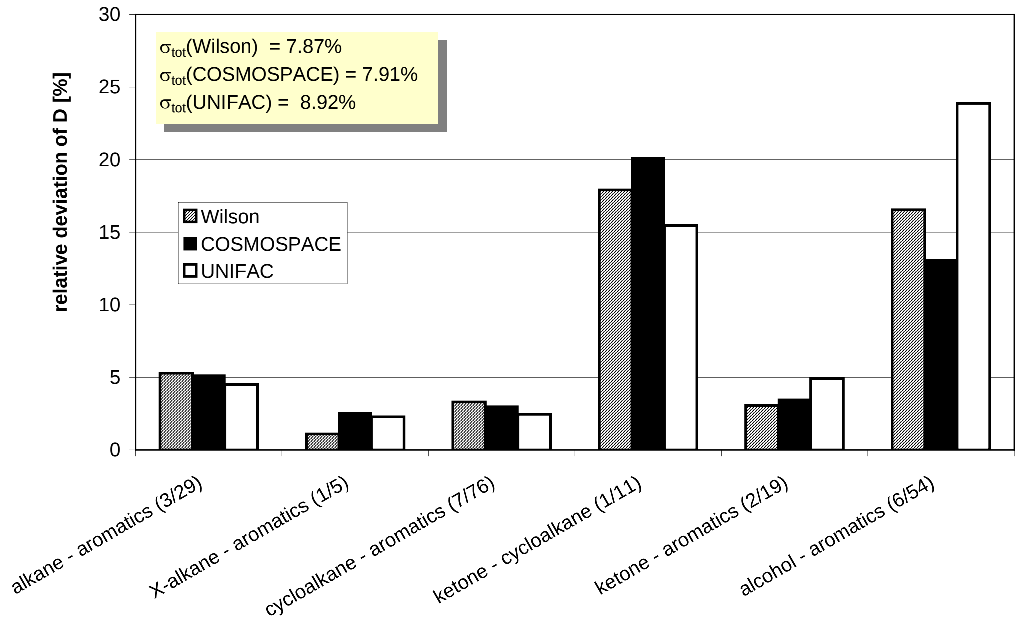

Figure 5.6. Relative deviations of diffusivity calculations in % with the Bosse-model and various g^E-models.

appendix.

As expected, the thermodynamically weakly nonideal systems (alkane – aromatics, X-alkane – aromatics, cycloalkane – aromatics) show the smallest deviations between experiment and model prediction and the results are almost independent from the choice of the g^E -model. A similar result is obtained for the class ketone – aromatics.

The largest prediction errors occur for the ketone – cycloalkane-systems (see Fig. 5.7). Interestingly, UNIFAC yields the smallest deviation for this case. Instead, the comparison of COSMOSPACE and Wilson reveals some deficiency of the COSMOSPACE model for this mixture class. The model inaccuracy is caused by the acetone sigma profile which was adopted from COSMO-RS. VLE predictions with COSMO-RS deviate largely from reality for ketone – cycloalkane-systems. However, due to the small database for this class of mixtures (only a single data set) a founded statement cannot be made which of the g^E-model is most suitable for the case considered hitherto.

A different conclusion can be drawn for the alcohol – aromatics systems (see also Fig. 5.8). In this case the COSMOSPACE-Bosse combination is to be favoured over the others. Especially the large deviations resulting from the UNIFAC calculations are striking. Summarising it can be said

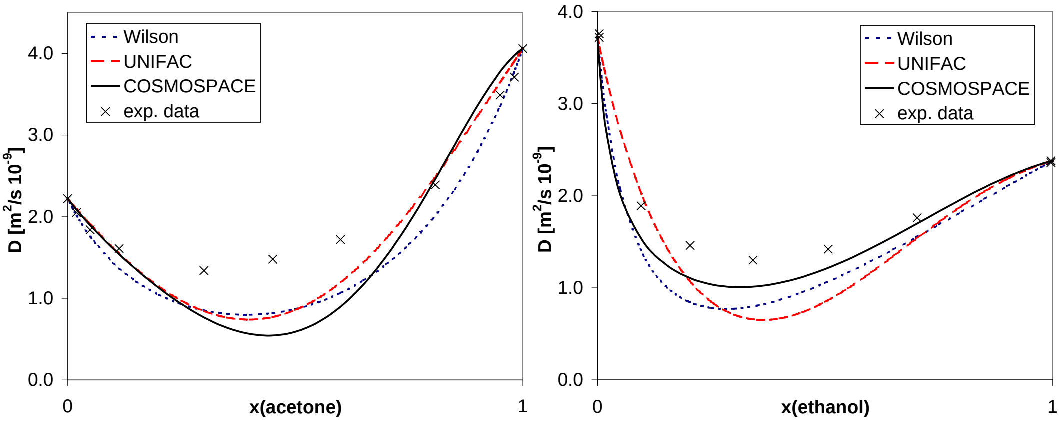

Figure 5.7. Prediction results with UNIFAC + Bosse and Vignes for the system acetone-cyclohexane at 25 °C (left).
Figure 5.8. Prediction results with UNIFAC + Bosse and Vignes for the system ethanol-benzene at 40 °C (right).

Table 5.1. Relative mean deviations ΔD for diffusivity calculations with COSMOSPACE for the thermodynamics and the models Vignes and Bosse for the MS-diffusivity.

	ΔD/%		
	Vignes	Bosse	Bosse (fit)
alkane – aromatics	8.59	5.16	1.47
X-alkane – aromatics	4.22	2.56	1.00
cycloalkane – aromatics	9.39	3.02	0.45
ketone – cycloalkane	29.05	20.15	19.68
ketone – aromatics	4.55	3.49	2.34
alcohols– aromatics	22.26	13.33	8.08

that for weakly nonideal systems the choice of the g^E-model plays only a secondary role while for associating systems the calculations with COSMOSPACE are superior to the other alternatives. Finally, all results obtained from the COSMOSPACE approach combined with the Vignes-model and the Bosse correlation are listed in Table 5.1.

In principal, an additional improvement of the diffusivity prediction can be achieved by using different sets of interaction parameters for the g^E-models used within the calculations of MS-diffusion coefficient and the thermodynamic correction factor. This can be realized by fitting the parameters of the Bosse model to experimental diffusivity data while the parameters for the correction factor are still adopted from the VLE-fitting. However, for an industrial application this alternative is questionable. This technique would require a reliable diffusivity database which does not exist for most of the systems of interest. Due to the positive experience made it is, therefore, suggested to simply apply the interaction parameters of the fitted VLE-data also to the MS-diffusivity model. Furthermore, the molecular interactions are consistently accounted for by a unique set of parameters. However, to show the potential of this additional fitting technique the results are tabulated in the third column of Table 5.1.

To perform a final assessment of the new approach, the Bosse model is tested against the model developed by Li et al. (Li et al. 2001). This model is one of the new developments that allows an improved prediction of diffusion coefficients. As already stated in the introduction, this model relies on several other physical properties in addition to the diffusivities at infinite dilution. Within this work the additional parameters are obtained as follows. The self diffusion coefficients are computed with the Dullien equation as suggested by Li et al. (Li et al. 2001). Mixture viscosities are calculated as aforementioned and the pure component properties are taken from the DIPPR database. Since the Wilson model accounts for the thermodynamics in the Li model, this g^E-expression is also used to compute the thermodynamic correction factor for the Bosse model. The relative mean deviations for the different mixture types are tabulated in Table 5.2, detailed results may be found in the Appendix. As the results show, with an average relative deviation of 7.28 % the model by Li et al. is slightly superior to the Bosse model (7.87 %). Since the Li model is not always superior a founded statement cannot be made which of the two models should be recommended. However, the advantage of the Bosse model is that it can be combined with any g^E-expression while the Li model is restricted to systems where Wilson parameters and the other physical properties are available.

Table 5.2. Relative mean deviations in ΔD for diffusivity calculations with Wilson for the thermodynamics and the models Bosse and Li for the MS-diffusivity.

	ΔD/%	
	Bosse	Li
alkane – aromatics	5.30	5.55
X-alkane – aromatics	1.11	2.16
cycloalkane – aromatics	3.31	5.90
ketone – cycloalkane	17.91	13.49
ketone – aromatics	3.06	4.51
alcohols– aromatics	16.55	12.11

5.5 Summary

In this work a new model for the prediction of Maxwell-Stefan diffusion coefficients has been developed. Eyring's absolute reaction rate theory, well-known for many theoretical derivations published in the literature, forms the basis of this approach. The new model has been presented in two alternative forms, the Bosse correlations as a modification of the Vignes-equation and the Bosse-LVS approach as a modification of the Leffler-Cullinan-model. Bosse-LVS differs from Bosse in the additional viscosity correction which has been successfully applied in many diffusivity models to improve the prediction quality, e.g. Leffler-Cullinan.

In a first comparison between Bosse and Vignes the influence of the additional energy contribution (excess Gibbs energy) has been examined. It has been clearly shown that for all systems this energy part leads to an improved description of the diffusion coefficients.

In further investigations the two new approaches have been compared with two models commonly used to test the effect of the viscosity. As the results have shown, the viscosity correction applied to Bosse-LVS does not lead to smaller deviations compared to Bosse. Overall the best results have been obtained with the Bosse model followed by Bosse-LVS. The average relative error has been reduced from 12.78 % to 7.81 %.

Depending on the choice of the g^E-model used within the new diffusivity approaches, association and solvation effects can be explicitly accounted for. Therefore, the influence of thermodynamics has also been investigated by means of the Wilson equation, UNIFAC, and COSMOSPACE. As expected, the choice of a g^E -expression plays only a secondary role for weakly nonideal systems. In contrast, the accuracy of the diffusivity predictions of alcohol systems depends strongly on the proper choice of a thermodynamic model. Here, it has been shown that COSMOSPACE-Bosse is superior to the other model combinations.

In a final assessment the Bosse model has been compared to the Li model. The results show that the Bosse model performs similar to the Li model but requires no additional parameters. Since only information of the diffusivities at infinite dilution and the thermodynamics are crucial, the Bosse model is widely applicable for the prediction of diffusion coefficients in liquid systems.

The thermodynamic correction factor should be in the focus of future work to enhance the prediction of diffusion coefficients. In contrast to other properties like diffusivities at infinite dilution or mixture viscosity data, this property is not accessible by experiment. Instead, it must be computed from the slope of the concentration dependence of the activity coefficients. Since VLE measurements are usually conducted in the mid-concentration range, this slope shows the largest uncertainties in the diluted concentration range. To obtain a more reliable curvature of the thermodynamic correction factor, the focus of VLE measurements should be direct not only to the mid-concentration range but also to the diluted and close to the infinitely diluted region. In this way, the calculation of VLE data may be greatly enhanced which in turn has a positive impact on the prediction of diffusion coefficients. In this way, it may be possible to reduce the average relative error for diffusion coefficient predictions below 2 %.

5.6 Symbols

D	Fick diffusion coefficient ($m^2\ s^{-1}$)
$Đ$	Maxwell-Stefan diffusion coefficient ($m^2\ s^{-1}$)
K	equilibrium constant (-)
N	number of data points (-)
P	pressure (Pa)
R	molar gas constant (8.3144 J mol^{-1} K^{-1})
T	temperature (K)

g	Gibbs energy (J mol^{-1})
h	Planck constant ($6.626 \cdot 10^{-34}$ m^2 kg s^{-1})
k_B	Boltzmann constant ($1.38 \cdot 10^{-23}$ m^2 kg s^{-2} K^{-1})
k	rate constant in Eyring's theory (s^{-1})
x	mole fraction of liquid phase (-)

Greek Symbols

Δg	standard free energy per mole (J mol^{-1})
Γ	thermodynamic correction factor (-)
Ω	partition sum (-)
γ	activity coefficient (-)
ε_0	activation energy per molecule at 0 °K (J)
η	dynamic viscosity (Pa s)
λ	distance between two successive equilibrium positions (m)

Subscripts

i	component i

Superscripts

+	activated state
∞	infinite dilution
E	excess
calc	calculated value
exp	experimental value

5.7 References

Bosse, D. and Bart, H. J.: *Binary Vapor-Liquid Equilibrium Predictions with COSMOSPACE*. Ind. Eng. Chem. Res. **44**(23): 8873-8882 (2005a).

Bosse, D. and Bart, H. J.: *Viscosity Calculations on the Basis of Eyring's Absolute Reaction Rate Theory and COSMOSPACE*. Ind. Eng. Chem. Res. **44**(22): 8428-8435 (2005b).

Cullinan, H. T., Jr.: *Concentration Dependence of the Binary Diffusion Coefficient*. Ind. Eng. Chem. Fundam. **5**(2): 281-283 (1966).

Cussler, E. L.: *Cluster Diffusion in Liquids*. AIChE J. **26**(1): 43-51 (1980).

Darken, L. S.: *Diffusion, mobility and their interrelation through free energy in binary metallic systems*. Trans. Am. Inst. Mining, Met. Eng. **175**: 184-201 (1948).

Fei, W. and Bart, H. J.: *Predicting Diffusivities in Liquids by the Group Contribution Method*. Chem. Eng. Proc. **40**: 531-535 (2001).

Fei, W. and Bart, H.-J.: *Prediction of diffusivities in liquids*. Chem. Eng. Tech. **21**(8): 659-665 (1998).

Fredenslund, A., Jones, R. L., and Prausnitz, J. M.: *Group-Contribution Estimation of Activity Coefficients in Nonideal Liquid Mixtures*. AIChE J. **21**(6): 1086-1099 (1975).

Glasstone, S., Laidler, K., and Eyring, H.: The Theory of Rate Processes. McGraw-Hill, New York (1941).

He, C.: *Prediction of the Concentration Dependence of Mutual Diffusion Coefficients in Binary Liquid Mixtures*. Ind. Eng. Chem. Res. **34**: 2148-2153 (1995).

Hsu, Y.-D. and Chen, Y.-P.: *Correlation of the mutual diffusion coefficients of binary liquid mixtures*. Fluid Phase Equilibria **152**: 149-168 (1998).

Hsu, Y.-D., Tang, M., and Chen, Y.-P.: *A group contribution correlation of the mutual diffusion coefficients of binary liquid mixtures*. Fluid Phase Equilibria **173**: 1-21 (2000).

Klamt, A., Krooshof, G. J. P., and Taylor, R.: *COSMOSPACE: Alternative to Conventional Activity-Coefficient Models*. AIChE J. **48**(10): 2332-2349 (2002).

Krishnamurthy, R. and Taylor, R.: *A Nonequilibrium Stage Model of Multicomponent Separation Processes*. AIChE J. **31**: 449-456 (1985).

Leffler, J. and Cullinan, H. T.: *Variation of Liquid Diffusion Coefficients with Composition*. Ind. Eng. Chem. Fundam. **9**(1): 84-88 (1970).

Li, J., Liu, H., and Hu, Y.: *A mutual-diffusion-coefficient model based on local composition*. Fluid Phase Equilibria **187-188**: 193-208 (2001).

Martins, R. J., de M. Cardoso, M. J. E., and Barcia, O. E.: *Excess Gibbs Free Energy Model for Calculating the Viscosity of Binary Liquid Mixtures*. Ind. Eng. Chem. Res. **39**: 849-854 (2000).

Martins, R. J., de M. Cardoso, M. J. E., and Barcia, O. E.: *Calculation of Viscosity of Ternary and Quaternary Liquid Mixtures*. Ind. Eng. Chem. Res. **40**: 1271-1275 (2001).

Rutten, P. W. M.: Diffusion in Liquids. Delft University Press, Delft (1992).

Taylor, R. and Krishna, R.: Multicomponent Mass Transfer. John Wiley & Sons, New York (1993).

Tyrrell, H. J. V. and Harris, R. Q.: Diffusion in Liquids. Butterworths (1984).

Vignes, A.: *Diffusion in Binary Solutions*. Ind. Eng. Chem. Fundam. **5**(2): 189-199 (1966).

Wilson, G. M.: *Vapor-Liquid Equilibrium. XI. A New Expression for the Excess Free Energy of Mixing*. J. Am. Chem. Soc. **86**: 127-130 (1964).

Appendix

A Detailed Results of the Diffusivity Predictions

Table A provides the detailed results of the diffusivity predictions. The third column displays the temperatures at which the experiments were conducted. The fourth column provides the number of data points gathered for the system described by the first two columns. Columns 5-7 refer to the results of the Bosse model with the excess Gibbs energy expressions Wilson, UNIFAC, and COSMOSPACE while the last column labelled Li refers to the calculated relative mean deviations as were computed with the Li model for the diffusion coefficients and the Wilson model for the thermodynamics.

Table A. Relative mean deviation ΔD computed with the Bosse model for the diffusivity approach and Wilson, UNIQUAC, and COSMOSPACE for the gE-model. The results of the Li-model for the diffusion coefficient calculation with the Wilson equation are also displayed.

				ΔD/%			
System		T/°C	N	Wilson	UNIFAC	COSMOSPACE	Li
alkane-aromatics				5.30	4.51	5.16	5.55
Benzene	n-heptane	45	7	8.60	7.67	5.93	6.86
Benzene	n-heptane	55	11	3.18	3.79	6.53	6.75
Benzene	n-hexane	25	11	4.12	2.07	3.02	8.52
X-alkane-aromatics				1.11	2.28	2.56	2.16
carbon tetrachloride	benzene	40	5	1.11	2.28	2.56	2.16
cycloalkane-aromatics				3.31	2.46	3.02	5.90
Benzene	cyclohexane	25	15	2.64	2.04	2.19	5.71
Benzene	cyclohexane	25	4	2.43	1.85	2.39	4.78
Benzene	cyclohexane	25	11	2.79	2.08	2.47	7.02
Benzene	cyclohexane	25	13	2.94	2.34	2.49	5.49
Benzene	cyclohexane	40	11	3.95	3.19	3.59	6.43
Benzene	cyclohexane	60	11	2.62	2.69	2.27	5.12

System		T/°C	N	ΔD/%			
				Wilson	UNIFAC	COSMOSPACE	Li
cyclohexane	toluene	25	11	5.79	3.00	5.74	6.74
ketone-cycloalkane				17.91	15.47	20.15	13.49
Acetone	cyclohexane	25	11	17.91	15.47	20.15	13.49
ketone-aromatics				3.06	4.93	3.49	4.51
Acetone	benzene	25	5	3.51	6.15	3.58	3.74
alcohol-aromatics							
Ethanol	benzene	25	8	12.11	19.05	5.83	7.73
Ethanol	benzene	25	11	9.06	19.44	7.76	4.28
Ethanol	benzene	25	10	13.71	20.21	8.66	9.70
Ethanol	benzene	40	9	17.23	15.75	11.09	15.27
Methanol	benzene	25	5	24.85	32.23	10.04	20.54
Methanol	benzene	25	11	22.30	36.57	35.19	15.16
			overall	**7.87**	**8.92**	**7.91**	**7.28**

B Literature References to Diffusivity Data

Alimadadian, A. and Colver, Ph., Can. J. Chem. Eng., **54**: 208-213 (1976).

Alizadeh, A.A. and Wakeham, W.A., Int. J. Thermophysics, **3**(4): 307-323 (1982).

Anderson, D.K., Hall, J.R., and Babb, A.L., J. Phys. Chem., **62**: 404-409 (1958).

Anderson, D.K. and Babb, A.L., J. Phys. Chem., **66**: 899-901 (1962).

Anderson, D.K. and Babb, A.L., J. Phys. Chem., **67**: 1362-1363 (1963).

Baldauf, W. and Knapp, H., Ber. Bunsenges. Phys.Chem., **87**: 304-309 (1983).

Bidlack, D.L. and Anderson, D.K., J. Phys. Chem., **68**: 3790-3794 (1964).

Caldwell, C.S. and Babb, A.L., J. Phys. Chem., **60**: 51-56 (1956).

Hammond, B.R. and Stokes, R.H., Trans. Far. Soc., **52**: 781-787 (1956).

Harned, H.S., Disc. Far. Soc., **24**: 7-16 (1957).

Harris, K.R., Pua, C.K., and Dunlop, P.J., J. Phys. Chem., **74**: 3518-3529 (1970).

Irani, R.R. and Adamson, A.W., J. Phys. Chem., **64**: 199-204 (1960).

Kelly, C.M., Wirth, G.B., and Anderson, D.K., J. Phys. Chem. (1971).

Kulkarni, M.V., Allen, G.F., and Lyons, P.A., J. Phys. Chem., **69**: 2491-2493 (1965).

Levien, B.J. and Mills, R., Aust. J. Chem., **33**: 1977-1985 (1980).

Rodwin, L., Harpst, J.A., and Lyons, P.A., J. Phys. Chem., **69**: 2783-2785 (1965).

Rowley, R.L., Sung, Chul Yi, Gubler, D.V., and Stoker J.M., J. Chem. Eng. Data, **33**: 362-366 (1988).

Sanchez, V., Oftadeh, H., Durou, C., and Hot, J-P., J. Chem. Eng. Data, **22**: 123-125 (1977).

Sanchez, V. and Clifton, M., J. Chem. Eng. Data, **23**: 209-212 (1978).

Sanni, S.A. and Hutchison, P., J. Chem. Eng. Data, **18**: 317-322 (1973).

Tasic, A. Z., Djordjeciv, B. D., Serbanovic, S. P., and Grozdanic, D. K., J. Chem. Eng. Data, **26**: 118-120 (1981).

Tyn, M.T. and Calus, W.F., J. Chem. Eng. Data, **20**(3): 310-316 (1975).

List of Publications and Conference Contributions

Bosse, D., Bart, H.-J., *Diffusion in flüssig-assoziierenden Systemen*, Presentation at the DECHEMA/GVC-Fachausschusstagung Extraktion 2001 in Frankfurt (Germany).

Bosse, D., Bart, H.-J., *Diffusion in Liquid Associating Systems*, Presentation at the 1st symposium of the TU Kaiserslautern and the TU Twente 2001 in Kaiserslautern (Germany).

Bosse, D., Bart, H.-J., *Diffusion in assoziierenden Flüssigkeiten*, Presentation at the BASF-workshop 2001 in Ludwigshafen (Germany).

Bosse, D., Bart, H.-J., *Stoffdaten aus assoziierenden Systemen*, Presentation at the COGNIS-workshop 2001 in Düsseldorf (Germany).

Bosse, D. und H.J. Bart. *Prediction of Diffusivities in Liquid Associating Systems on the Basis of a Multicomponent Approach*. in *Proceedings of the International Conference on Distillation & Absorption (CD-Rom)*. 2002. Baden-Baden (Germany): VDI-Gesellschaft Verfahrenstechnik und Chemieingenieurwesen GVC.

Bosse, D., Bart, H.-J., *Prediction of Diffusivities in Liquid Associating Systems*, Poster contribution at the ISEC 2002 in Cape Town (South Africa).

Bosse, D., Bart, H.-J., *Diffusion in Liquid Associating Systems*, Presentation at the Int. Conference of Distillation & Absorption 2002 in Baden-Baden (Germany).

Bosse, D. und H.J. Bart, *Diffusion in Liquid Associating Systems.* Chem. Eng. Tech., 2003. **26**(11): 1184-1188.

Bosse, D., Bart, H.-J., *Modellierung von Diffusionskoeffizienten in binären Flüssiggemischen*, Presentation at the DECHEMA/GVC-Fachausschusssitzung Thermisches Zerlegen 2003 in Weimar (Germany).

Bosse, D., Bart, H.-J., *Prediction of Diffusion Coefficients in Fluid Systems*, Presentation at the ECCE 2003 in Granada (Spain).

Bosse, D. und H.J. Bart, *Prediction of Diffusion Coefficients in Liquid Systems.* Ind. Eng. Chem. Res. (accepted for publication), 2005.

Bosse, D., Bart, H.-J., *Vorausberechnung von Diffusionskoeffizienten in fluiden Systemen*, Presentation at the DECHEMA/GVC-Fachausschusssitzung Thermisches Zerlegen 2004 in Leipzig (Germany).

Bosse, D. und H.-J. Bart, *Measurement of Diffusion Coefficients in Thermodynamically Nonideal Systems.* J. Chem. Eng. Data, 2005, **50**(5): 1525-1528.

Bosse, D. und H.J. Bart, *Viscosity Calculations on the Basis of Eyring's Absolute Reaction Rate Theory and COSMOSPACE.* Ind. Eng. Chem. Res., 2005, **44**(22): 8428-8435.

Bosse, D. und H.J. Bart, *Binary Vapor-Liquid Equilibrium Predictions with COSMOSPACE*, Ind. Eng. Chem. Res., 2005, **44**(23): 8873-8882.

List of Research Projects Supervised

Drumm, C., *Modellierung von Diffusionskoeffizienten in binären Flüssiggemischen*, Studienarbeit, Universität Kaiserslautern, 2003.

Stickland, D., *Statistical Thermodynamic Modelling of Liquid Viscosities – Prediction of Pure Component and Mixture Viscosities*, Studienarbeit, Universität Kaiserslautern, 2003

Lebenslauf

Persönliche Daten

Name:	Dennis Bosse
Adresse:	Lilienweg 32 53123 Bonn
Geburtsdatum	28. November 1973
Geburtsort	Remscheid
Staatsangehörigkeit:	deutsch
Familienstand:	verheiratet

Schulausbildung

08.1980 – 06.1984	Gemeinschaftsgrundschule Siepen, Remscheid
08.1984 – 06.1993	Ernst-Moritz-Arndt-Gymnasium, Remscheid Abschluss Abitur

Hochschulausbildung

10.1993 – 10.1999	Universität Dortmund Studium der Fachrichtung Chemietechnik Abschluss Diplom-Ingenieur
04.1999 – 10.1999	externe Diplomarbeit an der University of Bradford, Großbritannien

Berufserfahrungen

12.1999 – 04.2004	wissenschaftlicher Mitarbeiter am Lehrstuhl für Thermische Verfahrenstechnik, TU Kaiserslautern
seit 05.2004	Systemingenieur bei der innotec GmbH, Alfter-Oedekoven